

**AgSPA2 and AgBOI Control Landmarks of Filamentous
Growth in the Filamentous Ascomycete *Ashbya
gossypii***

Inauguraldissertation

zur

Erlangung der Würde eines Doktors der Philosophie

vorgelegt der

Philosophisch-Naturwissenschaftlichen Fakultät

der Universität Basel

von

Philipp Knechtle

aus Appenzell AI

Basel, 2002

Genehmigt von der Philosophisch-Naturwissenschaftlichen Fakultät
auf Antrag von

Prof. T. Boller

Dr. M.-P. Gulli

Prof. P. Philippsen

Basel, den 4. Juni 2002

Dekan

Prof. Dr. Andreas D. Zuberbühler

Summary	1
General Introduction	3
Mutations in AgSPA2 Have an Impact on the Hyphal Tip Growth Speed.....	8
Introduction	8
Results	9
AgSpa2p is a Conserved Protein with an Extended Internal Domain.....	9
AgSpa2p Localizes Permanently to Sites of Polarised Growth	11
AgSpa2p is Required for Fast Radial Growth	13
AgSpa2p Limits Early Hyphal Tip Growth Speed	15
Branching and Septation Temporarily Slows Down Hyphal Tip Growth Speed	16
Mutations in AgSPA2 have an Impact on the Branching Frequency	18
Mutations in AgSPA2 have an Impact on the Hyphal Tip Growth Speed Potential ..	20
The Hyphal Diameter is Decreased in AgSPA2 Δ P and Increased in Agspa2 Δ C Compared to Wild-type.....	21
Discussion	22
Perspectives	24
AgBoip is Required for Establishment and Maintenance of Polarised Growth in <i>A.gossypii</i>	25
Introduction	25
Results	26
AgBOI is Conserved Among Ascomycetes	26
AgBoi Δ Displays a Temperature Sensitive Phenotype.....	26
AgBoip is Required for Germination at Elevated Temperatures	27
Branching Frequency is Reduced in Agboi Δ	29
AgBOI is Required to Maintain Permanent Polarised Growth at the Tip	30
The Polarity Marker AgSpa2p Delocalises From the Tip During Spherical Enlargement in Agboi Δ Strains.....	31
Localisation of AgBoip	31
Discussion	34
Perspectives	36
Current Model of <i>A.gossypii</i> Morphogenesis	37

Construction of a Versatile Module for C-terminal GFP Fusion.....	39
Introduction	39
Results and Discussion.....	40
Cloning of a Universal GFP Cassette for C-terminal GFP Fusion via PCR Based Gene Targeting	40
Construction of an Integration Module Based on the AgADE2 Marker.....	44
Introduction	44
Results and Discussion.....	45
Generation of an Integration Module with AgADE2 as New Selection System.....	45
Integration of AgCAP1-GFP and AgCAP2-GFP Fusions Using the pAIC Module	47
Materials and Methods.....	49
Molecular Cloning	49
Methods in <i>A.gossypii</i> Genetics.....	50
Microscopy	52
Cloning of pAGSPA2.....	53
Generation of AgSPA2 Δ P and Agspa2 Δ C Strains	53
Methods in Yeast Genetics.....	53
Generation of AgSPA2-GFP and AgSPA2 Δ P-GFP Strains.....	53
Cloning of pAGBOI	54
Generation of Agboi Δ and Agboi Δ SPA2-GFP	54
Generation of AgBOI-GFP	54
Appendix I.....	55
Appendix II.....	56
Appendix III.....	57
References	58
Acknowledgements.....	62
Curriculum vitae	63

Summary

The morphological requirements for the development of a fungal mycelium include the emergence of germ tubes, a permanent hyphal tip extension, lateral and apical branching and septation. The basis for each of these events, also termed landmarks of filamentous growth, is polarised growth. Thus polarised growth is essential for hyphal and mycelial morphogenesis. We wanted to investigate genes in the filamentous ascomycete *Ashbya gossypii* that are involved in polarised growth and control landmarks of filamentous growth.

In "Chapter 1" and "Chapter 2" I described the identification of two genes that are involved in polarised growth and I highlighted their roles in landmarks of filamentous growth. At the end of the first two chapters I draw a refined model of the developmental pattern in *A.gossypii* with the insight gained from these first two chapters. In "Chapter 3" and "Chapter 4" I described two novel tools that were established for the functional analysis of the genes investigated in the first two chapters. These two methods were the construction of a versatile module for C-terminal GFP fusion and an integration module based on the AgADE2 marker.

Chapter 1 We wanted to identify genes in *A.gossypii* that are important for hyphal morphogenesis. As polarised growth is crucial for morphogenesis in *A.gossypii* and *S.cerevisiae* we hypothesised that a similar set of genes is required for polarised growth in *A.gossypii* and *S.cerevisiae*; however, differences in orthologous proteins might have an impact on the regulation of polarised growth and thus guide the process of filamentation in *A.gossypii* and budding in *S.cerevisiae*. We screened for *A.gossypii* proteins that have an orthologue in *S.cerevisiae* implicated in polarised growth and that display a significant difference in the primary structure compared to the *S.cerevisiae* orthologue. This revealed AgSpa2p, a homologue of ScSpa2p. AgSpa2p is more than twice as long as ScSpa2p due to an extended internal domain without significant homology to ScSpa2p. AgSpa2p localises permanently to hyphal tips and transiently to sites of septation. We constructed two AgSPA2 mutants, a partial deletion of the internal domain alone and a complete deletion. We could show that these mutant strains display alterations in the branching frequency and in the hyphal tip growth speed potential. The branching frequency and the hyphal tip growth speed potential are two factors that

have an impact on the hyphal tip growth speed. The two mutants behave opposing in respect of each of these factors and the two factors have a competing effect on the hyphal tip growth speed. We suggest that AgSpa2p is required to balance these two factors to achieve an efficient hyphal tip growth speed and the extended internal domain in AgSpa2p plays an important role in this process.

Chapter 2 We screened an existing *A.gossypii* knock out library for strains that show defects in landmarks of filamentous growth. We identified a strain that frequently displayed spherically enlarged hyphal tips. The deleted gene in that strain was identified as AgBOI. AgBoip represents an orthologue of the redundant proteins in *S.cerevisiae* ScBoi1p and ScBoi2p, which are implicated in polarised growth. We could show that AgBoip is required for the emergence of germ tubes and for the initiation of lateral branches. Moreover AgBoip is required for permanent hyphal tip extension, as polarisation of hyphal tips is not permanently maintained in Agboi Δ strains. We could show that prior to a spherical enlargement of hyphal tips in Agboi Δ the polarisation marker AgSpa2p delocalises from the tip. Tips can be repolarised which goes in parallel with a relocalisation of AgSpa2p. In spherically enlarged tips the actin cytoskeleton is also depolarised. AgBoip itself localised to sites of polarisation similar to cortical actin patches. We suggest that AgBoip is required for establishment of cell polarity to initiate germ tubes and lateral branches and for maintenance of cell polarity to allow a permanent hyphal tip extension.

Chapter 3 The green fluorescent protein (GFP) is of extraordinary value in molecular biology. It allows the visualisation of proteins in organisms and together with advanced microscopy techniques it enables dynamic studies in living cells. We constructed a versatile module for PCR based C-terminal GFP-fusion and established microscopy techniques for dynamic GFP studies in *A.gossypii*. The studies described in "Chapter 1" and "Chapter 2" would not have been possible without the development of this module.

Chapter 4 The functional analysis of genes often requires the expression of truncated alleles, e.g. reporter modules as the GFP, tagged proteins for biochemical analyses, mutant alleles or overexpression constructs. As it was of importance in this work to express certain GFP fusion proteins as second copies we constructed an integration

module on the basis of the AgADE2 marker. The mode of action of the integration module is the reconstitution of a truncated AgADE2 ORF thereby co-integrating the fragment of interest.

General Introduction

The ability of cells to polarise is an important component in the overall process of cellular morphogenesis (Drubin and Nelson, 1996). It allows the cell to establish and maintain spatially restricted components that mediate functions as diverse as vectorial transport in epithelial cells, directed cell movement in amoeba or leukocytes, cell shape development in early embryogenesis, neurite outgrowth or polarised growth in fungi. The establishment of cell polarity consists of three hierarchical and interdependent steps. First a response to intra and/or extracellular signals, second the generation of an axis of polarity in response to this signal and third the subsequent asymmetric distribution of cellular components along this axis. Feedback loops reinforce the ordering of these events resulting in the maintenance of cell polarity.

At a molecular level cell polarity has been most intensively investigated in the budding yeast *S.cerevisiae*. Studies on cell polarity in other eukaryotic organisms as the fission yeast *S.pombe*, *C.elegans*, *Drosophila* or cultured mammalian cells suggest that the molecular mechanism underlying cell polarity is conserved among eukaryotes. A variety of studies from all of these systems demonstrate that the Cdc42p GTPase and other Rho-type GTPases are key players in the establishment and maintenance of cell polarity. Locally activated Cdc42p signals downstream to a variety of effectors that mediate rearrangements of the actin cytoskeleton and transcriptional activation. The actin cytoskeleton serves as the structural basis for cell polarity. The activity of Cdc42p is controlled via its nucleotide bound state. Cdc42p bound to GTP is active whereas Cdc42p bound to GDP is inactive. Guanine nucleotide exchange factors (GEFs) and GTPase activating proteins (GAPs) are regulators of Cdc42p. GEFs catalyse the transition from the GDP to the GTP bound form thereby activating Cdc42p whereas GAPs activate the intrinsic GTPase activity of Cdc42p, which leads to a hydrolysis of the bound GTP to GDP and a subsequent inactivation of Cdc42p. The regulators of Cdc42p respond to intra and/or extracellular signals to activate or inactivate Cdc42p. (Hall, 1998; Johnson, 1999).

In filamentous fungi, cell polarity is the basis for hyphal morphogenesis. The establishment of cell polarity directs polarised growth spatially to initiate germ tubes and lateral branches. Filamentous fungi maintain cell polarity at tips of hyphae,

which results in a permanent apical extension. Apical branching is an event that was so far only observed in filamentous fungi and occurs when the tip of a single growing hypha divides symmetrically to produce two equal tips. Polarised growth is maintained during apical branching since growth does not stop. A polarisation within hyphae directs the formation of a septum, the incomplete cytokinesis in filamentous fungi that lacks cell-cell separation. Branching, permanent polarised growth and septation are landmarks of filamentous growth (Christiansen et al., 1999; Harris, 1997; Heath, 1995; Lengeler et al., 2000; Momany and Hamer, 1997; Momany and Taylor, 2000; Spohr et al., 1998; Trinci, 1970; Wendland, 2001). We wanted to investigate genes in the filamentous ascomycete *Ashbya gossypii* (Ashby and Nowell, 1926), which are involved in polarised growth and control landmarks of filamentous growth.

Recent work has demonstrated that Rho-type GTPases and their regulators are crucial for hyphal morphogenesis in *A.gossypii*. Deletion of a CDC42 homologue in *A.gossypii*, AgCDC42, or its putative GEF, AgCDC24, still allowed the initial isotropic growth phase of the spore but prevented the establishment of cell polarity (Wendland and Philippsen, 2001). The function of the rhoGAP AgBem2p in *A.gossypii* was associated with the determination of cell polarity in germinated spores and hyphal tips (Wendland and Philippsen, 2000) and the PAK kinase AgCla4p, a potential effector of AgCdc42p, with maturation of hypha (Ayad-Durieux et al., 2000). Thus, many of the signaling networks crucial for polarity are conserved in *A.gossypii* and contribute to filamentous growth.

The completion of a whole genome sequencing approach in *A.gossypii* revealed a relatively small genome of only 9 Mbp encoding about 4800 genes with very few gene duplications (Dietrich et al., 2001). Interestingly 97 % of all genes identified had an orthologue in the budding yeast *S.cerevisiae* and for nearly all genes implicated in cell polarity in *S.cerevisiae* orthologues could be identified in *A.gossypii*. This included Rho-type and Ras GTPase modules, regulators of these modules, scaffold proteins, formin homologues and PAK kinases. A current view of the interaction of these proteins in *S.cerevisiae* is represented in Figure 1 (acc. to Casamayor and Snyder, 2002; Chant, 1999; Gulli and Peter, 2001; Johnson, 1999; Madden and Snyder, 1998; Pruyne and Bretscher, 2000a; Pruyne and Bretscher, 2000b).

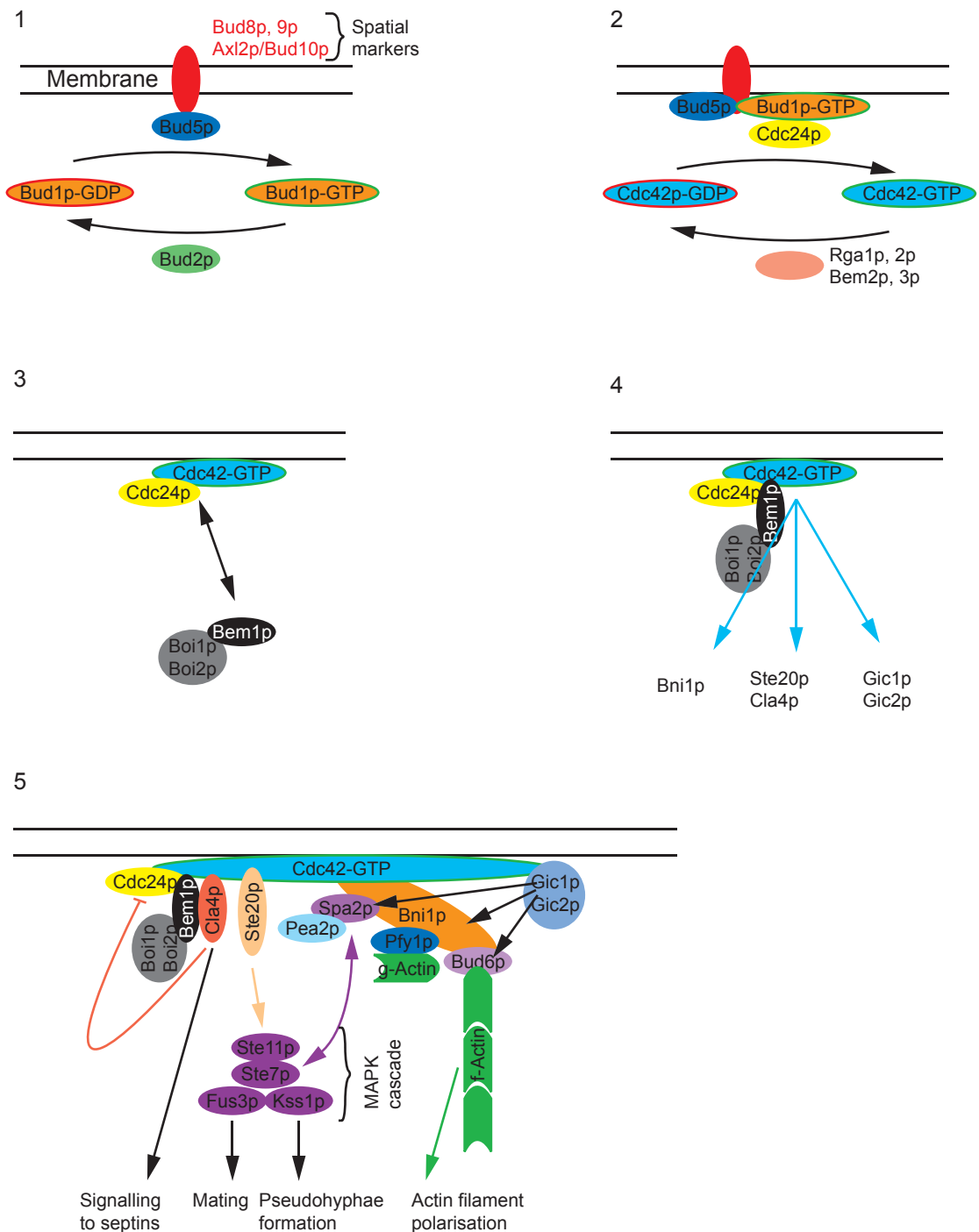


Figure 1
Establishment of cell polarity in *S.cerevisiae*

This sketch represents a very simplified and thus incomplete model of how cell polarity is established in *S.cerevisiae*. (1) Localised activation of the GEF Bud5p by bud tag proteins. Bud5p in turn catalyses the activation of the Ras GTPase Bud1p at the membrane. (2) Active Bud1p locally activates the GEF Cdc24p. Cdc24p in turn locally activates the Rho-type GTPase Cdc42p at the membrane. (3) Cdc24p is stabilised by the scaffold Bem1p that binds to Cdc24p, Cdc42p, Boi1p and Boi2p. (4) Active Cdc42p signals to a variety of effectors including Bni1p, Ste20p, Gic1p and Gic2p and Cla4p, resulting in the organisation of the actin cytoskeleton at sites of growth (5). *A.gossypii* genes encoding orthologous proteins were identified for all proteins drawn, except that for the duplicated genes in *S.cerevisiae* only one is present in *A.gossypii*.

Potentially a very similar set of genes is responsible for two such distinct cellular morphogeneses as budding in *S.cerevisiae* and filamentous growth in *A.gossypii*. One strategy to

identify genes that are involved in polarised growth and control landmarks of filamentous growth was based on a sequence comparison of *A.gossypii* proteins with their orthologues in *S.cerevisiae*.

We hypothesised that differences in the primary structure in conserved proteins in *A.gossypii*, which are implicated in polarised growth in *S.cerevisiae*, guide the process of filamentous growth. Thus we screened conserved proteins for the presence of additional domains or the absence of individual domains, major differences in length or mutations at conserved residues. In "Chapter 1" of this work we identified an orthologue in *A.gossypii* of the *S.cerevisiae* polarisome protein ScSpa2p, which is more than twice as long as ScSpa2p. We suggest that AgSpa2p balances the branching frequency versus the hyphal tip growth speed potential to achieve a maximal hyphal tip growth speed.

In a second strategy we visually screened an existing *A.gossypii* knock out mutant collection for strains with alterations in landmarks of filamentous growth. We identified a strain carrying a deletion of an orthologue to the redundant proteins ScBoi1p and ScBoi2p in *S.cerevisiae*. These proteins in *S.cerevisiae* are implicated in cell polarity but their function is not well characterised. In "Chapter 2" of this work we report that AgBoip is required for establishment of cell polarity to initiate germ tubes and lateral branches and for maintenance of cell polarity to allow a permanent hyphal tip extension.

The developmental pattern of *A.gossypii* starts with an isotropic growth phase (Figure 2A & 2B and supplemental movie 1 and movie 4). The middle of a needle shaped spore starts to enlarge spherically to form the germ bubble and actin patches are distributed randomly at the periphery. Then, actin patches begin to localise perpendicular to the axis of the spore at the cortex of the germ bubble marking the site of polarisation. Polarised growth leads to the initiation of the first germ tube to form the unipolar germling. Cortical actin patches are localised to the tip of the germ tube. Patches localise also randomly but less frequent to the hyphal cortex. Actin cables emanate from the tip into the hypha. The established germ tube maintains polarisation and extends permanently. A second site of polarisation is established at the periphery of the germ bubble to induce a second germ tube and this generates the bipolar germling. Additional sites of polarity are established at the hyphal cortex to initiate lateral branches. Actin rings, a prerequisite of septum formation, develop at the hyphal cortex. The first septum arises preferentially at the neck between the germ bubble and the first germ tube, actin patches localise temporary to that site spanning the cross-section of a hypha. Further septa are formed during development of a young mycelium.

Maturation of hypha leads to an increase of the hyphal tip growth speed and apical branching (Ayad-Durieux et al., 2000; Wendland and Philippsen, 2000; Wendland and Philippsen, 2001 and our unpublished results).

Several properties and established techniques make *A.gossypii* an interesting model organism, e.g. homologous recombination functions as the main mechanism for DNA integration (Steiner et al., 1995) replicative plasmids bearing CEN/ARS elements from *S.cerevisiae* are maintained under appropriate conditions (Wright and Philippsen, 1991), PCR based gene targeting works as an efficient tool for the generation of deletions (Wendland et al., 2000) and the genome is completely sequenced and annotated (Dietrich et al., 2001). Some biological questions we were interested in, however, could not be answered adequate with the existing methods. For this reason this work also includes the development and establishment of new techniques. "In Chapter 3" we describe the construction of a versatile GFP module for C-terminal GFP fusion and in "Chapter 4" the construction of an integration module based on a novel marker.

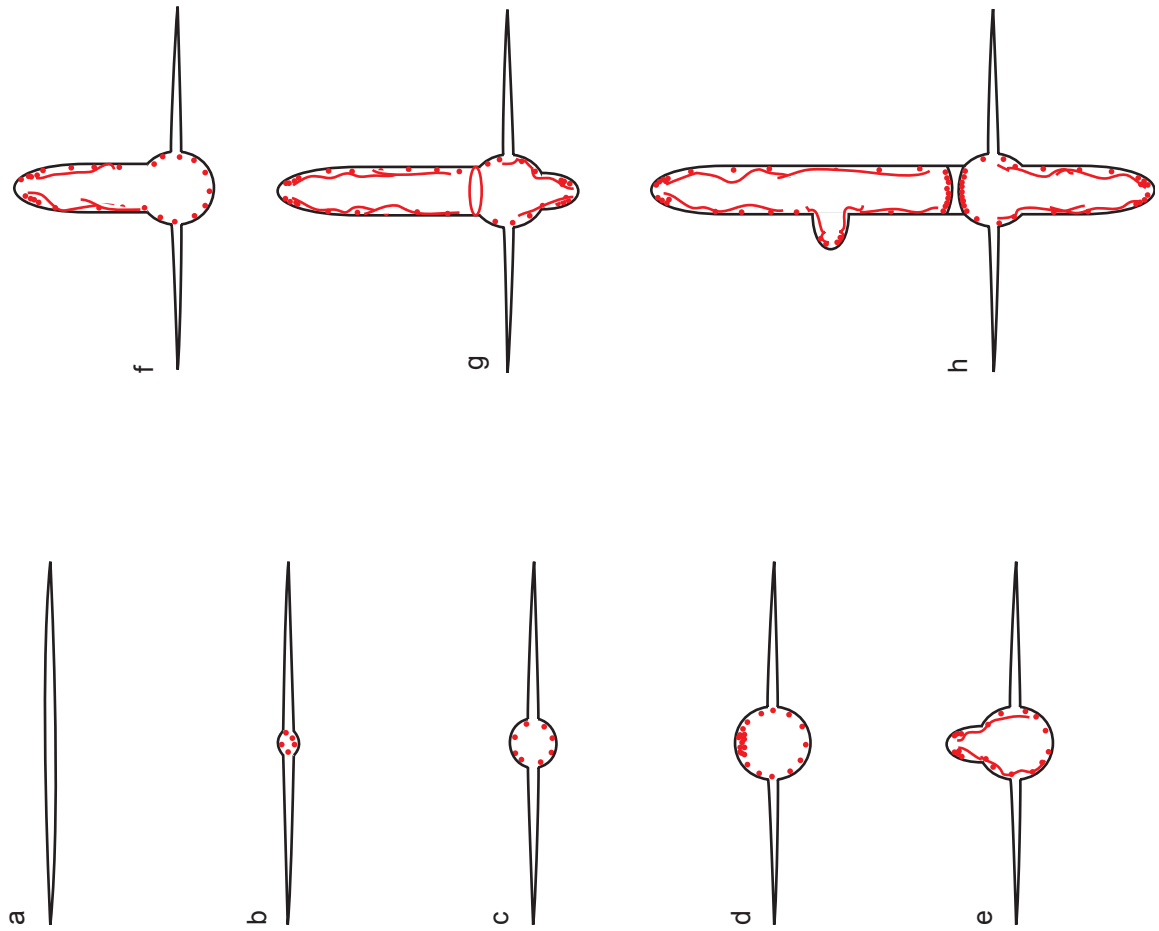


Figure 2A
Schematic representation of the development from a spore to a young mycelium in *A.gossypii*. The individual pictures represent cross sections. The outline is in black, red represents the actin distribution. Dots mark actin patches, lines actin cables and rings actin rings. a) Ungerminated spore; b) & c) Isotropic growth phase in the germ bubble. Actin patches are distributed evenly at the cell cortex; d) Concentration of actin patches to the site of branch emergence; e) Unipolar germling. Actin patches are concentrated to the site of growth and actin cables emanate from the tip. f) Continued apical growth phase in the unipolar germling. Actin patches are concentrated at the tip, the very apical part is free of actin patches. Actin cables emanate at the cortex from the tip into the hyphae. g) Emergence of a second germ tube. An actin ring localises to the neck between the first germ tube and the germ bubble as a precursor for septation. h) Emergence of the first lateral branch and induction of a septum at the neck where the actin ring was localised. Actin patches localise transiently to the site of septum formation. i) Continued apical growth at all tips. The generated septum is free of actin. j) Apical branching in mature hyphae. Refer also to Figure 2B.

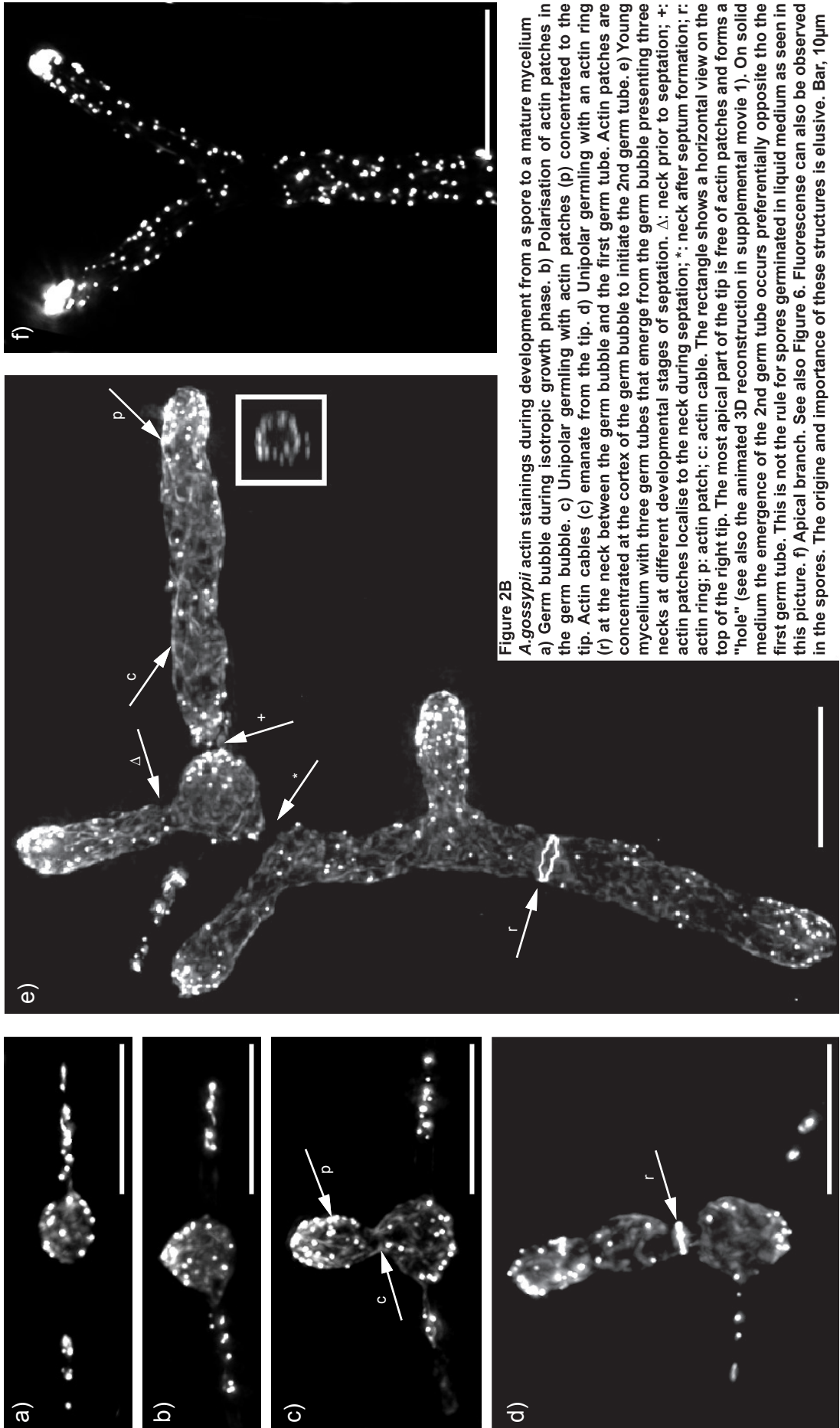


Figure 2B

A.gossypii actin stainings during development from a spore to a mature mycelium
 a) Germ bubble during isotropic growth phase. b) Polarisation of actin patches in the germ bubble. c) Unipolar germling with actin patches (p) concentrated to the tip. Actin cables (c) emanate from the tip. d) Unipolar germling with an actin ring (r) at the neck between the germ bubble and the first germ tube. Actin patches are concentrated at the cortex of the germ bubble to initiate the 2nd germ tube. e) Young mycelium with three germ tubes that emerge from the germ bubble presenting three necks at different developmental stages of septation. Δ: neck prior to septation; +: actin patches localise to the neck during septation; *: neck after septum formation; r: actin ring; p: actin patch; c: actin cable. The rectangle shows a horizontal view on the top of the right tip. The most apical part of the tip is free of actin patches and forms a "hole" (see also the animated 3D reconstruction in supplemental movie 1). On solid medium the emergence of the 2nd germ tube occurs preferentially opposite to the first germ tube. This is not the rule for spores germinated in liquid medium as seen in this picture. f) Apical branch. See also Figure 6. Fluorescence can also be observed in the spores. The origine and importance of these structures is elusive. Bar, 10µm

Mutations in AgSPA2 Have an Impact on the Hyphal Tip Growth Speed

Introduction

We identified an orthologue of the *S.cerevisiae* ScSpa2p in *A.gossypii* termed AgSpa2p. AgSpa2p differs significantly in length compared to ScSpa2. In *S.cerevisiae* ScSpa2p localises to sites of polarised growth independent of actin. During the mitotic cycle ScSpa2p can be found at bud tips and at the site of cytokinesis, upon pheromone induction ScSpa2p localises to sites of projection formation (Gehring and Snyder, 1990; Snyder, 1989; Snyder et al., 1991). ScSpa2p together with ScBud6p (ScAip3) and ScPea2p is part of a protein complex termed the polarisome. A deletion of any of these genes causes similar phenotypes. Cells are rounder than wild-type, defective in mating projection formation and bud site selection in diploid cells (Gehring and Snyder, 1990; Sheu et al., 1998). ScPea2p binds to an internal region of ScSpa2p, which is important for ScSpa2p stability and localisation (Sheu et al., 1998, Valtz and Herskowitz, 1996) and ScBud6 binds actin (Amberg et al., 1997). It is thought that the polarisome proteins are involved in regulation of the actin cytoskeleton. The formin homologue ScBni1p, which is also implicated in actin organisation, interacts with polarisome proteins. The C-terminal part of ScSpa2p binds internally to ScBni1p whereas ScBud6p binds to the C-terminus of ScBni1p. In addition the Rho-type GTPases ScCdc42p and ScRho1p interact with ScBni1p in their activated form and probably activate ScBni1p (Fujiwara et al., 1998, Evangelista et al., 1997). ScPfy1, another binding partner of ScBni1p (Imamura et al., 1997), can promote the incorporation of actin monomers on barbed ends of actin filaments (Pantaloni and Carlier, 1993). The localisation of ScBni1p at bud tips absolutely depends on ScCdc42p, largely on ScSpa2p and partly on ScBud6p (Ozaki-Kuroda et al., 2001). Recently it has been shown that ScBni1p directs actin filament assembly to sites of polarisation where ScSpa2p mediates localisation and ScBud6p activation (Evangelista et al., 2002; Sagot et al., 2002, see also Figure 2).

ScSpa2p interacts also with members of MAPK cascades in *S.cerevisiae* as shown with the two-hybrid system. The MEK ScSte7p from the Fus3p-Kss1p pathway and the MEK ScMkk1p from the Slt2p pathway interacted with ScSpa2p (Sheu et al., 1998).

Thus ScSpa2 plays a key role in polarity

establishment and maintenance putatively through contributing to actin cable assembly.

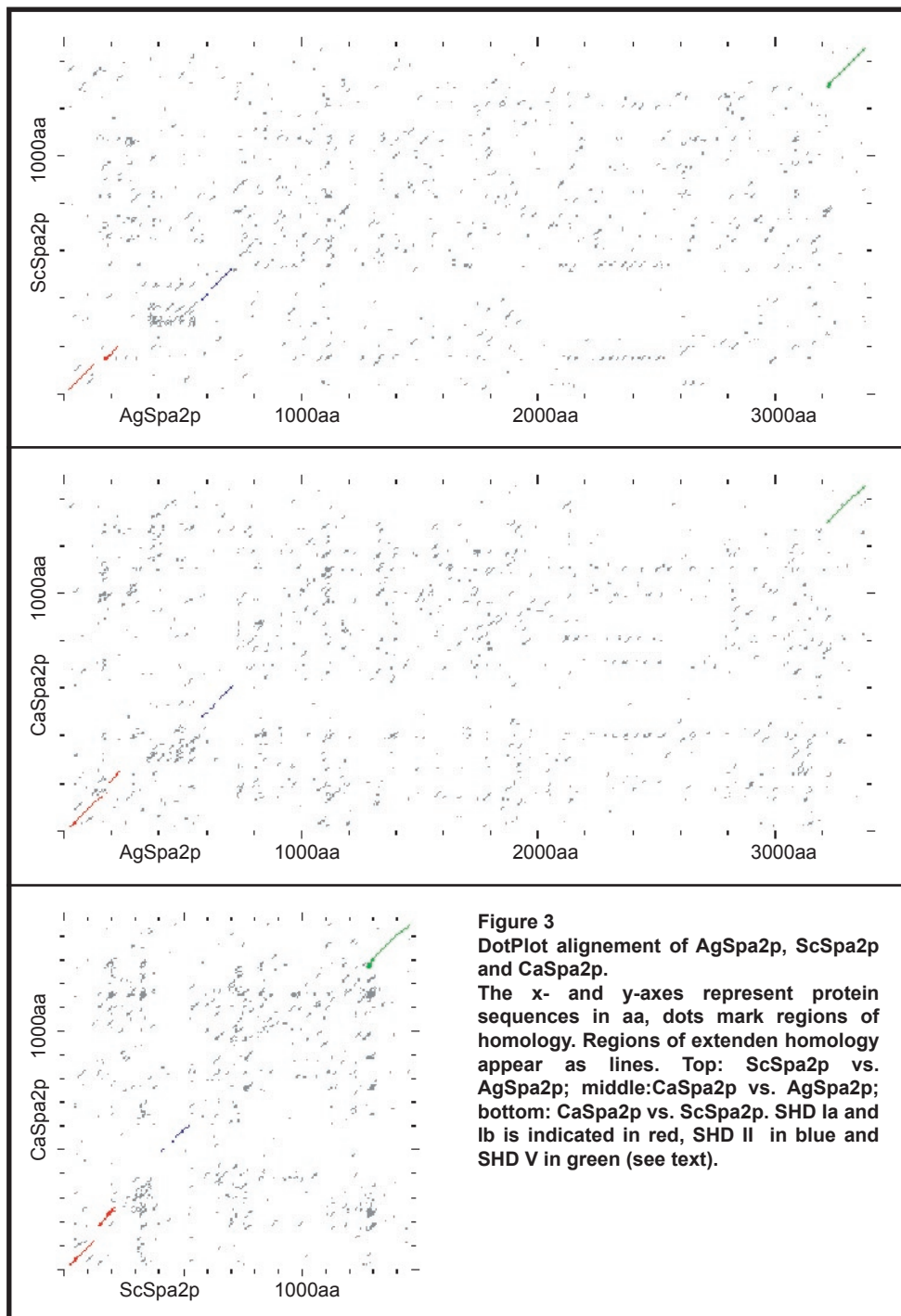
AgSpa2p in *A.gossypii* is more than twice as large as ScSpa2p due to an extended internal domain without homology to ScSpa2p. We found that this domain plays an important role in the branching frequency and the hyphal tip growth speed potential in *A.gossypii*. We suggest that AgSpa2p balances the branching frequency versus the hyphal tip growth speed potential to optimise the hyphal tip growth speed.

Results

AgSpa2p is a Conserved Protein with an Extended Internal Domain

The AgSPA2 ORF was identified during the *A.gossypii* sequencing project (Dietrich et al., 2001). It encodes a protein with homology to ScSpa2p (Snyder, 1989) and CaSpa2p (renamed, originally IPF11245, Brown et al., 2001). Both the *S.cerevisiae* and the *C.albicans* proteins are

1466 aa in length whereas the *A.gossypii* protein is 3392 aa in length with a predicted molecular weight of about 360 kD. The size of the *A.gossypii* protein is due to an extended internal domain, which is about three times as large as in the *S.cerevisiae* or *C.albicans* protein as judged by



DotPlot analysis (Maizel and Lenk, 1981). No significant homology can be located in this internal domain comparing the three proteins to each other (Figure 3). AgSPA2 bears a highly repetitive region in the internal domain of about 800 aa in length. It is made up of a 10 aa repeat of the sequence SPA(R,L)G(E,D)(L,V)(I,K)S(T,V) that is repeated 30 times (with 2 substitutions allowed). A 9 aa repeat was identified previously in ScSpa2p (Snyder, 1989). The repetitive region in ScSpa2p is also localized towards the end of the internal domain as in AgSpa2p. Both repeats harbour a single Ser-Pro unit but further homology between the two repetitive regions could not be observed. The AgSPA2 ORF is also highly repetitive in the coding region for the AgSpa2p repeat. However this cannot be observed in the ScSPA2 ORF (Figure 4). Repetitive sequence could not be identified in CaSpa2p, neither in the protein sequence nor in its coding region. ClustalW analysis (Thompson et al., 1994) was made to identify homologous regions between AgSpa2p, ScSpa2p and CaSpa2p. Four domains with significant homology could be identified termed Spa2p Homology Domain (SHD) Ia, Ib, II and V (acc. to Roemer et al., 1998, Figure 5). A region with predicted coiled coils (Steinert and Roop, 1988) located between HD Ib and HD II in all three proteins. The original SHD I domain was split into two separate domains since it was interrupted by a region of weak homology. It was previously shown for SHD Ia in *S.cerevisiae* that it interacts with members of the Fus3-Kss1 and Slt2 MAPK cascades. The non-kinase domain of the MEKs

ScSte11p, ScMkk1p and ScMkk2p interacted with the first 150 aa of ScSpa2p (Sheu et al., 1998). SHD II was shown to be necessary and sufficient

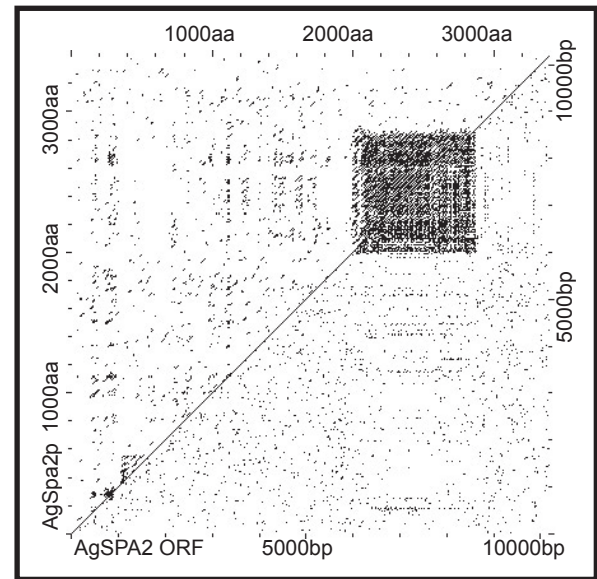


Figure 4
Repetitive regions in the AgSPA2 ORF and AgSpa2p protein represented in a DotPlot alignment
 The x- and y-axes represent protein sequences in aa and nucleotide sequences in bp, respectively. Dots mark regions of homology.
 Left: AgSpa2p protein aligned against itself; right: AgSPA2 ORF aligned against itself. Highly repetitive regions appear in the AgSpa2p between app. 2000 aa and 2850 aa. This corresponds to the region between app. 6000 bp and 8500 bp in the AgSPA2 ORF. In addition a repetitive region is located only in the protein sequence between 200 aa and 400 aa representing potential coiled coils.

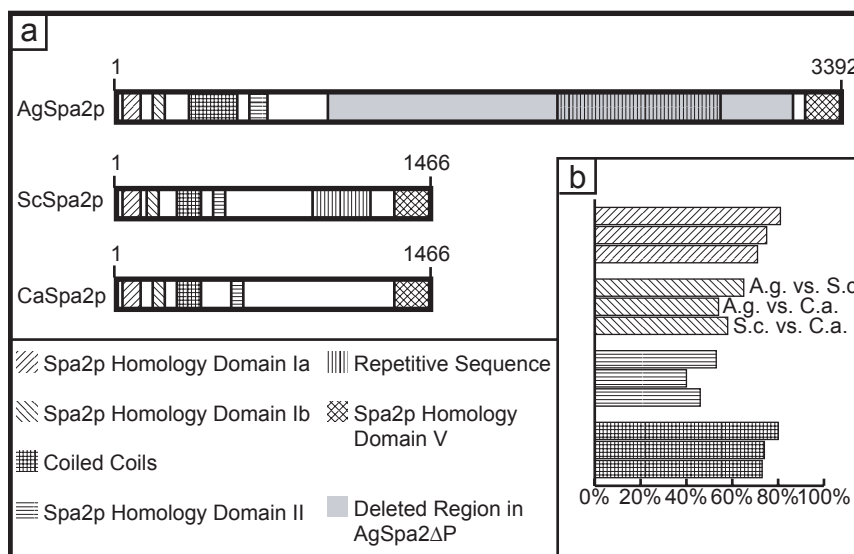


Figure 5
Conserved regions in AgSpa2p
 a) The position of the homology domains according to a ClustalW alignment are as follows: AgSpa2p SHD Ia: 20-121, SHD Ib:169-216, CC: 340-466, 470-516, 519-562, SHD II: 624-695, SHD V:3229-3386. ScSpa2p SHD Ia: 19-121, SHD Ib:144-186, CC: 283-388, SHD II: 444-516, SHD V:1304-1461. CaSpa2p SHD Ia: 10-114, SHD Ib:176-288, CC: 278-392, SHD II: 523-596, SHD V:1307-1457. The corresponding domains carry the same hatching. The shaded region in AgSpa2p indicates the deletion set in AgSpa2ΔP (see text). b) Comparison of the four corresponding domains. Each set carries the hatching of the respective domain. Top

is always *A.gossypii* vs. *S.cerevisiae*, middle *A.gossypii* vs. *C.albicans* and bottom *S.cerevisiae* vs. *C.albicans*. The bars give similarities in %

for localisation of ScSpa2p (Arkowitz and Lowe, 1997) and to bind ScPea2p (Valtz and Herskowitz, 1996). SHD V in ScSpa2p binds to ScBni1p (Fujiwara et al., 1998). All interactors of ScSpa2p in *S.cerevisiae* were found to have an orthologue protein in *A.gossypii*.

AgSpa2p also showed homology to ScSph1 (Roemer et al., 1998), a duplicated ORF of ScSpa2p. However the homology was restricted to the SHD Ia, Ib and II domains. The SHD V domain of ScSph1p displayed only weak homology to SHD V of AgSpa2p compared to ScSpa2p and CaSpa2p. Therefore ScSph1p was not included in the comparison. A screen of the *A.gossypii* protein database with ScSpa2p or ScSph1p gave only AgSpa2p as a hit suggesting that there is no duplication of the AgSPA2 ORF in *A.gossypii*.

AgSpa2p Localizes Permanently to Sites of Polarised Growth

We wanted to investigate whether AgSpa2p localises to sites of polarised growth as seen for ScSpa2p in *S.cerevisiae*. We therefore made a C-terminal GFP fusion to the endogenous copy of the AgSPA2 ORF in the *Agleu2Δthr4Δ* background strain (see "Chapter 3"; *Agleu2Δthr4Δ* is referred to as wild-type). The radial growth rate, the morphology and pattern of the actin cytoskeleton did not differ in the AgSPA2-GFP strain from what was observed in wild-type. In contrast, a strain carrying a complete deletion of the AgSPA2 locus had a severe radial growth defect (see below). A plasmid bearing either the full length AgSPA2 ORF

or the full length ORF fused to the GFP module could complement this radial growth defect to the same extent as it was for the wild-type strain bearing the vector control alone (data not shown). We therefore conclude that the GFP tag did not impair the function of AgSpa2p.

The gene product of AgSPA2-GFP localized to the tips of mycelia as a bright dot. AgSpa2p-GFP could also be observed within hyphae spanning the cross-section of a hypha. In a co-staining with Rhodamine-Phalloidine AgSpa2p-GFP localised to tips and sites of septation as seen for cortical actin patches, however, AgSpa2p did not co-localise with actin patches. Spa2p-GFP could neither be observed at sites where an actin ring localised nor could it be seen associated with actin cables (Figure 6). Thus AgSpa2p appears to be at sites of polarised growth.

To determine the temporal organization of AgSpa2p-GFP in a developing mycelium a time-lapse series was acquired. First we started with a unipolar germling that already had AgSpa2p-GFP localised to its tip. Pictures were taken over a time period of 7 h at a frequency of 0.2 min⁻¹. AgSpa2p-GFP remained localised to the original tip without delocalisation. The emergence of a novel lateral branch was preceded by a concentration of AgSpa2p-GFP at the cell cortex. These newly initiated branches also maintained AgSpa2p-GFP at the tip. AgSpa2p-GFP was also observed transiently at sites of septation but the signal was weak under time-lapse conditions (Figure 7 and supplemental movie 2).

Second we started a time-lapse acquisition

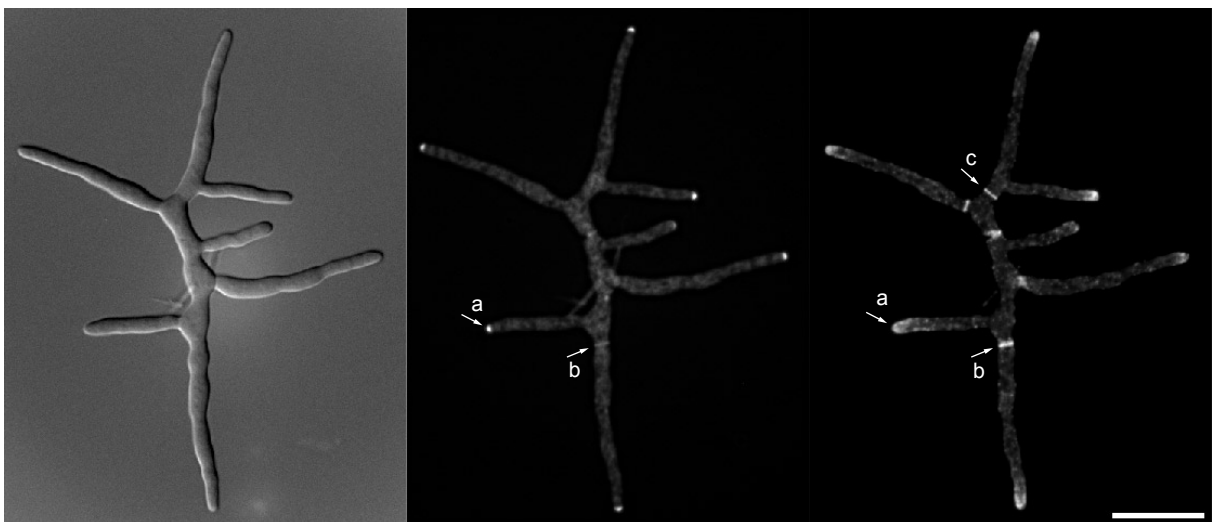


Figure 6
AgSpa2p-GFP / Rhodamine-Phalloidin double staining
Left: Nomarski illumination; middle: GFP; right: Rhodamine-Phalloidin. Localisation of AgSpa2p-GFP and actin at hyphal tips (a) and at sites of septation (b). AgSpa2p-GFP does not localise with the actin ring (c). Bar, 20 μ m

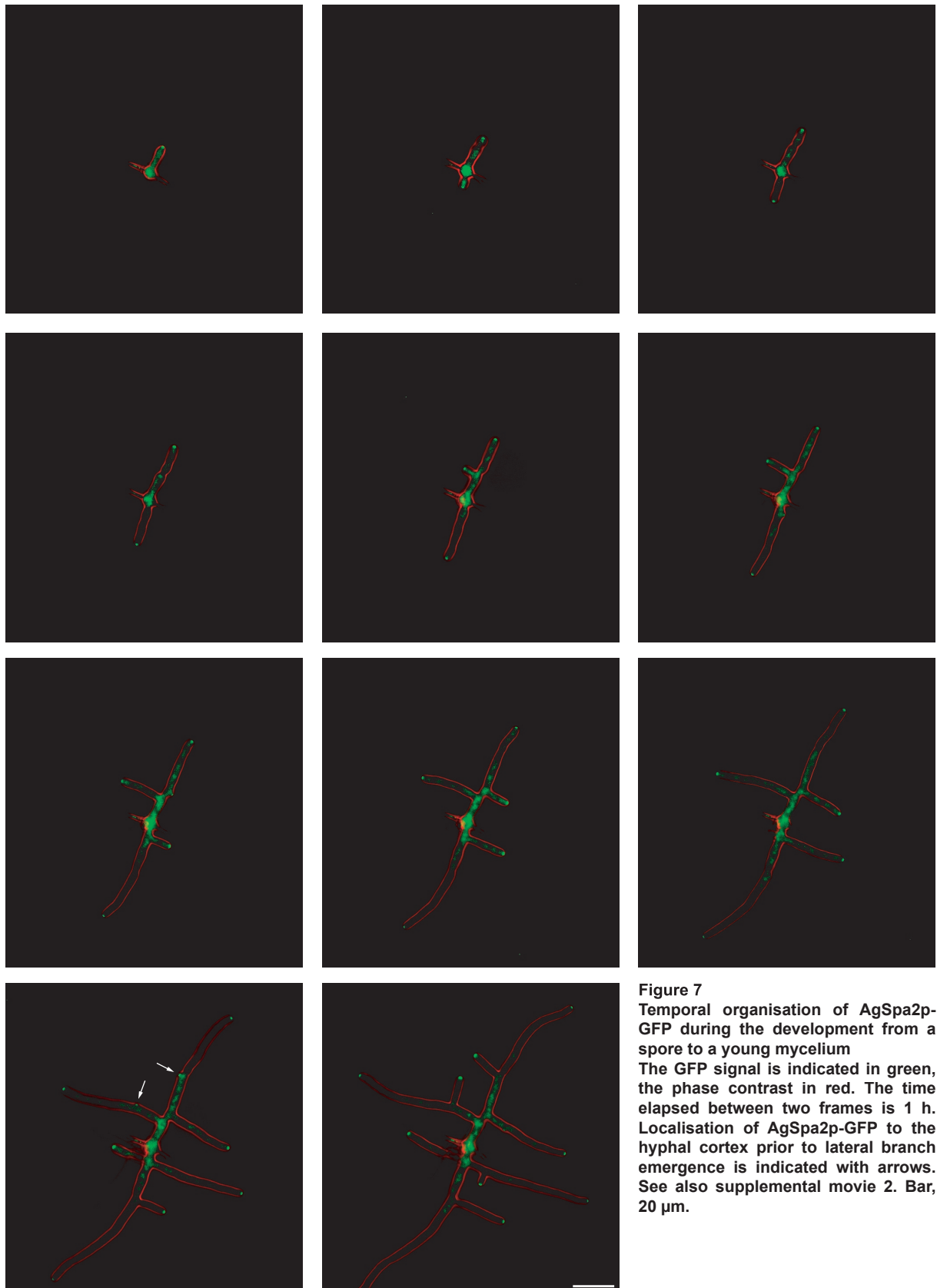


Figure 7
 Temporal organisation of AgSpa2p-GFP during the development from a spore to a young mycelium
 The GFP signal is indicated in green, the phase contrast in red. The time elapsed between two frames is 1 h. Localisation of AgSpa2p-GFP to the hyphal cortex prior to lateral branch emergence is indicated with arrows. See also supplemental movie 2. Bar, 20 μm .

from a mature hypha and followed the formation of an apical branch. The picture acquisition frequency was 0.5 min^{-1} , the total duration 46

min. AgSpa2p-GFP permanently localised to the single growing hyphae. Prior to the apical branch initiation after 22 min the site of AgSpa2p-GFP

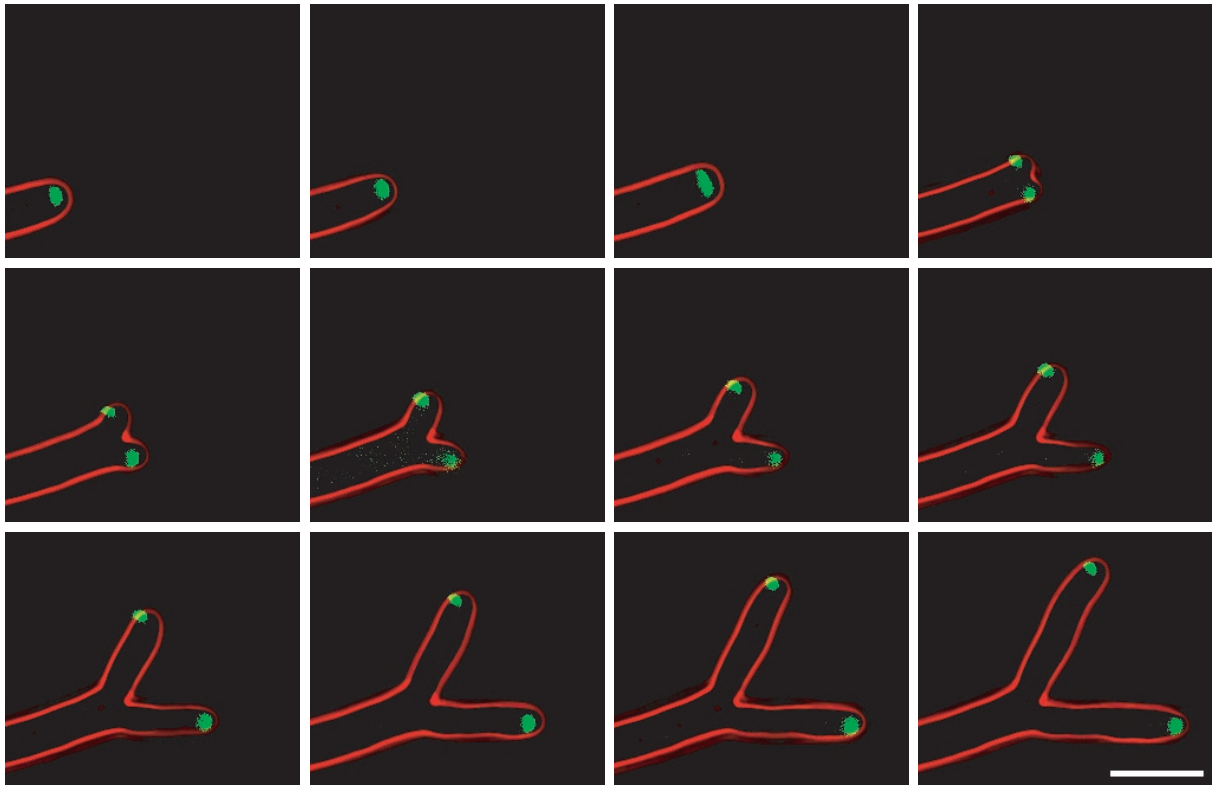


Figure 8
Temporal organisation of AgSpa2p-GFP during apical branch formation. The GFP signal is indicated in green, the phase contrast in red. The time elapsed between two frames is 2 min. Between frame 3 and 9 the GFP signal does not localise exactly to the hyphal tip. This is an artefact caused by different focal planes of the two tips. This is also the reason for the weak GFP signal for the lower tip in frame 6. See also supplemental movie 3. Bar, 10 μ m.

localisation enlarged and divided symmetrically. Two independent branches formed which again permanently localised AgSpa2p-GFP to their tip (Figure 8 and supplemental movie 3).

We demonstrate that permanent polarised growth in *A.gossypii* is maintained by a permanent polarisation of hyphal tips and neither lateral nor apical branching disrupts the polarisation at the tip. At the site of septation the polarisation is transient.

AgSpa2p is Required for Fast Radial Growth

To investigate the role of AgSpa2p in hyphal morphogenesis we generated two mutant alleles of AgSPA2. A complete deletion of the AgSPA2 ORF was generated by PCR based gene targeting (Wendland et al., 2000; Wach et al., 1994; Baudin et al., 1993). The complete coding region downstream of the start codon was deleted to generate the Agspa2 Δ C strain. Additionally an in frame deletion strain was generated in which the extended internal domain in AgSpa2p was eliminated. The region coding for 978 aa - 3163

aa in AgSPA2 was deleted from the endogenous copy generating an AgSPA2 Δ P strain. A C-terminal GFP tagged version of this strain was also constructed (see Figure 5 and "Materials and Methods").

The AgSPA2 Δ P and Agspa2 Δ C mutants had a radial growth defect, which was more pronounced in the complete deletion strain. When grown on AFM plates for 6 d the radial growth distance of the partial deletion strain was only 63 % compared to the wild-type. The complete deletion reached only 40 % of wild-type (Figure 9).

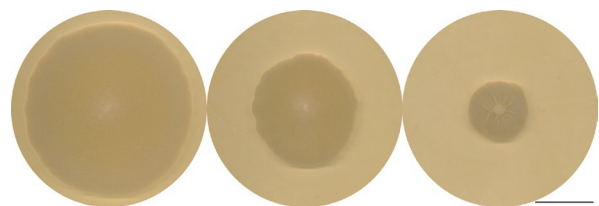


Figure 9
Radial growth defect in AgSPA2 Δ P and Agspa2 Δ C strains. Left: Wild-type; middle: AgSPA2 Δ P; right: Agspa2 Δ C. All mycelia were grown for 6 d at 30°C. Bar, 2 cm.

To determine whether this radial growth defect was the result of a decreased radial growth speed we determined the radial growth speed of wild-type, AgSPA2 Δ P and Agspa2 Δ C over a time frame of 7 d. Pre-grown mycelium was inoculated in the centre of AFM plates. The mycelia were cultured at 30°C and the radial diameter of the colony was measured every 24 h. All three strains reached their maximal radial growth speed after 3 d. For wild-type this was about 190 $\mu\text{m}/\text{h}$. AgSPA2 Δ P

the frequency of polarised cortical actin in that strain and compared it to wild-type. We also included the partially deleted and the two GFP fusion strains. Spores of all five strains were cultured in AFM at 30°C and fixed after 16 h. The mycelia were stained for actin and polarised actin localization was quantified. It was observed in all strains at a frequency of 98% or more ($n > 100$). We conclude that AgSpa2p is required for fast radial growth and that the extended internal

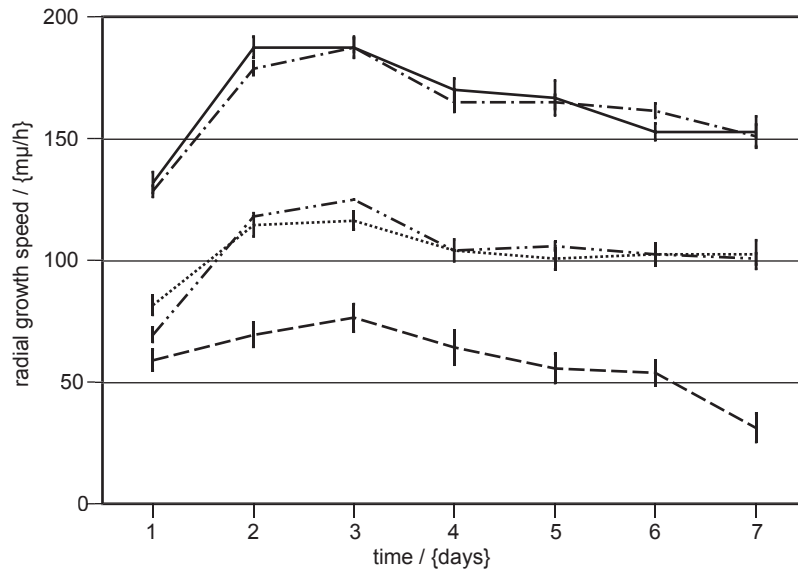


Figure 10
Radial growth speed of strains carrying different AgSPA2 alleles
The x-axis represents the time in days, the y-axis the radial growth speed in $\mu\text{m}/\text{h}$. wild-type(—), AgSPA2-GFP(---), AgSPA2 Δ P(· · ·), AgSPA2 Δ P-GFP(- · - ·) and Agspa2 Δ (- - -). The value measured after the first day was the difference between the inoculums (1 mm in diameter) and the radial growth distance after 1 d divided by 24 h. The inoculums were taken from plates that had already been growing for 3 d and should have reached the maximal radial growth speed. We suppose therefore that the value for day 1 (especially for the strains carrying the full length and partially deleted alleles) is too low. Bar, SEM.

reached a maximal radial growth speed of about 120 $\mu\text{m}/\text{h}$ and Agspa2 Δ C about 80 $\mu\text{m}/\text{h}$ (Figure 10). The radial growth speed decreased slowly after passing the maximum for all strains. The radial growth speed was also determined from the GFP tagged strains and compared with the untagged strains. The pattern obtained for the AgSPA2-GFP strain did not differ significantly to the one observed for wild-type. Similarly the AgSPA2 Δ P-GFP strain did not differ significantly from the untagged version.

AgSpa2 Δ Pp-GFP had a similar localisation pattern as the full-length protein. It was found at hyphal tips and at sites of septation. To rule out that the decreased radial growth speed observed for AgSPA2 Δ P was due to an unstable localisation of AgSpa2 Δ Pp we compared the frequency of apical GFP localisation between AgSpa2p-GFP and AgSpa2 Δ Pp-GFP. 91 % of all hyphae had the full length protein localised to tips and 90 % the partially deleted protein ($n > 80$, Figure 11).

To exclude that the observed decrease in radial growth speed in Agspa2 Δ C was due to a less frequent polarisation of hyphal tips we determined

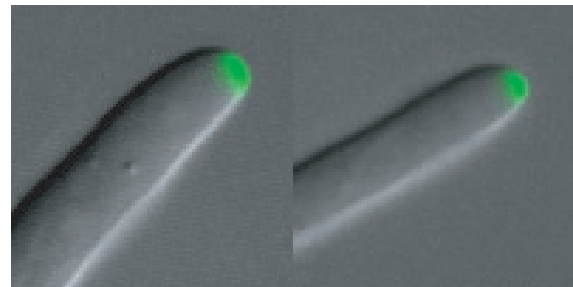


Figure 11
Localisation of AgSpa2 Δ Pp
Left: AgSpa2p-GFP; right: AgSpa2 Δ Pp-GFP. Nomarski illumination in grey with the GFP signal in green.

domain plays an important role in that process. AgSpa2p is not required to polarise cortical actin to tips but we do not exclude that it has a regulatory function on polarised actin.

AgSpa2p Limits Early Hyphal Tip Growth Speed

We wanted to investigate whether the decreased radial growth speed observed in the AgSPA2 Δ P and Agspa2 Δ C strains was the result of a decreased hyphal tip growth speed.

Spores from wild-type, AgSPA2 Δ P and Agspa2 Δ C were cultured on slides at 30°C. After 8 h individual spores that had developed to a unipolar

primary germ tube extended and subsequently a second germ tube emerged generating the bipolar germling. Then lateral branches were initiated to form a young mycelium (Figure 12, 13 & 14).

To determine the growth speed of individual hyphae we measured the increase in length of the primary tip in time intervals of 2 h. The hyphal tip growth speeds were determined over a period of 16 h and plotted against time (Figure 15).

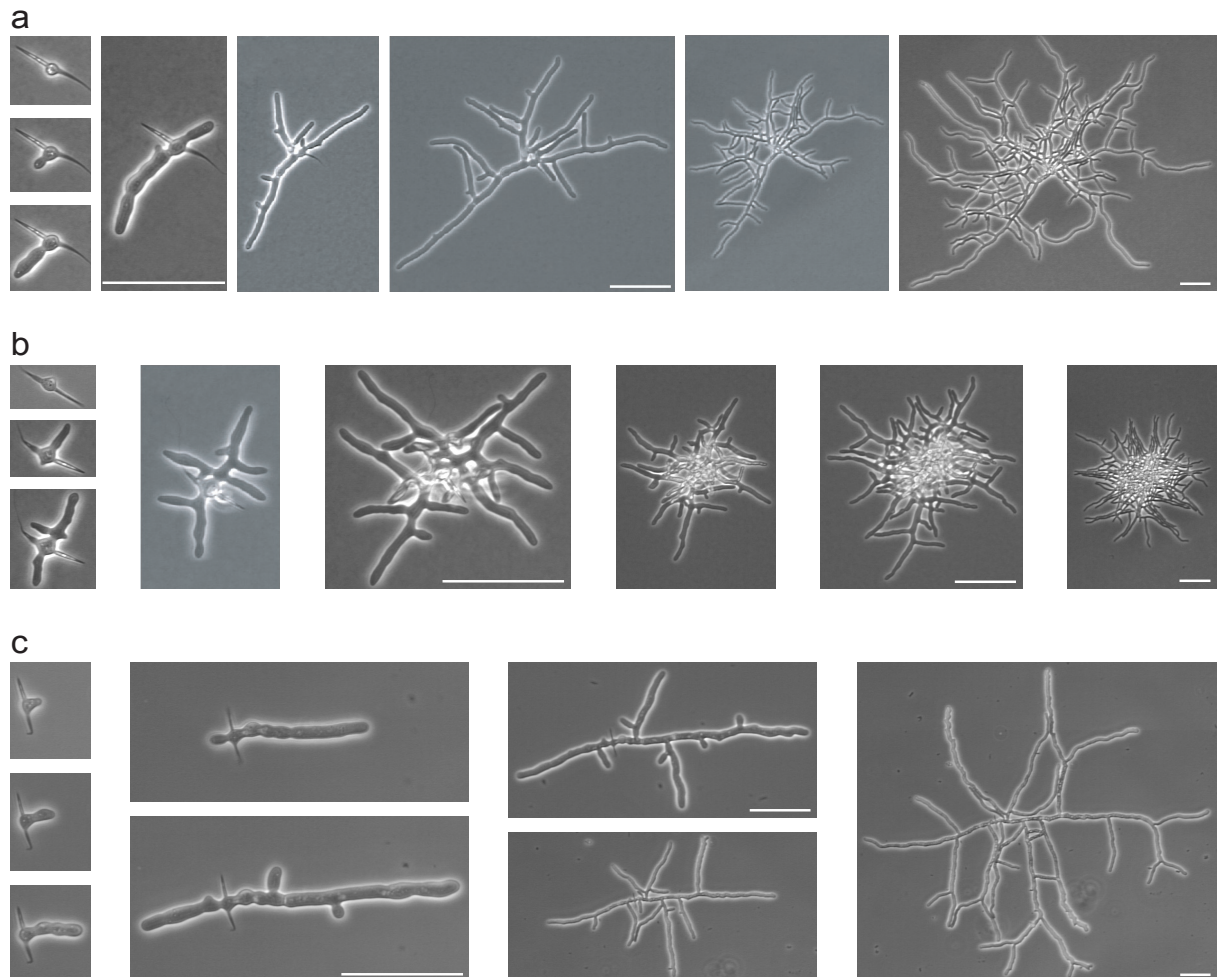


Figure 6
Time-lapse acquisition of wild-type, AgSPA2 Δ P and Agspa2 Δ C during development from a spore to a mature mycelium (a) wild-type, (b) AgSPA2 Δ P and (c) Agspa2 Δ C. The time elapsed between two frames is 2 h. Bar, 50 μ m.

germling were followed over a time period of 16 h at a picture acquisition frequency of 0.5 h⁻¹ (see "Materials and Methods").

The general growth pattern was the same for all three strains. Growth started with an initial isotropic growth phase generating a germ bubble. Next the switch to polarised growth lead to a first germ tube forming a unipolar germling. The

The growth speed in wild-type behaved logarithmic over the entire time followed. After 16 h the speed reached 92 μ m/h, which is in the same range as previously reported (Ayad-Durieux et al., 2000). The maximal value observed was 167 μ m/h. This is also in accordance with the radial growth speed of 190 μ m/h after 3 d of growth on plates (see above).

The hyphal tip growth speeds measured for AgSPA2 Δ P were decreased compared to wild-type at all time points measured. The hyphal tip growth speed reached a value of 49 $\mu\text{m}/\text{h}$ after 16 h of growth.

The initial hyphal tip growth speed (2 - 12 h) measured for Agspa2 Δ C was increased compared to wild-type. At 14 h the acceleration decreased and the hyphal tip growth speed reached a value of 66 $\mu\text{m}/\text{h}$ after 16 h. The discontinual behaviour of the growth speed between 10 and 14 h could be associated with premature apical branching in Agspa2 Δ C (Figure 16). Neither in wild-type nor in AgSPA2 Δ P apical branches could be observed

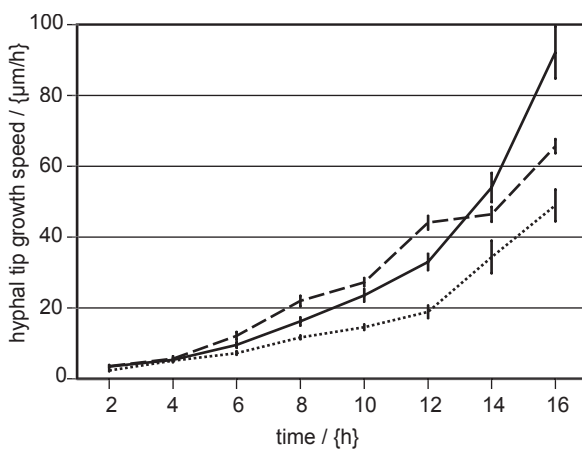
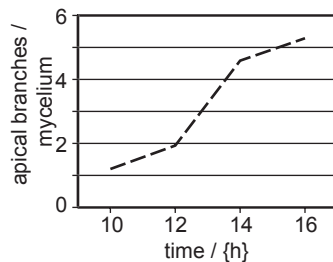


Figure 15
Hyphal tip growth speed of strains carrying different AgSPA2 alleles
 The x-axis represents the time in hours, the y-axis the hyphal tip growth speed in $\mu\text{m}/\text{h}$. wild-type(—); AgSPA2 Δ P(- -) and Agspa2 Δ C (· · ·). Error bar, SEM. n>20 for each point

Figure 16
Agspa2 Δ C displays premature apical branching
 The x-axis represents the time in hours, the y-axis the average number of lateral branches in the Agspa2 Δ C strain. n>20 for each point. Refer also to Figure 15



during the 16 h of growth followed, however both strains exhibit apical branches after 20 h of growth.

AgSpa2p is required for fast radial growth but limits the initial hyphal tip growth speed. Moreover

the two AgSPA2 mutants AgSPA2 Δ P and Agspa2 Δ C behave opposite. The initial hyphal tip growth speed for Agspa2 Δ C is increased compared to AgSPA2 Δ P but the radial growth speed is decreased. We conclude that the decreased radial growth speed observed for AgSPA2 Δ P and Agspa2 Δ C cannot be the result of a decreased hyphal tip growth speed potential, i.e. the capability of growth at the tip, alone in these mutants. It appears that other factors, which might be regulated by AgSpa2p, make an impact on the hyphal tip growth speed. We hypothesised that these might be morphogenetic events as branching or septation.

Branching and Septation Temporarily Slows Down Hyphal Tip Growth Speed

To investigate whether branching or septation are factors that make an impact on the hyphal tip growth speed the development of a single spore to a young mycelium was followed in a time-lapse acquisition.

Spores from the wild-type strain were allowed to germinate on time-lapse slides at room temperature (24°C). Pictures from a single spore were acquired over a time period of 15 h at a frequency of 0.5 min⁻¹ (see "Materials and Methods"). The hyphal tip growth speed of the first germ tube that emerged (the main tip) was determined every 10 min and plotted against time (Figure 17, supplemental movie 4 and Figure 18). The hyphal tip growth speed of the emerging tip was between 5 and 6 $\mu\text{m}/\text{h}$ during the first 1h 30'. Growth speed started to increase after 1h 30' and reached a maximum at 1 h 40'. Growth speed dropped to reach a minimum at 2 h 10'. This drop coincided with the initiation of the 2nd germ tube at 2 h 06'. Growth speed increased again and reached a top at 3 h 00'. It dropped, reached a minimum at 3 h 10' and increased again to reach the next maximum at 3 h 50'. The first septum formed at the neck between the germ bubble and the 1st germ tube at 3 h 18' coincided with the drop in hyphal tip growth speed at 3 h 10'. Growth speed dropped at 4 h 00', reached a minimum at 4 h 50' and increased again to reach a maximum at 5 h 00'. The first lateral branch was initiated at 4 h 20' coinciding with the drop in hyphal tip growth speed at 4 h 20' localising just after the first septum. Growth speed dropped, reached a minimum at 5 h 40', increased in speed again to reach the next maximum 6 h 00'. The second lateral branch was initiated at 5 h 20' coinciding with the drop in hyphal tip growth speed at 5 h 40' at the position that the main branch reached at 3 h 34'.

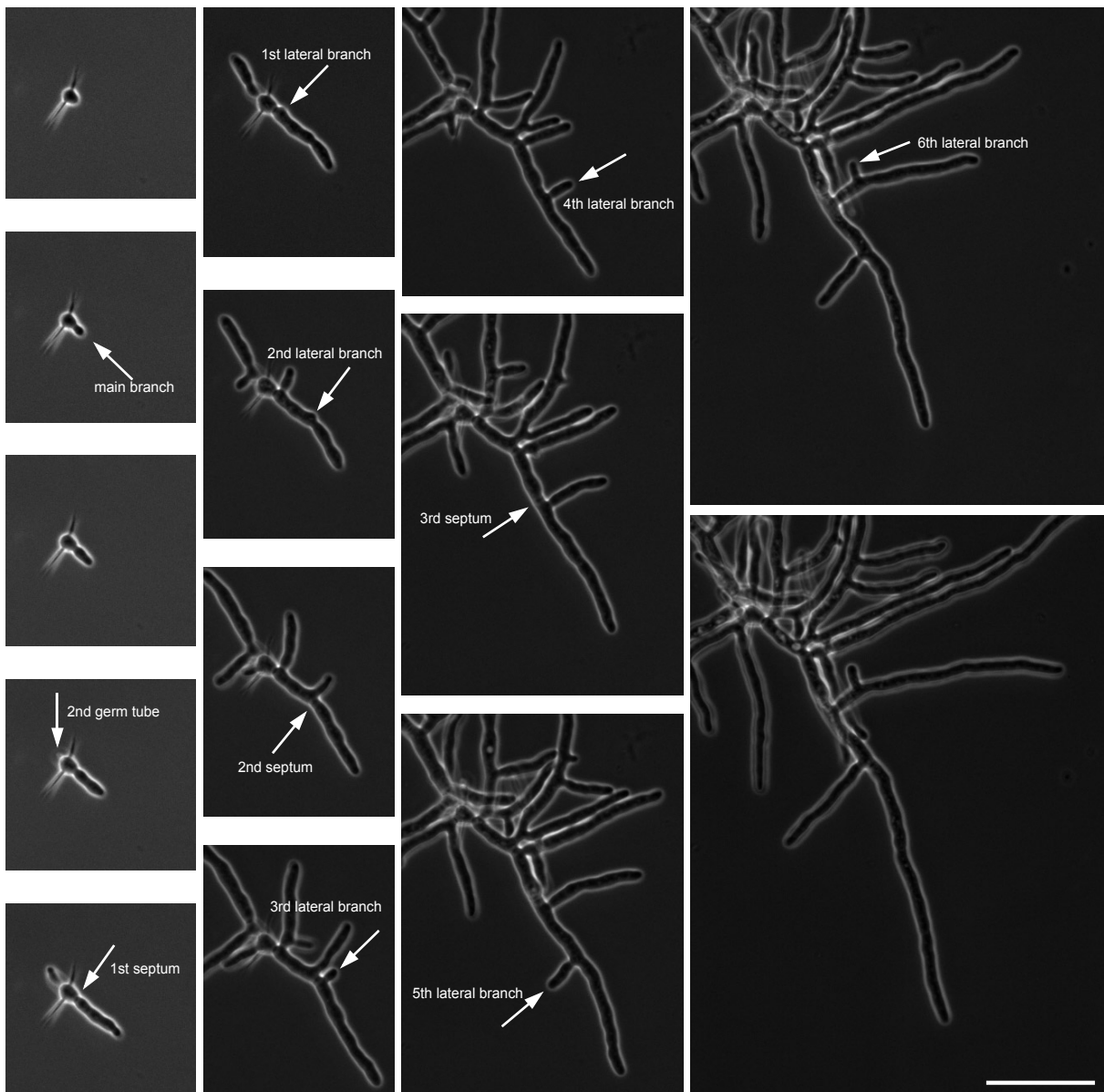


Figure 17
Medium resolution time-lapse acquisition of wild-type
 The time elapsed between two frames is 1 h with the first frame as time point 0 h. We followed the development of the first emerging germ tube (main tip). Sites of septation and lateral branch emergence are marked by arrows and labeled. We show the emergence of 6 lateral branches out of 9 observed and 3 septations out of 4 observed. Bar, 50 μm .

During the barely 15 h of growth we could follow the formation of 9 branches and 4 septa. These were all initiated in the apical compartment, i.e. not interrupted by a septum from the main tip. Each of these polarisation events caused the hyphal tip growth speed of the main tip to slow down. After each polarisation event the hyphal tip growth speed of the main tip increased to reach the next maximum. Initiations of branches or septa in compartments that were separated from the main tip by one or more septa did not have an effect on the hyphal tip growth speed of the main tip. The hyphal tip growth speed determined

after 14 h was 26 $\mu\text{m}/\text{h}$ which is about half of what was determined in the previous experiment which might be due to different culture temperatures. A decrease in hyphal tip growth speed could also be observed during apical branching (Figure 8 and 19). The hyphal tip growth speed was determined every 10 min and plotted versus time. The hyphal tip growth speed was in a range between 80 and 100 $\mu\text{m}/\text{h}$ within the first 16 min. The hyphal tip growth speed dropped and an apical branch was initiated after 22 min. The hyphal tip growth speed of the 2 new branches started to increase again and reached 80 $\mu\text{m}/\text{h}$ after 40 min.

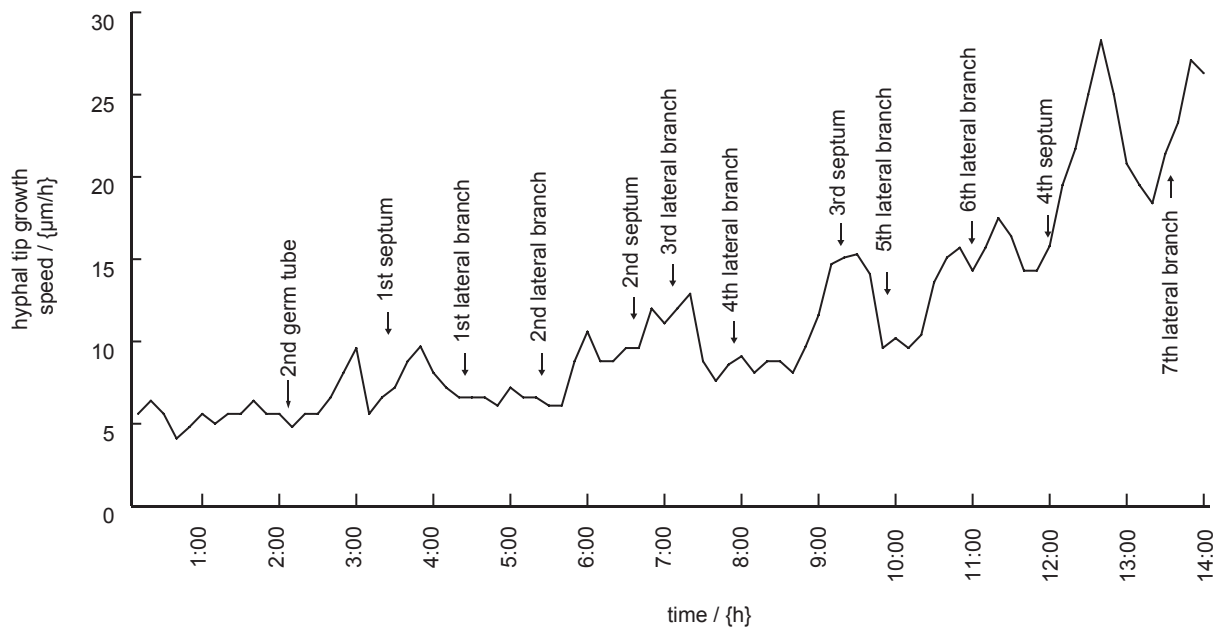


Figure 18

Hyphal tip growth speed of wild-type determined in a medium resolution time-lapse

The basis for this graph is the supplemental movie 4. Single frames are shown in Figure 17. The x-axis represents the elapsed time in min and the y-axis the hyphal tip growth speed in $\mu\text{m/h}$. Labelled arrows mark the initiation of septa and branches. Lateral branches appear 10-20 minutes after a hyphal tip growth speed decrease whereas septa seem to appear slightly later. The reason for this might be that the beginning of a septum formation cannot be seen in phase contrast microscopy. We marked the emergence of 7 lateral branches out of 9 observed and 4 septations out of 4 observed.

We conclude that branching and septation are factors that make an impact on the hyphal tip growth speed. Both these morphogenetic events transiently decrease the hyphal tip growth speed. Spatial analysis of lateral branching and septation revealed furthermore that the site selection of these events was not random. The initiation of a lateral branch or a septum caused the hyphal tip growth speed to decrease transiently (as shown above). The position that the main tip was exposed to during a hyphal tip growth speed decrease must have been marked. Exclusively these sites served as potential initiation points for new septa or lateral branches. For example, the position that the main tip reached during the emergence of the second septum served as initiation point for the fourth lateral branch and the third septum, respectively (Figure 17 & 36). The first potential site for septation or branching is established during initiation of the first germ tube as seen by a frequent septum formation at the neck between the germ bubble and the first germ tube in unipolar germlings.

Mutations in AgSPA2 have an Impact on the Branching Frequency

The initiation of branches or septa is one factor that has an impact on the hyphal tip growth

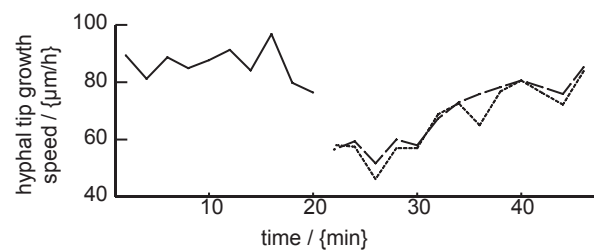


Figure 19

Hyphal tip growth speed of wild-type during apical branching

The basis for this graph is the supplemental movie 3. Single frames are shown in Figure 8. The x-axis represents the elapsed time in min and the y-axis the hyphal tip growth speed in $\mu\text{m/h}$. Apical branching occurs after 22 min. The solid line shows the hyphal tip growth speed prior to the apical branch, the dashed and dotted lines the hyphal tip growth speeds after the apical branch.

speed. As the AgSPA2 Δ P and Agspa2 Δ C mutations alter the hyphal tip growth speed we wanted to investigate whether the frequency of lateral branching is affected in these mutants. We therefore determined a branching index for the AgSPA2 Δ P and Agspa2 Δ C strains and compared it to wild-type.

The branching index is defined as the overall hyphal length of single mycelia divided by the number of tips it presents and represents the

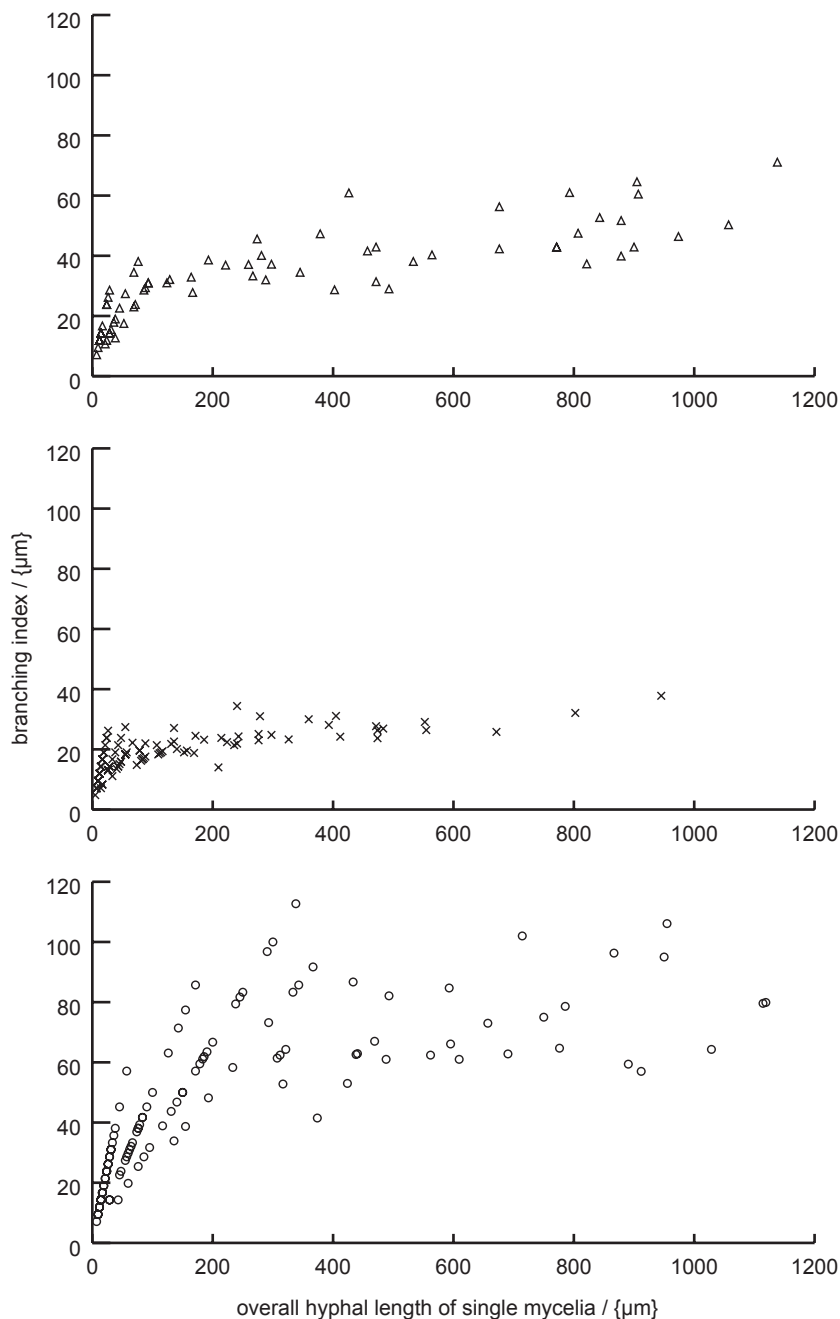


Figure 20
Branching index versus the overall hyphal length of single mycelia
 The x-axes represent the overall hyphal length of individual mycelia and the y-axes the branching indices determined in these mycelia. Top: wild-type (Δ); middle: AgSPA2 Δ P (x); bottom: Agspa2 Δ C (o). The average branching index was determined between 200 and 1200 μm overall hyphal length ($n > 25$). In the diagram for the Agspa2 Δ C strain it appears that the data points are distributed on lines. The reason for this is that the values on the x-axis are multiples of the values on the y-axis ($y = x/a$, whereas $a = \text{"tip number"}$). Thus the most vertical "line" represents the distribution of unipolar germlings, the next "line" bipolar germlings and so on. This pattern can also be observed for wild-type and AgSPA2 Δ P but less pronounced.

average distance between two lateral branches (acc. to Trinci, 1970). A decreased branching index represents an increased branching frequency and vice versa.

The branching index was determined for different developmental stages from germinating spores to young mycelia (Figure 12, 13 & 14) and plotted versus the overall hyphal length. The branching index behaved logarithmic with increasing hyphal length of single mycelia. It reached constancy after an overall hyphal length of single mycelia of about 200 μm . We determined an average branching index for all strains. For the wild-type strain this was 45 μm , for the AgSPA2 Δ P strain 27 μm and

for the Agspa2 Δ C strain 72 μm (Figure 20).

Evidence for an effect on branching frequency in AgSPA2 Δ P and Agspa2 Δ C could also be obtained from analysing the morphology of germlings. Spores of the three strains were cultured in AFM for 8 h at 30°C and the population of individual stages counted: germinated spores without polarisation (germ bubble), germinated spores with one tip (unipolar germling), with two tips (bipolar germling), with three, four, five or more than five tips (Figure 21). The distribution of germlings carrying the AgSPA2 Δ P mutation was shifted towards more tips compared to the wild-type whereas the distribution of germlings carrying

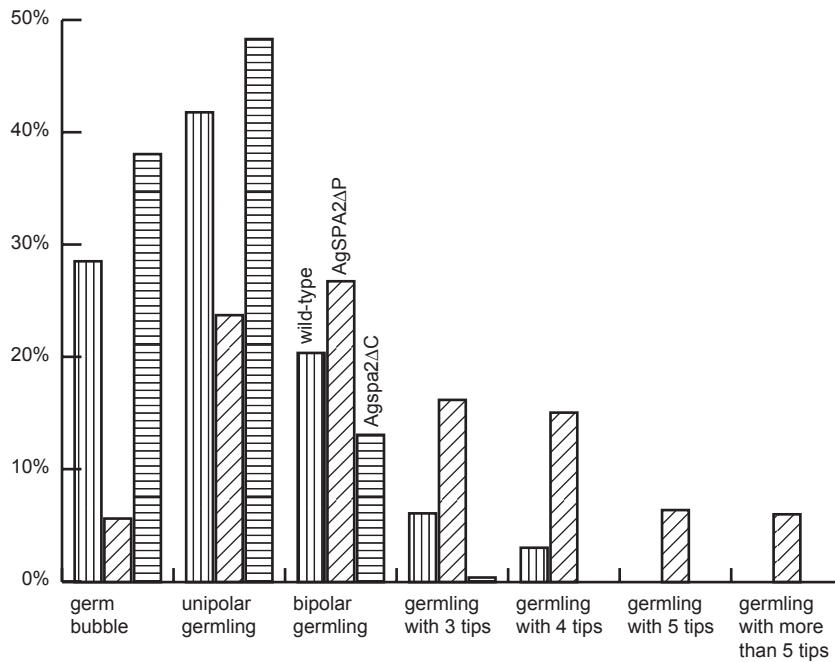


Figure 21
Altered germling distributions of strains carrying different AgSPA2 alleles
 The distribution of germlings is given in %, the respective germling morphology mentioned. Wild-type is represented with vertically hatched bars, AgSPA2ΔP with diagonally hatched bars and Agspa2ΔC with horizontally hatched bars; (n>100 for each strain).

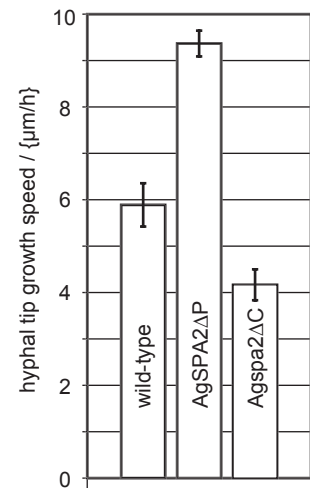


Figure 22
Hyphal tip growth speed potential of unipolar germlings carrying different AgSPA2 alleles
 The hyphal tip growth speed is given in μm/h (n=3). Error bar, SEM.

the Agspa2ΔC mutation was shifted towards less tips.

We conclude that mutations in AgSPA2 have an impact on the branching frequency. A deletion of the extended internal domain leads to an increased branching frequency whereas a complete deletion leads to a decreased branching frequency. Moreover the branching frequency is not constant during the development of a spore to a young mycelium. At early stages the branching frequency is increased and decreases during development to reach a constant frequency.

Mutations in AgSPA2 have an Impact on the Hyphal Tip Growth Speed Potential

Each branching event causes the hyphal tip growth speed to decrease. A mutant with an increased branching frequency should therefore grow slower than wild-type and a mutant with a decreased branching frequency faster than wild-type. This is indeed the case considering the initial growth phase of the AgSPA2ΔP and Agspa2ΔC strains. Considering the radial growth speed, however, wild-type grows fastest followed by AgSPA2ΔP and Agspa2ΔC strains. Therefore the altered branching frequency cannot be the sole

reason for the radial growth defect observed in these mutants. We hypothesised that the hyphal tip growth speed potential could also be affected in AgSPA2ΔP and Agspa2ΔC.

To compare the hyphal tip growth speed potential between wild-type, AgSPA2ΔP and Agspa2ΔC we determined the hyphal tip growth speed in unipolar germlings of these strains. Unipolar germlings display the only stage during *A. gossypii* development in which the hyphal tip growth speed is neither affected due to branch or septum initiation nor due to entering logarithmic growth phase. The hyphal tip growth speed is linear during that developmental process (Figure 18, 0 h 50' - 1 h 30').

Wild-type, AgSPA2ΔP and Agspa2ΔC spores were allowed to germinate on time-lapse slides. The individual development from germ bubbles to stages of unipolar germlings was followed in time-lapse acquisitions. The hyphal tip growth speed measured for wild-type was 5.9 μm/h, for AgSPA2ΔP 9.4 μm/h and for Agspa2ΔC 4.2 μm/h (Figure 22).

These results indicate that the hyphal tip growth speed potential is increased in AgSPA2ΔP and decreased in Agspa2ΔC compared to wild-type.

The Hyphal Diameter is Decreased in AgSPA2 Δ P and Increased in Agspa2 Δ C Compared to Wild-type

Mutations in AgSPA2 alter the hyphal tip growth speed potential. We wanted to investigate whether the hyphal diameter is also altered in the AgSPA2 Δ P and Agspa2 Δ C mutants implying that the increased hyphal tip growth speed potential could be the consequence of thinner hyphae.

The hyphal diameter is very heterogeneous, especially at early developmental stages. The hyphal diameter was therefore determined in hyphal stretches that had a constant diameter over at least 25 μ m. For wild-type we determined a diameter of 4.2 μ m, for AgSPA2 Δ P 3.7 μ m and for Agspa2 Δ C 5.8 μ m (Figure 12, 13, 14 & 23).

We also measured the expansion of the GFP signal at the tip in the AgSPA2-GFP and the AgSPA2 Δ P-GFP strain. For AgSpa2p-GFP we determined an expansion of 2.3 μ m and for AgSPA2 Δ Pp-GFP 1.9 μ m (Figure 24).

This suggests that mutations in AgSPA2 have an influence on the hyphal diameter. The hyphal diameter remains constant after the tip has determined it once (Figure 12, 13, 14 & 17). Thus changes in the hyphal diameter as seen in AgSPA2 Δ P and Agspa2 Δ C represent changes in the growth area at the tip. Therefore we conclude that AgSPA2 has an impact on the area of polarised growth at the tip. This is also supported by a decreased GFP expansion in the AgSPA2 Δ P-GFP strain compared to AgSPA2-GFP. We hypothesise that the increased hyphal tip growth speed potential is the consequence of a smaller area of growth at the tip.

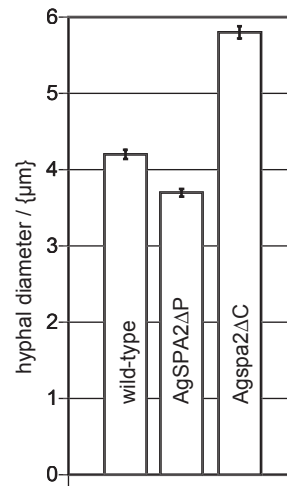


Figure 23
Hyphal tip diameter of strains carrying different AgSPA2 alleles
The hyphal tip diameter is given in μ m ($n > 20$). Error bar, SEM.

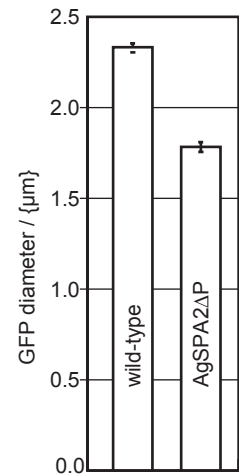


Figure 24
Expansion of the GFP signal at the tip in the AgSPA2-GFP strain and the AgSPA2 Δ P-GFP strain
The expansion is given in μ m ($n > 30$). Error bar, SEM.

Discussion

Spatial organisation of polarisation in *A.gossypii*. The localisation pattern of AgSpa2p is similar to polarised actin. AgSpa2p can be found permanently at the hyphal tip and transiently at the site of septum formation suggesting that AgSpa2p localises to sites of polarised growth, however AgSpa2p-GFP does not co-localise with actin. Thus the AgSPA2-GFP strain is also an excellent tool to study polarisation in mutant strains (see "Chapter 2" of this work and Bauer and Philippsen, 2002).

Permanent hyphal tip extension is a hallmark of filamentous growth. The permanent localisation of AgSpa2p to hyphal tips demonstrates that permanent hyphal tip extension is a consequence of permanently maintained polarised growth at hyphal tips. Neither septation nor branching disrupts the polarisation. Uniquely to filamentous growth is apical branching, which clearly differs from lateral branching. Apical branching represents the division of an existing polarisation whereas lateral branching is the initiation of a new polarisation. The spatial organisation of apical branching, however, is unclear.

In *S.cerevisiae* the polarised growth phase established for the formation of a new bud is transient. An isotropic growth phase with a subsequent polarisation of the mother/bud neck for septation ends the initial polarised growth phase. In *A.gossypii* polarisation at the tip is neither lost during septation nor during the initiation of a new lateral branch. However, growth speed is decreased during these processes. A decrease of the hyphal tip growth speed during lateral or apical branching has already been described in the filamentous ascomycetes *Aspergillus nidulans* (Trinci, 1970) and *Aspergillus oryzae* (Spohr et al., 1998, Christiansen, 1999 #7)

Yeast cells have a tightly regulated budding pattern, i.e. the emergence of a new bud is spatially determined. We could show in *A.gossypii* that branching or septation does neither occur at random sites. Site markers might be set at the tip in response to a lateral branching or septation event. We suggest that these markers persist at their initiation site to direct future branching or septation events.

Hyphal growth in *A.gossypii* can mostly be compared with the bipolar budding pattern in yeast diploids. Daughter cells bud uniquely distal to the mother/bud neck which leads to the formation of a filament like structure after several divisions on solid medium. Proximal or distal budding in mother cells resembles the formation of a lateral branches in *A.gossypii*.

AgSpa2p balances the branching frequency versus the hyphal tip growth speed potential.

We could identify two factors that have an effect on the hyphal tip growth speed. First the branching frequency and second the hyphal tip growth speed potential. In the AgSPA2 Δ P strain the branching frequency is increased whereas in the Agspa2 Δ C strain the branching frequency is decreased compared to wild-type. As branching slows down the hyphal tip growth speed (see above) we suggest that the observed alterations in the hyphal tip growth speeds during early stages of growth (2 - 12 h) are a direct consequence of the altered branching frequencies in the two mutants.

Whereas in the partial deletion strain the increased branching frequency has a negative effect on the hyphal tip growth speed the increased hyphal tip growth speed potential has a positive effect on the hyphal tip growth speed. In the complete deletion strain this is exactly opposite. Whereas the decreased branching frequency has a positive effect on the hyphal tip growth speed the decreased hyphal tip growth speed potential has a negative effect. Thus in these mutants an increase in the branching frequency is associated with an increase in the hyphal tip growth speed potential and vice versa. We suggest that alterations in the branching frequency and the hyphal tip growth speed potential in AgSPA2 Δ P and Agspa2 Δ C are the result of alterations in the same pathway and that AgSpa2p is involved in the regulation of this pathway.

The branching index behaves logarithmic during the development from a spore to a young mycelium. At early stages of growth the branching frequency is increased, decreases during early development and reaches a constant value. This pattern could be observed for wild-type, AgSPA2 Δ P and Agspa2 Δ C. We suggest therefore that the hyphal tip growth speed potential and the branching frequency have different impacts on the hyphal tip growth speed during the development from a spore to a mycelium. At early stages of development the branching frequency has a higher impact on the hyphal tip growth speed than at later stages. And conversely the hyphal tip growth speed potential has a higher impact on the hyphal tip growth speed at later stages of development since then the hyphal tip growth speed is less frequent subjected to a decrease induced by a branching event.

Taken together we suggest that AgSpa2p has an impact on two factors that determine hyphal tip growth speed: the branching frequency and the hyphal tip growth speed potential. These two

factors are out of balance in the AgSPA2 Δ P and Agspa2 Δ C strains resulting in a decreased radial growth speed in both mutant strains. Apparently AgSpa2p is required to balance these two factors for an efficient hyphal tip growth speed and the extended internal domain in AgSpa2p plays an important role in this process.

Molecular implication of AgSpa2p. At a molecular level the cause of the phenotypes in the AgSPA2 Δ P and Agspa2 Δ C mutations is elusive. We hypothesise that the primary defects of the mutations occur at the same molecular level where AgSpa2p functions, however the consequences of the mutations are opposing.

One hypothesis is that the observed phenotypes for AgSPA2 Δ P and Agspa2 Δ C depend solely on the expression level of the AgSpa2p. Thus not the truncation of AgSpa2 Δ Pp but its altered expression level would induce the observed phenotype. In *S.cerevisiae* it was shown that a deletion of the region coding for the C-terminal 933 aa (which includes the internal domain and the SHD V domain and therefore expands the deleted region we set in AgSPA2 Δ P) does not change the expression level (Sheu et al., 1998). We could show that AgSpa2 Δ Pp is expressed. From GFP intensity quantification experiments in the AgSPA2-GFP and the AgSPA2 Δ P-GFP strain we do not expect a major difference between the two protein levels. Thus we do not think that the branching frequency and the hyphal tip growth speed potential is a consequence of the expression level of AgSpa2p.

Another explanation could be found in the spatial organisation of AgSpa2p binding proteins. In *S.cerevisiae* it was shown that ScSte7p, a member of the Ste20 MAPK cascade, binds to SHD I (Sheu et al., 1998), SHD II is important for localisation and binds to ScPea2p (Arkowitz and Lowe, 1997; Sheu et al., 1998) and SHD V binds to ScBni1p (Fujiwara et al., 1998). For all these interaction partners orthologues were also identified in *A.gossypii*. We hypothesise that a shortened internal domain between SHD II and SHD V, as in AgSpa2 Δ Pp, might affect the spatial interaction of AgBni1p with AgPea2p, AgSte7p, ScBud6p or an up to now unidentified interaction partner. Thus this internal domain could act as a spacer. In the Agspa2 Δ C strain such an interaction would be exacerbated.

We think that AgSpa2p has an influence of the area of growth at the tip and that the extended internal domain is involved in the determination of this area. This would also be in agreement with the finding that ScSPA2 deletion strains in *S.cerevisiae* fail to properly localise the secretion

marker ScSec4p (Sheu et al., 2000). In addition it is thought that ScSpa2p localises ScBni1 and that ScBni1p directs actin filament assembly to sites of growth (Evangelista et al., 2002; Sagot et al., 2002). Thus the area of growth could be more compact and stable in the AgSPA2 Δ P strain leading to a smaller area of growth and a facilitated induction of a new lateral branch. In the Agspa2 Δ C strain the area of growth could be less compact and stable leading to a larger area of growth and a less efficient induction of a new lateral branch.

The deletion of AgSTE7 in *A.gossypii* does not have an effect on growth under standard growth conditions. However, under nitrogen limitation the branching frequency is increased in wild-type but not in the Agste7 Δ strain (Mohr, 1997; AgSTE7 was originally named APK1). ScSpa2 was shown to interact with ScSte7p (Sheu et al., 1998). Moreover ScSpa2 was required for processes as mating and pseudohyphae formation, which both depend on a functional ScSte7p (Mosch et al., 1996; Errede et al., 1993). This suggests that AgSte7p might regulate AgSpa2p under nitrogen limitation. The higher branching frequency, likely associated with a thinner hyphal diameter, might facilitate invasive growth seen in *A.gossypii* during nitrogen limitation. Similarly ScSte7p in *S.cerevisiae* might regulate the diameter of the bud tip via ScSpa2p under nitrogen limitation or projection formation.

It might also be possible that the internal domain between SHD II and SHD V serves as an interaction domain rather than a spacer. Although homology is missing in that region both internal domains bear a repetitive region and the repeats in both internal domains bear a Ser-Pro unit.

Perspectives

In future work we would like to investigate a potential regulation of AgSpa2p by AgSte7p and the role of the extended internal domain of AgSpa2p in such a regulation. We hypothesise that AgSte7 regulates AgSpa2p under nitrogen limitation to induce a higher branching frequency and a decreased hyphal diameter, which might facilitate invasive growth observed under these environmental conditions.

First we want to confirm the increased branching frequency in *A.gossypii* upon nitrogen limitation and the dependence on AgSte7p as it was shown previously (Mohr, 1997). It would be of interest to see whether the increased branching frequency upon nitrogen limitation is also associated with a decreased hyphal diameter and an increased hyphal tip growth speed potential, respectively, as this was observed for AgSPA2ΔP. Further we would like to determine the branching index under nitrogen limitation in the AgSPA2ΔP and the Agspa2ΔC strain in the presence and absence of AgSte7p. This should reveal a potential regulation of AgSpa2p by AgSte7p. In addition we might test an interaction between AgSpa2p and AgSte7p by two-hybrid as it has been shown in *S.cerevisiae* (Sheu et al., 1998) and try to construct an AgSPA2 allele whose product is deficient for AgSte7p interaction but does not affect the branching frequency under full medium conditions. The branching frequency of this AgSte7p - AgSpa2p interaction deficient strain should also be tested under nitrogen limitation in the presence and absence of AgSte7p to further test the hypothesis of a regulation of AgSpa2p by AgSte7p.

Second we would like to express AgSpa2p and AgSpa2ΔPp in *S.cerevisiae* Scspa2Δ strains to see to what extents these proteins can complement ScSpa2p. Complementation could be evaluated by analysing the diameter of the cells. Further we would also like to analyse the morphological effect of nitrogen limitation and pheromone induction in the heterologously complemented *S.cerevisiae* strains. This should also be done in the presence and absence of ScSte7p. Additionally the converse experiment in which ScSpa2p is should also be expressed in *A.gossypii* Agspa2Δ strains and compared with *A.gossypii* wild-type and AgSPA2ΔP strains may also be informative. These complementation experiments have the potential to shed light on the importance of the extended internal domain in AgSpa2p.

Third we would like to investigate the function of the AgSpa2 internal domain. As the repeated Ser-Pro residues are conserved in the internal

domains of AgSpa2p and ScSpa2p, respectively, we would like to generate a motif and screen protein databases for similar domains.

We hypothesise that a deletion of the extended internal domain in AgSpa2ΔPp mimics the regulation of AgSpa2p via AgSte7p under nitrogen limiting conditions. Thus we would like to see whether AgSte7p could induce a conformational change in AgSpa2p. An in vivo approach would be to express an AgSpa2p protein that is N-terminally fused to CFP and C-terminally fused to YFP. A conformational change, which could have an impact on the C- and N-terminal interdependence, might be visualised by FRET.

AgBoip is Required for Establishment and Maintenance of Polarised Growth in *A.gossypii*

Introduction

We identified a mutant in our *A.gossypii* knock out collection that frequently displayed spherically enlarged hyphal tips. The gene deleted in that strain was identified as an orthologue of the duplicated genes in *S.cerevisiae*, ScBoi1p and ScBoi2p.

ScBoi1p and ScBoi2p were implicated in cell polarity in *S.cerevisiae*. Both proteins were identified in two-hybrid screens as interactors of the scaffold protein ScBem1p. The deletion of ScBoi1p and ScBoi2p, but not one alone, caused a temperature sensitive phenotype. At elevated temperature Scboi1 Δ boi2 Δ cells arrested as large, round and unbudded cells with delocalised cortical actin and a fair fraction of the cells appeared to be lysed at a budded stage. At 20°C the cells grew only somewhat slower than wild-type although 30 % of the cells were dead. Expressing the C-terminal part of ScBoi1p or ScBoi2p alone that contained a PH-domain could complement the double knock-out. Overexpression of either ScBoi1p or ScBoi2p resulted in unbudded cells with delocalised cortical actin as seen for the double knock-out. This could be counteracted by co-overexpression of ScCdc42p (Akada et al., 1997; Bender et al., 1996; Matsui et al., 1996; see also Figure 2). These data suggest that Scboi1p and ScBoi2p are involved in establishment and/or maintenance of polarised growth.

A homologue of ScBoi1p and ScBoi2p was also identified in *S.pombe* termed Pob1p. Deletion of SpPOB1 lead to a quick cessation of cellular elongation and cells started to swell. SpPob1p was also shown to be essential for cell separation. It localised at cell tips during interphase and at the division plane during cytokinesis (Toya et al., 1999).

In *S.cerevisiae*, the Rho-type GTPase ScRho3p could serve as a multicopy suppressor of the Scboi1 Δ boi2 Δ defect (Bender et al., 1996; Matsui et al., 1996). ScRho3p was implicated in distinct functions of cell polarity as the organisation of the actin cytoskeleton (Kagami et al., 1997; Matsui and Toh, 1992), transport of exocytotic vesicles from the mother cell to the bud and docking and fusion of vesicles (Adamo et al., 1999; Robinson et al., 1999). A homologue of ScRho3p in the filamentous fungus *Trichoderma reesei* could suppress secretion defects in *S.cerevisiae* when overexpressed and the deletion of TrRHO3 in

T.reesei caused a secretion defect (Vasara et al., 2001a; Vasara et al., 2001b). The deletion of AgRho3p, the orthologue of ScRho3p, in *A.gossypii* caused periodic swelling of hyphal tips (Wendland and Philippsen, 2001) similarly as observed for Agboi Δ strains. These data indicate that the Boip's might link the actin cytoskeleton to secretion.

Despite these data the function of the Boip's is still elusive. We wanted to investigate the role of AgBoip during filamentous growth in *A.gossypii*. We show that AgBoip in *A.gossypii* is required for the establishment of germ tubes and lateral branches and for the maintenance of permanent hyphal tip extension.

Results

AgBOI is Conserved Among Ascomycetes

We isolated a clone containing the coding region of the AgBoip flanked by promoter and terminator sequences (see "Materials and Methods"). The complete AgBOI sequence encoded a protein of 984 aa in length. The orthologous proteins in *S.cerevisiae*, ScBoi1p and ScBoi2p are 980 aa and 1040 aa in length, respectively (Bender et al., 1996; Matsui et al., 1996), SpPob1 in *S.pombe* 871 aa (Toya et al., 1999) and CaBoi2p in *C.albicans* 1172 aa (Brown et al., 2001). AgBoip is closest related to ScBoi1p and ScBoi2p, followed by CaBoi2p and SpPob1p. ClustalW (Thompson et al., 1994) was used for a multiple alignment of the five proteins. Four regions with significant homology throughout all five proteins were identified. For each of these four regions one specific profile could be defined in all five proteins (Pagni et al., 2001). These were an SH3 domain (Mayer, 2001), a SAM domain (Stapleton et al., 1999), a proline rich region (Mayer, 2001) and a PH domain (Rebecchi and Scarlata, 1998). The proline rich regions were weak hits in all proteins (Figure 25A & 25B).

AgBoiΔ Displays a Temperature Sensitive Phenotype

The AgboiΔ strain identified from our knock out collection carried only a partial deletion of the AgBOI ORF. To characterise the function of

AgBoip we deleted the complete AgBOI ORF via PCR based gene targeting with the GEN3 marker (Wendland et al., 2000; Wach et al., 1994; Baudin et al., 1993) in the Agleu2Δthr4Δ background strain (referred to as wild-type; see "Materials and Methods"). When we isolated single spores from the primary heterokaryotic transformants we observed that spores carrying the AgBOI deletion were unable form mycelia at 30°C. The spores had to be incubated at 20°C to obtain mycelia. We therefore wanted to investigate the temperature sensitivity of AgboiΔ spores.

Spores from the wild-type and the AgboiΔ strain were spread on AFM plates and incubated at 20°C, 30°C and 37°C. After an incubation time of 5 d at 20°C and 3 d at 30°C or 37°C, respectively, the rate of mycelium formation was determined on the individual plates. Whereas the temperature did not have an effect on the mycelium formation rate in wild-type mycelium formation was nearly abolished in the AgboiΔ strain at 30°C and 37°C (Figure 26A & 26B).

To estimate whether the formation of mycelia from spores at 20°C occurred at a similar rate in wild-type and in AgboiΔ we isolated single wild-type and AgboiΔ spores and incubated them at 20°C. 14 out of 20 isolated AgboiΔ spores formed a mycelium after 5 d at 20°C and 13 out of 20 wild-type spores. The same experiment at 37°C gave no colonies for AgboiΔ and 13 colonies for wild-type (Figure 26C).

It is possible that AgBoip is simply required for

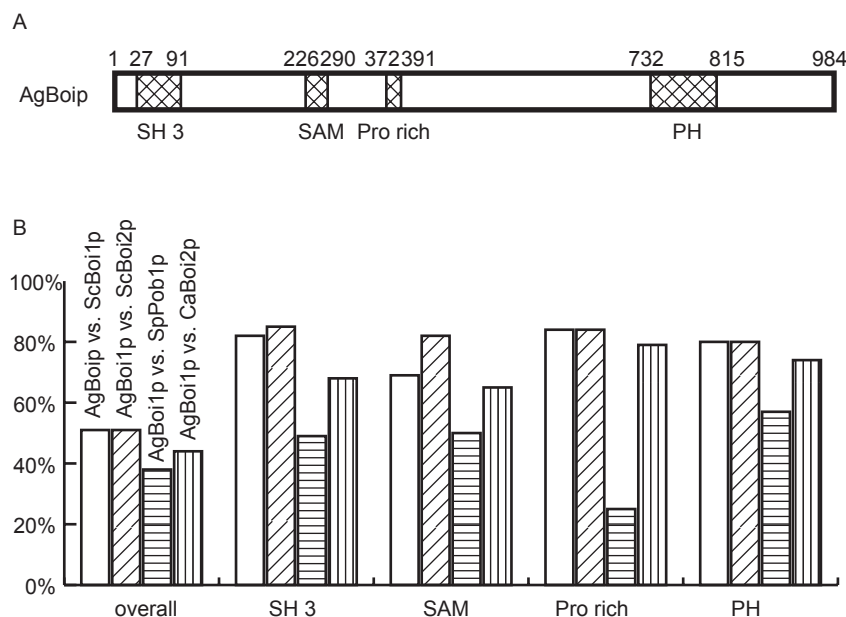


Figure 25
AgBoip structure and homology to ScBoi1p, ScBoi2p, SpPob1p and CaBoi2p

A) Domains identified in AgBoip are indicated as boxes. The SH3 domain is located from 27 - 91 aa, the SAM domain from 226 - 290 aa, the proline rich region from 372 - 391 aa and the PH domain from 732 - 815 aa.

B) The bars show homology in % similarity, the different hatchings represent the individual comparisons. The first group is a comparison of the full length proteins, the second the SH3 domain, the third the SAM domain, the fourth the Pro-rich region and the fifth the PH-domain.

proper germination and growth of young mycelium but not during radial growth in mature mycelium. To investigate the role of AgBoip during later stages of mycelium growth we incubated Agboi Δ mycelium, which was pre-grown at 20°C, 30°C and 37°C and compared the radial diameter to wild-type after an incubation time of 6 d. At all temperatures the radial diameters of the Agboi Δ mycelia were decreased compared to wild-type

1 d and 2 d, respectively, and then incubated for 2 d. The shorter incubation period of just 1 d at 37°C gave a denser population of mycelia at 20°C (Figure 27B). We therefore suggest that elevated temperatures are lethal for Agboi Δ spores and that lethality is restricted to early phases of development, probably germination of spores. We wanted to clarify at which morphological stage growth was arrested at elevated temperatures.

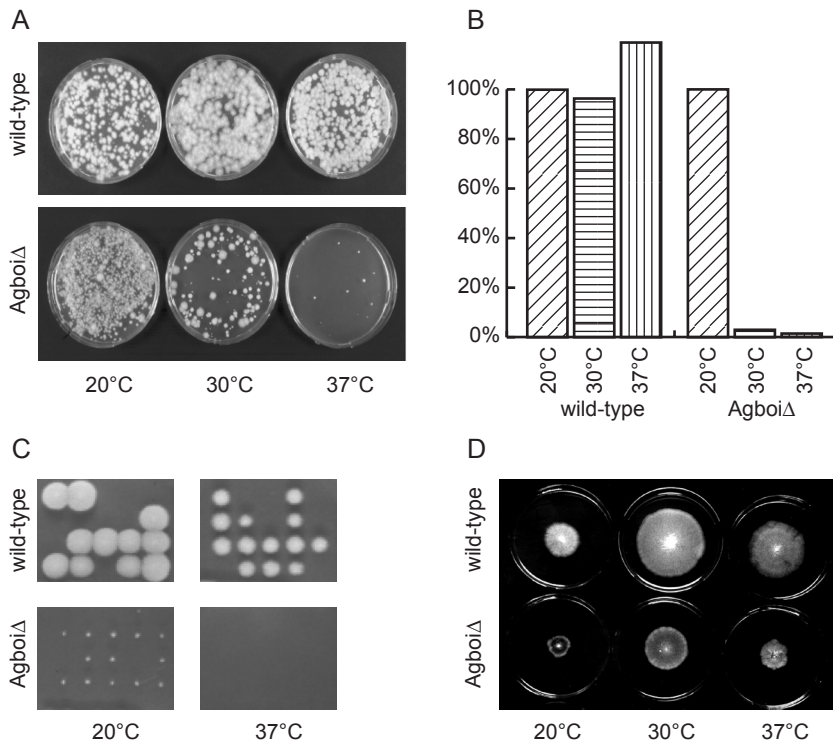


Figure 26
Temperature sensitivity observed in Agboi Δ
(A) wild-type and Agboi Δ spores spread on AFM plates and incubated at the indicated temperature. (B) Mycelium formation rate at different temperatures in %. The same hatching represents the same temperature. The reference mycelium formation rate was taken at 20°C for both of the strains. The value for the wild-type strain at 37°C might indicate a slight increase of the germination rate at elevated temperature. (C) 20 separated spores from wild-type and Agboi Δ incubated at the indicated temperatures. (D) Radial diameter after incubation of 6 d at the indicated temperatures.

(Figure 26D).

Thus the deletion of AgBOI prevented the formation of mycelia from spores only at elevated temperatures and AgBoip is required for efficient radial growth at all temperatures compared to wild-type.

AgBoip is Required for Germination at Elevated Temperatures

To investigate whether early developmental stages were more susceptible to elevated temperatures we made temperature shift experiments. Agboi Δ spores were spread onto AFM plates and incubated at 20°C for 1 d and 3 d, respectively and then shifted to 37°C and incubated for 2 d. The longer initial incubation period of 2 d at 20°C gave a significant denser population of mycelia at 37°C (Figure 27A). Spores were also incubated on AFM plates at 37°C and shifted to 20°C after

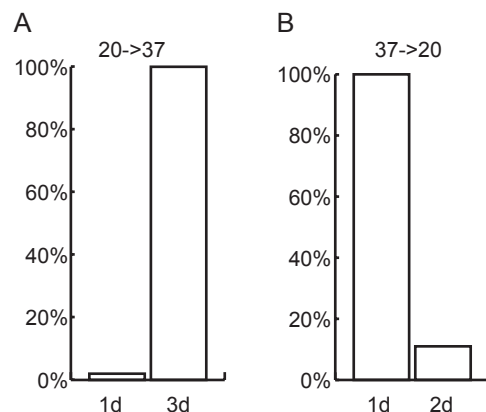


Figure 27
Temperature shift experiments of Agboi Δ
(A) Mycelium formation rate in % after a temperature shift from 20°C to 37°C after 1 d and 3 d, respectively. The reference mycelium formation rate was taken at 3 d. (B) Mycelium formation rate in % after a temperature shift from 37°C to 20°C after 1 d and 2 d, respectively. The reference mycelium formation rate was taken at 1 d.

Therefore we inoculated *Agboi* Δ spores on microscopy slides with an AFM agar layer at 37°C for 24 h (see "Materials and Methods"). 71% of the spores had started to germinate and had formed a first germ tube but then lysed. 15% of the spores did not reach that stage and had lysed as germ bubbles. A minority had lysed at the stage of two germ tubes or at later stages (Figure 28). Lysed unipolar and bipolar germlings mostly had enlarged tips where lysis might have originated. We also followed single *Agboi* Δ spores at 37°C from the first steps in germination to their lysis in a time-lapse acquisition. Spores were incubated on

microscopy slides (see "Materials and Methods") and pictures were acquired from individual spores at a frequency of 0.5 h⁻¹ (Figure 29). Germinating spores had either lysed at the stage of a germ bubble or as unipolar germlings with an enlarged tip. We could not find evidence that the polarised growth phase between germ tube emergence and lysis of the unipolar germlings was affected. Thus *AgBoip* is required for germination at elevated temperatures, eventually prior to the emergence of the first and the second germ tube.

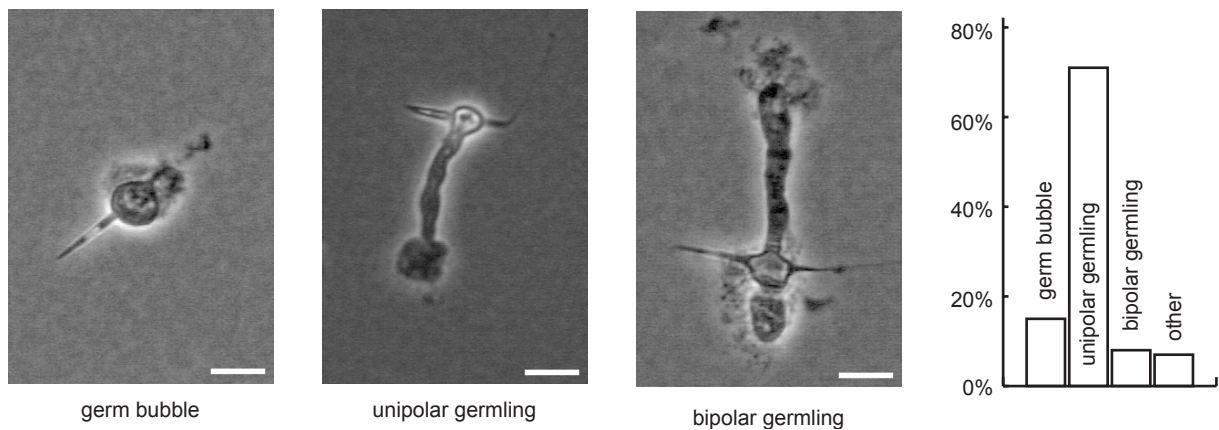


Figure 28
Fate and developmental stage of *Agboi* Δ at elevated temperatures
 The needle shaped spore from which growth originated is still visible in all pictures. Dark clouds might be cytoplasm that leaked from the germlings. The graph shows the populations of the different stages of lysis. Bar, 10 μ m.

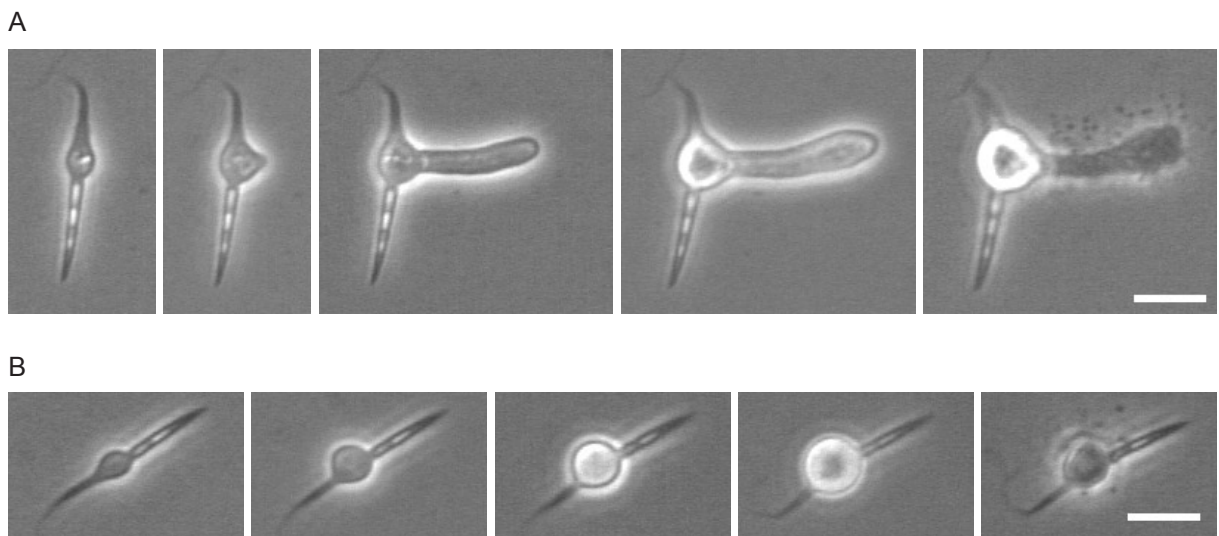


Figure 29
Time-lapse acquisition of *Agboi* Δ at 37°C
 (A) Development from a single spore to a unipolar germling with subsequent lysis. (B) Germination of a single spore with subsequent lysis. The time elapsed between two frames is 2 h. Bar, 10 μ m.

Branching Frequency is Reduced in Agboi Δ

Deletion of AgBOI caused lysis of germinated spores at elevated temperature. At 20°C spores formed mycelia at a similar rate as observed in wild-type, however, the radial diameter reached after 6 d incubation at 20°C was decreased compared to wild-type. We therefore wanted to investigate the growth pattern of Agboi Δ at 20°C. Spores were spread on microscopy slides covered with an AFM agar layer and incubated at 20°C (see "Materials and Methods"). Germinated spores were followed in a time-lapse acquisition over a time period of 16 h at a picture frequency of 0.25 h⁻¹ (Figure 30). The hyphal length of single mycelia was determined and plotted versus the number of tips.

At the same hyphal length the Agboi Δ strain displayed less lateral branches compared to wild-type. We also determined the average hyphal

length of unipolar germlings prior to the formation of the second germ tube and bipolar germlings prior to the formation of a first lateral branch in the wild-type and Agboi Δ strain. In wild-type the average hyphal length of unipolar germlings was 12.0 μm and in Agboi Δ 36.4 μm . Bipolar germlings had an average hyphal length of 49.9 μm in wild-type and 126.5 μm in Agboi Δ (Figure 31). We therefore suggest that the branching frequency is decreased in the Agboi Δ strain compared to wild-type.

A more precise determination of a branching index as presented in "Chapter 1" of this work requires overall hyphal lengths of single mycelia that exceed 200 μm . As Agboi Δ had to be incubated at 20°C the incubation time would have exceeded 24 h to reach 200 μm hyphal lengths of single mycelia. However, we only achieved an incubation time of 20 h.

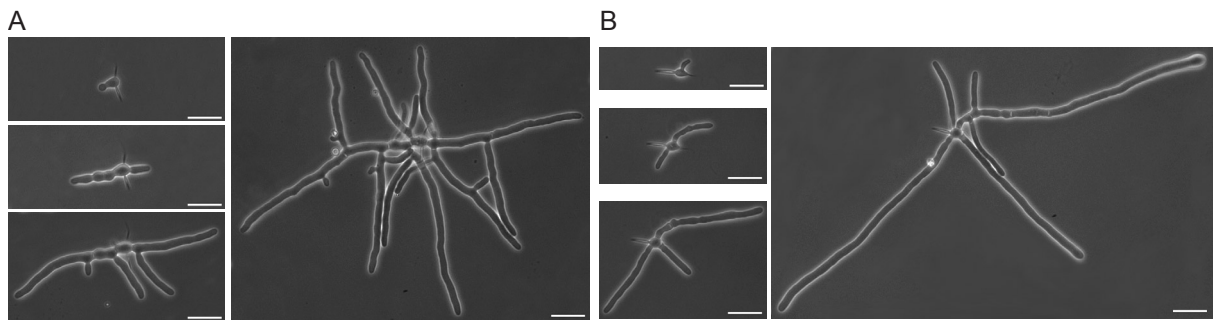


Figure 30
Time-lapse acquisition of wild-type and Agboi Δ at 20°C
(A) Development of a single wild-type spore to a small mycelium. (B) Development of a single Agboi Δ spore to a small mycelium. Arrow indicates enlarged tip (see text). The time elapsed between two frames is 4 h. Bar, 20 μm .

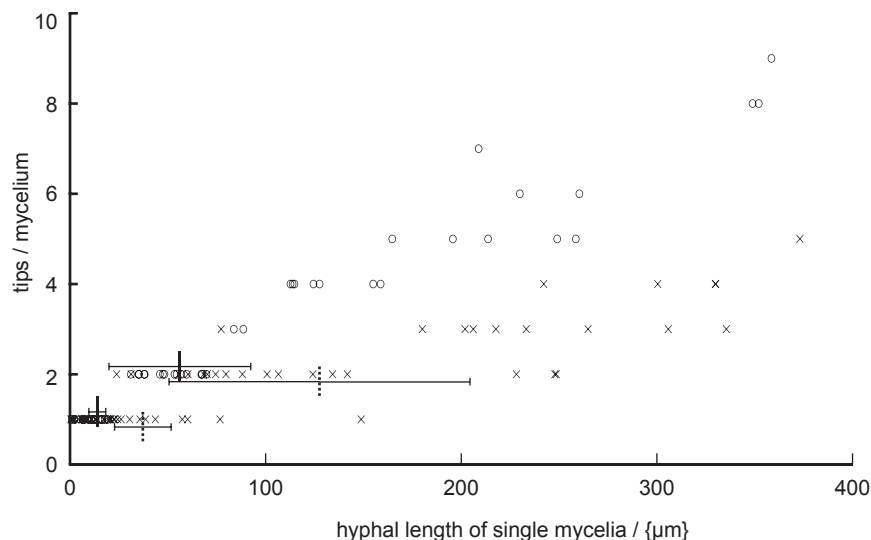


Figure 31
Branching frequency in wild-type and Agboi Δ during initial growth
The hyphal length of single mycelia was plotted versus the number of tips. Values for wild-type are plotted as circles (o), values for Agboi Δ as crosses (x). The vertical lines indicate the average length of unipolar and bipolar germlings, respectively. The straight line represents wild-type, the dotted line Agboi Δ . Error bar, SD; n>13.

AgBOI is Required to Maintain Permanent Polarised Growth at the Tip

Agboi Δ spores grown at 37°C lysed preferentially as unipolar germlings. It appeared as if lysis had occurred mostly at the tip in these unipolar germlings. When the Agboi Δ strain was grown at 20°C, we could also observe frequent enlargement of hyphal tips (Figure 30). We wanted to investigate

whether the deletion of AgBOI causes defects in the polarisation of tips and whether this defect was more pronounced at elevated temperatures.

Agboi Δ was cultured at 20°C for 34 h and then shifted to 37°C and cultured for 2 h. When cultured at 20°C without a temperature shift morphological changes at tips could already be observed. 11 % of all hyphal tips were spherically enlarged. The temperature shift to 37°C made this defect more pronounced with 26 % of all tips then enlarged.

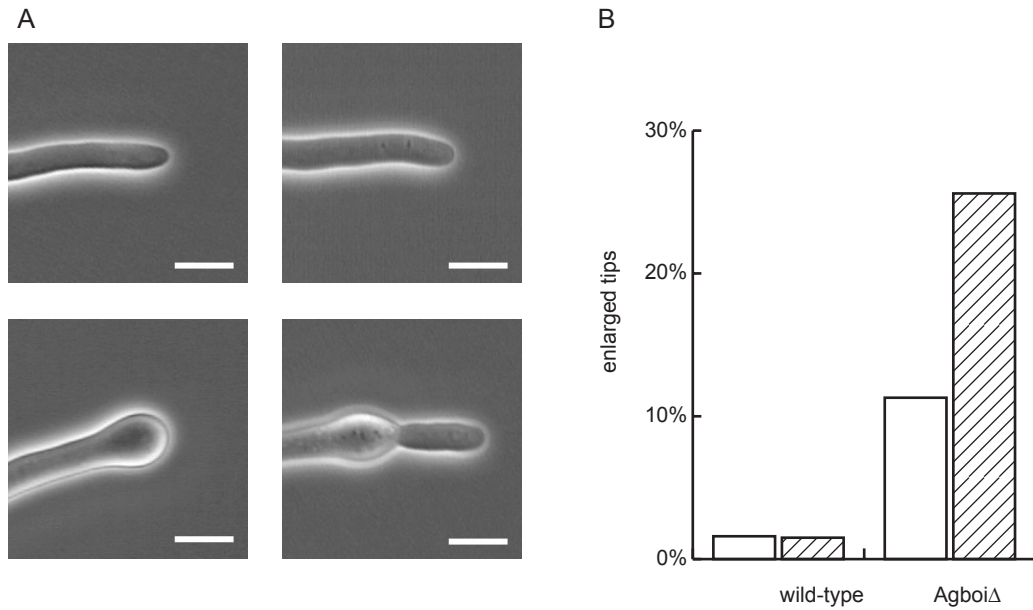


Figure 32
Spherical enlargement of hyphal tips in Agboi Δ
(A) Top left: wild-type tip. Top right: Agboi Δ tip not enlarged. Bottom left: Agboi Δ tip spherically enlarged. Bottom right: Agboi Δ tip that regained polarised growth after a spherical enlargement. Bar, 10 μ m. (B) Hyphae with enlarged tips in %. Clear bars represent fraction at 20°C, hatched bars after the temperature shift to 37°C.

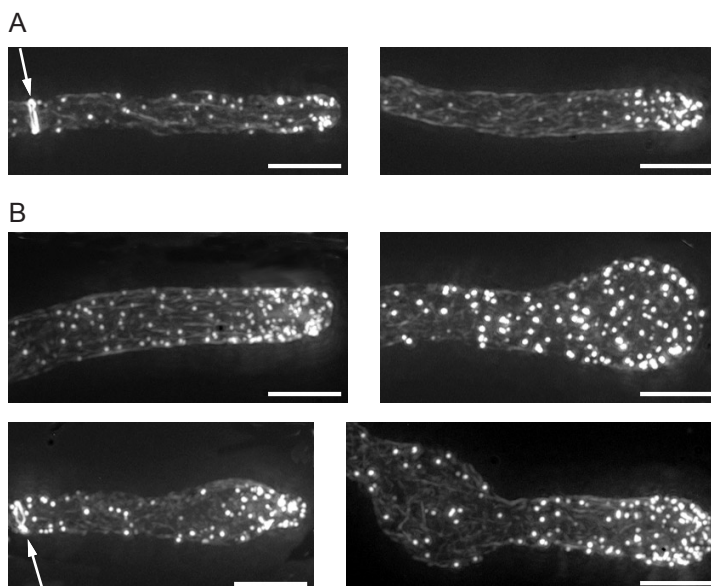


Figure 33
Localisation of actin in wild-type and Agboi Δ
(A) Both pictures show the distribution of actin in wild-type. Patches are localised to the tip and cables emanate from the tip. An actin ring is present at the cell cortex in the left picture (marked with an arrow; refer also to Figure 1B). (B) Staining of Agboi Δ . Top left: polar growing hypha with polarised actin patches at the tip and cables emanating from the tip. Top right: Spherically enlarged hyphal tip with depolarised actin patches and a disturbed actin cable network. Bottom left: Repolarisation of a spherically enlarged tip. Actin patches localise towards the newly initiated tip and cables emanate again from the tip. An actin ring localises at the cell cortex (marked with an arrow). Bottom right: Continued growth after a depolarisation. Bar, 10 μ m

The spherical enlargement was not a terminal phenotype. At 20°C or 37°C enlarged tips could repolarise and regain polarised tip growth. In wild-type not more than 2 % of all tips were enlarged even after a temperature shift (Figure 32). Lysed tips had also been observed in mycelia cultured at 20°C, 30°C and 37°C.

These enlarged tips prompted us to investigate the actin cytoskeleton of hyphal tips in the *Agboi*Δ strain. *Agboi*Δ spores were cultured for 48 h in AFM at 20°C and stained with Alexa-Phalloidin (see "Materials and Methods"). In growing *Agboi*Δ hypha actin patches were polarised localising towards the tips. Actin cables seemed to emanate from the tips as observed in wild-type. In spherically enlarged tips the actin patches were delocalised and the actin cable network seemed to be disorganised but still present. When a spherically enlarged tip repolarised actin patches localised again to the tip (Figure 33).

We suggest that the spherical enlargement of hyphal tips is the consequence of a failure to maintain polarised growth at the tip. The delocalisation of actin patches and actin cables in the enlarged tips indicates also that the polarised growth might have turned to an isotropic growth.

The Polarity Marker *AgSpa2p* Delocalises From the Tip During Spherical Enlargement in *Agboi*Δ Strains

AgSpa2p is a marker of polarised growth in *A.gossypii* that localises permanently to hyphal tips and transiently to sites of septation (see "Chapter 1"). We wanted to use *AgSpa2p*-GFP as a marker to visualise the polarisation at the tip in the *Agboi*Δ strain. We deleted the complete *AgBOI* ORF by PCR based gene targeting (Wendland et al., 2000; Wach et al., 1994; Baudin et al., 1993) in the *AgSPA2*-GFP background strain using *NAT1* as resistance marker (Goldstein and McCusker, 1999, see "Materials and Methods"). The GFP fusion to *AgSpa2p* did not affect the behaviour of the *Agboi*Δ strain. We followed the *Agboi*Δ*SPA2*-GFP strain in a time-lapse acquisition (see "Materials and Methods"). Pictures were acquired over a time period of 144 min at a picture frequency of 0.25 min⁻¹. During polarised growth of *Agboi*Δ*SPA2*-GFP *AgSpa2p*-GFP localised permanently to the tip. Prior to tip enlargement *AgSpa2p*-GFP delocalised from the tip. Repolarisation of the spherically enlarged tip was in parallel with a relocalisation of *AgSpa2p*-GFP (Figure 34 and supplemental movie 5).

Thus the deletion of *AgBOI* causes not only the loss of polarised actin but also polarity markers as

AgSpa2p.

Localisation of *AgBoip*

In order to determine the localisation pattern of the *AgBoip* we constructed a C-terminal GFP fusion to the endogenous copy of the *AgBOI* ORF (see "Chapter 3"). The growth morphology in the *AgBOI*-GFP strain did not differ from what was observed in wild-type suggesting that the GFP fusion did not disturb the function of the protein. *AgBoip*-GFP could be localised at tips during all stages of development. 71 % of all unipolar germlings displayed specific *AgBoip*-GFP fluorescence at the tip, 80 % of the tips in bipolar germlings, 98 % in small mycelia with 3 - 5 tips and more than 99 % of the tips in mature mycelia. Specific fluorescence could also be found within hyphae either as a "double disc" or a "single ring" structure. The "double disc" structure seems to consist of two separate discs that cover the intersection of the hyphal tube to generate a small interspace. The "single ring" structure consists of one cohesive ring-like structure that localises solely to the hyphal cortex (Figure 35).

AgBoip localises to hyphal tips as actin patches, as a "double disc" structure within hyphae as actin patches during septation and as a "single ring" similarly to the actin ring (Figure 1B). It is likely that the *AgBoip* localisation pattern coincides with what was observed for actin patches, however *AgBoip* does not co-localise with actin patches.

A Rhodamine-Phalloidine/GFP double staining as presented in "Chapter 1" of this work could not be achieved as the *AgBoip*-GFP signal was too weak and could not be observed any more upon fixation.

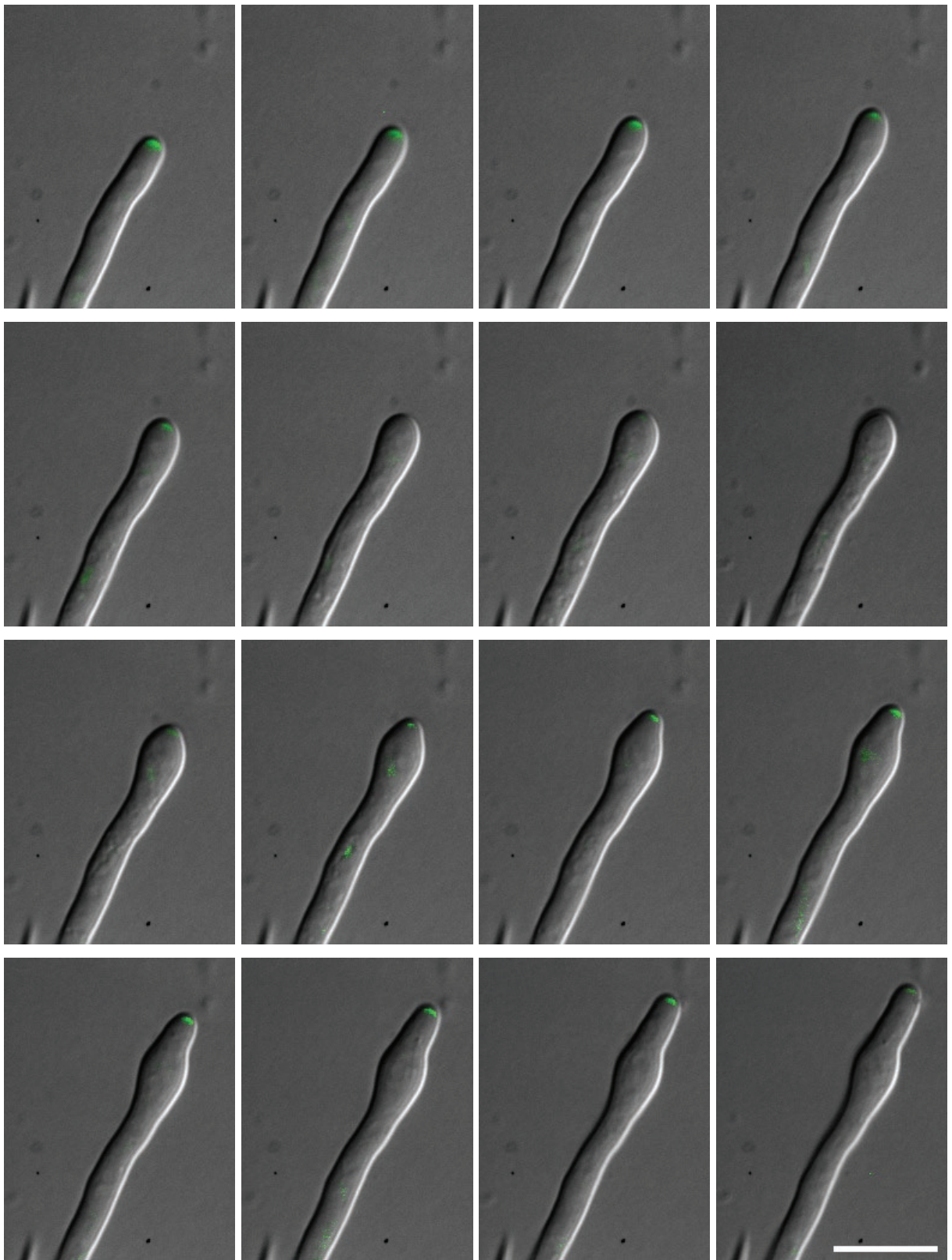
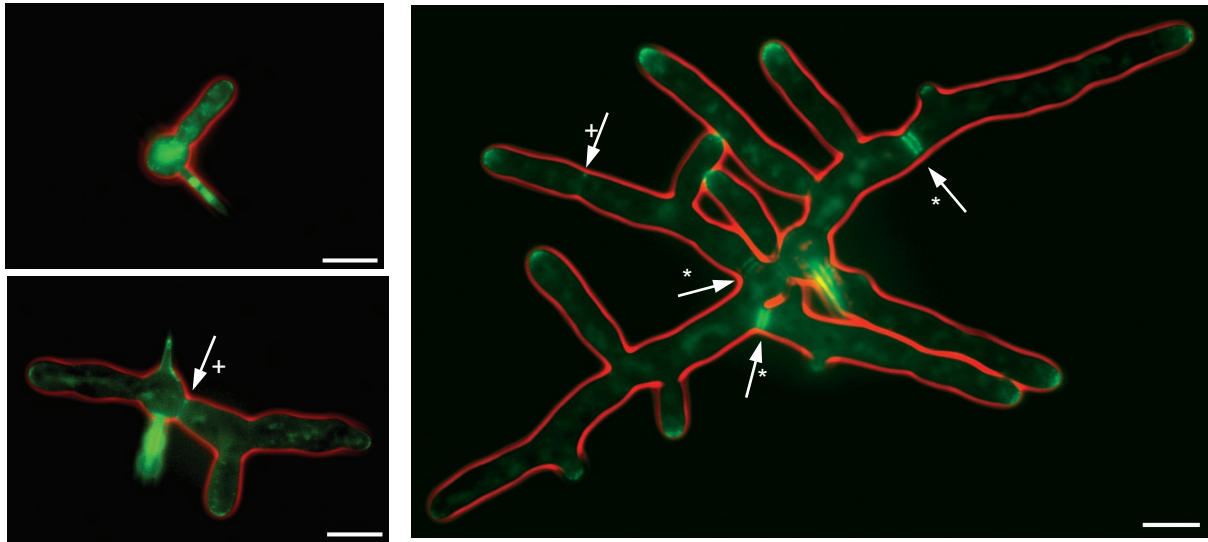
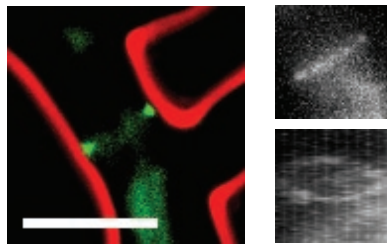


Figure 34
Time-lapse acquisition of Agboi Δ SPA2-GFP
The outline of the hypha is represented in grey, the AgSpa2p-GFP signal in green. The time elapsed between two frames is 4 min. Bar, 25 μ m

A



B



C

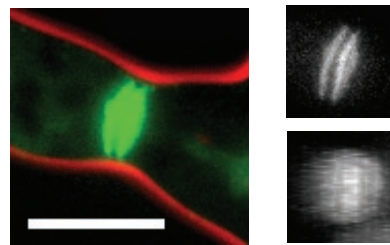


Figure 35

Localisation of AgBoip-GFP

(A) Overlay construction of phase contrast acquisitions (red) with GFP fluorescence acquisitions (green). Arrows indicate sites with "single ring" structures (marked with a "+") and "double plane" structures (marked with a "*"). Localisation to the tip is weaker at early stages but can be observed in all tips. Autofluorescence of the spore is observed in all pictures. (B) "Single ring" structure as overlaid picture (left). Ten planes of that "single ring" structure were acquired at a z-distance of 0.6 μm . The structure was three dimensionally reconstructed and viewed from top (top right) and 90° rotated at the x-axis (bottom right). (C) "Double plane" structure as overlaid picture (left). Ten planes of that "double plane" structure were acquired at a z-distance of 0.6 μm . The structure was three dimensionally reconstructed and viewed from top (top right) and 90° rotated at the y-axis (bottom right). Bar, 10 μm

Discussion

AgBoip is required to maintain polarisation at hyphal tips. We have demonstrated that AgBoip is required during germination of spores at elevated temperatures. The majority of the germinating Agboi Δ spores lysed as unipolar germlings and lysis occurred preferentially at the tip. At 20°C germination was successful but hyphal tips in Agboi Δ strains frequently lost polarisation and this portion was increased at elevated temperatures. A loss of polarisation at the tip was associated with a depolarisation of the actin cytoskeleton. Actin patches were delocalised from the tip and actin cables did not emanate from the tip any more. In addition, the polarisation marker AgSpa2p (see "Chapter 1") was also delocalised from the tip. We conclude therefore that AgBoip is required to maintain polarisation at hyphal tips to allow a permanent hyphal tip extension.

Whether the delocalised actin causes the spherical enlargement of hyphal tips or vice versa is unclear. However, as the delocalisation of AgSpa2p precedes slightly the spherical enlargement of hyphal tips and since AgSpa2p is thought to have a regulatory function on the actin cytoskeleton (see "Chapter 1"; Evangelista et al., 2002; Sagot et al., 2002) we hypothesise that AgBoip has a regulatory function on cell polarity upstream of AgSpa2p and actin.

In spherically enlarged tips polarity could be regained in the same direction established by the hyphae prior to the enlargement. Thus the direction of growth did not get lost during the depolarisation suggesting that spatial markers are maintained in spherically enlarged Agboi Δ tips.

AgBoip is required for establishment of cell polarity to initiate germ tubes and lateral branches. 15 % of Agboi Δ spores incubated at 37°C failed to initiate a germ tube. At 20°C, where germination was successful, the emergence of germ tubes was delayed. Agboi Δ unipolar and bipolar germlings reached about twice the hyphal length compared to wild-type prior to the initiation of the subsequent germ tube or lateral branch. During later development of Agboi Δ mycelia the branching frequency was reduced compared to wild-type. This suggests that AgBoip is also required for establishment of cell polarity to initiate germ tubes and lateral branches.

AgBoip localises to sites of polarised growth. An implication of AgBoip in cell polarity is also supported by its localisation pattern. AgBoip localises to tips and potentially to sites of septation as a "double disc" structure. Although

a smaller portion of tips localise AgBoip in unipolar and bipolar germlings compared to later developmental stages we do not think that AgBoip is expressed preferentially at later developmental stages as germination. We rather think that early stages of growth are more susceptible to stress and thus might delocalise e.g. AgBoip-GFP during microscopy procedures. The localisation pattern of AgBoip is in agreement with what was found for an orthologue of AgBoip in *S.pombe*, SpPob1. SpPob1p localises to tips and to the division plane similar to actin patches (Toya et al., 1999). Both proteins, AgBoip and SpPob1p were also found as a "single ring" like structure. In *S.pombe* the ring localised together with the actin ring. Although AgBoip potentially localises to sites of septation we could not detect a defect in septation. Septa were still successfully formed.

Conclusion. AgBoip might be implicated in establishment and maintenance of cell polarity to regulate the emergence of germ tubes and lateral branches and to maintain permanent hyphal tip extension in *A.gossypii*. A related role was also suggested for ScBoi1p and ScBoi2p in *S.cerevisiae*. Yeast Scboi1 Δ boi2 Δ cells arrest large round and unbudded with a delocalised actin cytoskeleton (Bender et al., 1996), which would implicate a failure to establish cell polarity. On the other hand the majority of dead cells upon a temperature shift were budded (Matsui et al., 1996) indicating a failure in maintenance of cell polarity.

However, we could also show that the majority of hyphal tips in the Agboi Δ strain maintained polarised growth even upon a shift from 20°C to 37°C and Agboi Δ germlings successfully maintained the polarised growth phase between emergence of the first germ tube and the subsequent lysis at the tip. Moreover AgSpa2-GFP and actin was properly maintained in Agboi Δ strains during polarised growth phases prior and after enlargement of tips. Thus AgBoip might not be required permanently during polarised growth of hyphal tips but only in response to distinct events. Such events might be the initiation of a septum, a germ tube or a lateral branch. All of these events cause the hyphal tip growth speed to slow down temporally even though polarisation at the tip is maintained (see "Chapter 1"; Christiansen et al., 1999; Spohr et al., 1998; Trinci, 1970). Thus AgBoip might be required for establishment of cell polarity to initiate germ tubes and lateral branches and for reinforcement of polarisation in response to septation or branching to maintain permanent

hyphal tip extension.

Perspectives

We hypothesise that AgBoip is not permanently required for polarised growth in *A.gossypii* but only at distinct points of development as the emergence of the first and second germ tubes, the emergence of lateral branches or upon branching or septation to reinforce existing polarisations. With reinforcement of polarised growth we defined the acceleration of the hyphal tip growth speed that was temporally decreased upon branching or septation. As the tip is also marked for future branching or septation events prior to reinforcement we think that rearrangements occur at a molecular level uniquely prior to reinforcements and not during polarised growth phases inbetween two reinforcements.

To test when exactly AgBoip is required during development we would like to analyse the germination of Agboi Δ spores at elevated temperatures in the AgSPA2 Δ P and Agspa2 Δ C background strain. The length of the first germ tube prior to the emergence of the second germ tube is decreased in the AgSPA2 Δ P strain and increased in the Agspa2 Δ C strain compared to wild-type. If our model was correct lysed unipolar Agboi Δ germlings should display a longer germ tube in the Agboi Δ spa2 Δ C strain and a shorter germ tube in the Agboi Δ SPA2 Δ P strain compared to the Agboi Δ strain. If our model is not correct and AgBoip is required during all phases of growth to the same extent, then we would expect the same germ tube lengths for all mutants.

If our model was correct this also would raise the question whether polarisation requires a positive feedback loop to be maintained or whether a once established polarisation is maintained intrinsically. Thus we would like to test if there was a molecular differentiation between polarity establishment and maintenance. We could make a temperature sensitive allele of AgCdc24p, inoculate spores at the permissive temperature, shift to the restrictive temperature at different time points and determine the length of the germ tube in unipolar germlings. If AgCdc24p was required at all stages of growth, i.e. maintained polarisation required a positive feedback loop, we would expect a relation between the germ tube length and the time after the shift to the restrictive temperature. If not, the germ tube length of unipolar germlings should be constant. As a control we would like to use a temperature sensitive allele of the AgAct1p. There, we expect a correlation between the temperature shift and the germ tube length of unipolar germlings. These experiments should also be made in the AgSPA2 Δ P and Agspa2 Δ C background strain.

We would further like to investigate where AgBoip

could be ordered in the hierarchy of polarity control proteins during establishment or maintenance of polarity. Therefore we would like to investigate the localisation of other polarity components during a spherical enlargement, e.g. AgCdc42p, AgCdc24p but also AgBud8p and AgAxl2/Bud10p as this was done for AgSpa2p.

Moreover we would be interested in the function of the PH-domain in AgBoip and whether this domain interacts with lipids and/or other proteins. Additionally we would like to investigate whether AgBoip is involved in secretion.

Current Model of *A.gossypii* Morphogenesis

During the functional analysis of the AgSPA2 and AgBO1 genes I also intensively concentrated on the morphogenesis of *A.gossypii* wild-type. Some of the insights gained were not discussed deeply in these chapters, as it was not relevant in the respective context. Thus I would like to mention again and discuss more deeply some aspects of *A.gossypii* morphogenesis and expand the initially drawn model of *A.gossypii* morphogenesis (Figure 1A & 36).

The hyphal tip growth speed increases exponentially. The hyphal tip growth speed of the first emerging germ tube was about 6 $\mu\text{m}/\text{h}$ whereas mature hyphae reached more than 180 $\mu\text{m}/\text{h}$. This is more than a 30-fold increase during development, which was achieved in an exponential acceleration.

It is likely that vesicles required for hyphal tip growth can be supplied from all over the apical compartment. Short branches, e.g. germ tubes, could therefore have a decreased delivery of vesicles to the tip than longer hyphae and as a consequence short branches have a decreased hyphal tip growth speed compared to longer branches. With the increase of the cytoplasmic volume during hyphal tip growth more vesicles could be delivered to the tip leading to an acceleration of the hyphal tip growth speed (Figure 36A).

The polarisation of hyphal tips is permanently maintained. AgSpa2p, a marker of polarisation in *A.gossypii*, localises permanently to sites of growth. Neither septation nor the initiation of a lateral branch causes AgSpa2p to delocalise from the tip. When a lateral branch is newly initiated the polarisation of AgSpa2p slightly precedes the emergence of the new branch. Thus the cause for the permanent hyphal tip extension in *A.gossypii* is likely the permanent polarisation of hyphal tips. Apical branching clearly differs from a lateral branching considering the state of the polarisation. Whereas a lateral branch displays the establishment of a new site of polarisation an apical branch displays a division of an existing polarisation.

AgSpa2p and actin also temporally localise to septa suggesting that these are also sites of polarisation (Figure 36A).

The hyphal tip growth speed is transiently decreased during the initiation of branches or septa but with the addition that this counts only for tips that share the same cytoplasm with the initiated septum or branch, i.e. the hyphal tip growth speed is not affected if septa or branches are initiated in a hyphal compartment that is

separated by one or more septa from that tip.

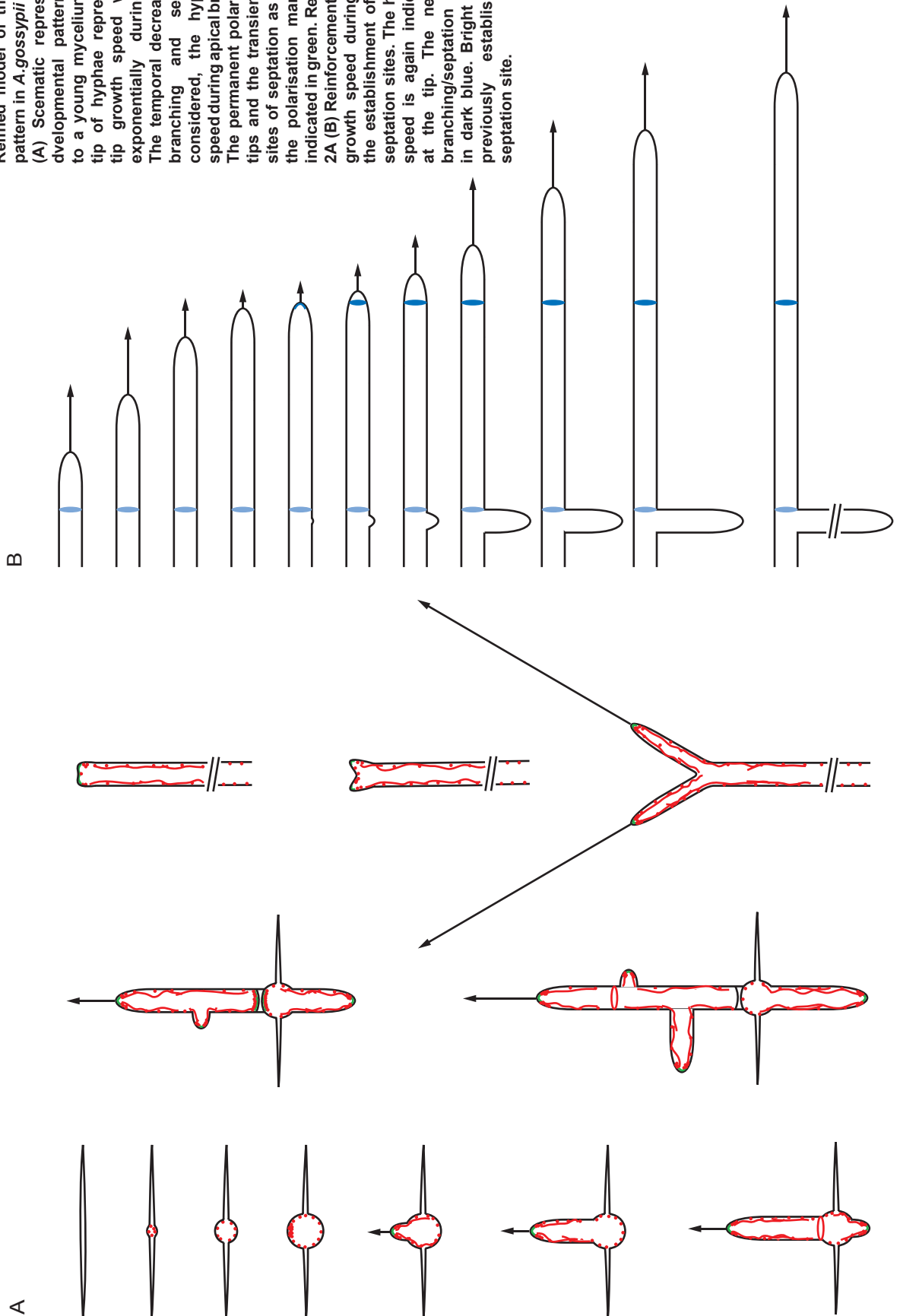
One possible explanation for the decrease is that vesicles are redirected to sites of lateral branch or septum initiation and no longer to the already existing tip. Thus the existing tip has a decreased supply of vesicles.

Apical branches also cause the hyphal tip growth speed to decrease transiently. The cause of this decrease might be that the supply of vesicles that was originally directed to one tip is now directed to two tips (Figure 36B).

Site selection for branching and septation is not random. During the temporal decrease of the hyphal tip growth speed as a consequence of a lateral branch or a septation event the hyphal tip must be marked since future lateral branches or septa are exclusively induced at these sites. One exception of this rule occurs during germination. The site selected for the initiation of the first germ tube cannot depend upon a previous septation or lateral branching event. However, the initiation site can serve for future septation or lateral branching events. Thus we suggest that sites for septation or lateral branching are established upon initiation of a germ tube or reinforcement of hyphal tip growth speed. As we could never observe a decrease of the hyphal tip growth speed without a branching or septation event but each branching or septation event caused the hyphal tip growth speed to decrease transiently we suggest that the decrease of the hyphal tip growth speed is the consequence of branching or septation and not vice versa, i.e. the hyphal tip growth speed is subjected to velocity fluctuations that might induce a lateral branch or a septum. Further we think that the hyphal tip is marked during emergence of the new branch (or initiation of the new septum), thus slightly prior to reinforcement of the main tip.

Figure 36
 Refined model of the developmental
 pattern in *A.gossypii*

(A) Schematic representation of the
 developmental pattern from a spore
 to a young mycelium. Arrows at the
 tip of hyphae represent the hyphal
 tip growth speed which increases
 exponentially during development.
 The temporal decrease during lateral
 branching and septation is not
 considered, the hyphal tip growth
 speed during apical branching omitted.
 The permanent polarisation of hyphal
 tips and the transient polarisation at
 sites of septation as visualised using
 the polarisation marker AgSpa2p is
 indicated in green. Refer also to Figure
 2A (B) Reinforcement of the hyphal tip
 growth speed during branching and
 the establishment of new branching/
 septation sites. The hyphal tip growth
 speed is again indicated as arrows
 at the tip. The newly established
 branching/septation site is marked
 in dark blue. Bright blue indicates a
 previously established branching/
 septation site.



Construction of a Versatile Module for C-terminal GFP Fusion

Introduction

The introduction of the green fluorescent protein (GFP) into heterologous organisms has been shown to be of extraordinary value. It allows the visualization of the temporal and spatial organisation of proteins. The recent development of GFP mutant alleles with different spectral properties and advances in microscopy enables more sophisticated techniques as expression profiling, video microscopy or studies on protein-protein interaction and signalling (van Roessel and Brand, 2002).

In Yeast a very efficient way for C-terminal GFP fusion has been developed (Wach et al., 1997). A universal module consisting of the coding region of the GFP, a terminator and a selection marker are amplified by PCR. The primers used carry 45 b extensions at their 3'-site. The extensions are homologous to the C-terminal coding region of the ORF to be tagged and to the terminator region following the endogenous stop codon. Homologous recombination of a generated cassette at the chosen locus leads to an extension of the respective ORF with the coding region of the GFP and during translation to a C-terminally labelled GFP fusion protein.

It was shown that PCR based gene targeting is an efficient method to generate knock out strains in *A.gossypii* (Wendland et al., 2000). Thus we wanted to construct a versatile module for C-terminal GFP fusion in *A.gossypii*. From previous studies we knew that critical factors for transformations in *A.gossypii* are the amount of DNA transformed and the length of the homology regions. Taking this into account we followed two strategies for C-terminal GFP fusion. On one hand we wanted to try C-terminal GFP fusion by PCR based gene targeting, i.e. the amplified PCR product is directly transformed. On the other hand the PCR product should be co-transformed into yeast with a plasmid that bears the *A.gossypii* GFP target locus of interest. We expected recombination of the PCR product on the plasmid. The introduced GFP cassette could then be subcloned from the generated plasmid and propagated in *E.coli* to get the amounts of DNA and length of homology flanks required for an efficient transformation of *A.gossypii*.

Results and Discussion

Cloning of a Universal GFP Cassette for C-terminal GFP Fusion via PCR Based Gene Targeting

The *A.gossypii* GFP module was based on the GFP module for PCR based GFP fusion in Yeast, pFA6a_GFP(S65T)_kanMX6 (Wach et al., 1997).

This module consists of the coding region of the GFP variant GFP(S65T) (Heim and Tsien, 1996), the *S.cerevisiae* ADH terminator and the kanMX6 (Wach et al., 1994) dominant drug resistance marker (Figure 37a). The kanMX6 marker consists of the open reading frame of the *E.coli* kan^R gene under the control of promoter and

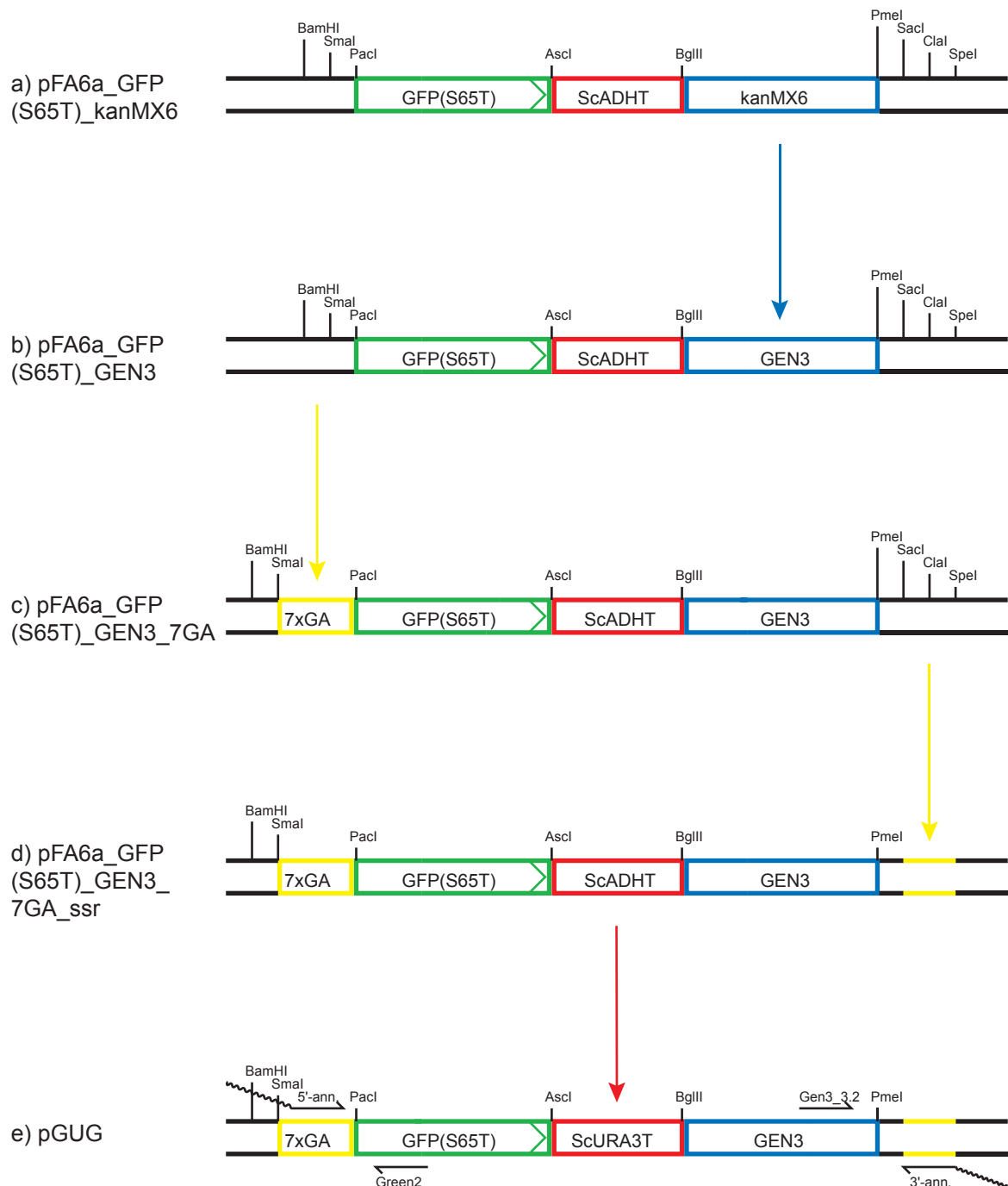


Figure 37
Construction of pGUG

Each arrow represents one cloning step, restriction sites are specified. Black arrows mark the new annealing sites for amplification of the GUG module and the standard annealing sites used for verification.

terminator sequences of the *A.gossypii* AgTEF gene. To avoid recombination at the *A.gossypii* TEF locus we had to replace the kanMX6 marker in a first step by GEN3 (Wendland et al., 2000). GEN3 consists of the open reading frame of the *E.coli* kan^R gene under the control of promoter and terminator sequences of the *S.cerevisiae* ScTEF2 gene.

GEN3 was amplified from pGEN3 by PCR with the oligonucleotide pair GEN3_BglII (bearing a BglII site) x GEN3_PmeI (bearing a PmeI site). The PCR product was digested BglII/PmeI and ligated into the BglII/PmeI locus in pFA6a_GFPS65T_kanMX6 generating pFA6a_GFPS65T_GEN3 (Figure 37b).

The oligonucleotide annealing sites in pFA6a_GFPS65T_kanMX6 were originally designed on the multicloning site of the vector. In a PCR reaction this lead to an amplification of restriction sites with the module, at the 5'-end the sites Sall, BamHI and SmaI, at the 3'-end ClaI and SacI. These restriction sites were undesired in the second GFP fusion strategy (see above) where the module should be re-cloned with longer homology flanks. Moreover the 5'-annealing site showed homology to a region 28 bp after the 3'-annealing site. The module could even be amplified with just the 5'-annealing oligonucleotide thus generating a false product with the same homology flanks at both ends. We therefore decided to construct new annealing sites.

At the 5'-site of pFA6a_GFPS65T_GEN3 two complementary oligonucleotides (7GAfor and 7GArev) of 42 bp in length were inserted into the SmaI site generating pFA6a_GFPS65T_GEN3_7GA (Figure 37c). The oligonucleotides encode a 7xGly-Ala linker. At the 3'-site the 26 bp SacI/SpeI fragment was replaced with two complementary oligonucleotides of 22 bp in length (GFP_3_W and GFP_3_C) generating pFA6a_GFP(S65T)_GEN3_7GA_ssr (Figure 37d). New annealing sites were chosen in accordance to each other. At the 5'-site this was a 19 bp stretch 5'-GGTGCAGGCGCTGGAGCTG-3' and at the 3'-site the 18 bp stretch 5'-AGGGACCTGGCACGGAGC-3'.

The newly constructed module was amplified by PCR to introduce a C-terminal GFP fusion. Several transformants were obtained in each transformation. However, a correct integration could not be obtained. We could show that pFA6a_GFP(S65T)_GEN3_7GA_ssr circularises or forms circular dimers after transformation in *A.gossypii*, which are maintained under selective conditions. Amplifying and transforming the resistance marker GEN3 alone did not give transformants. When the *S.cerevisiae* ScADH terminator was amplified

together with the GEN3 marker transformants were obtained indicating ARS activity in the ScADH terminator. We decided to replace the ScADH terminator by the *S.cerevisiae* ScURA3 terminator. 234 bp from position 116980-117213 on Yeast chromosome V (Dietrich et al., 1997) were amplified with oligonucleotides URA3t_AscI (bearing an AscI site) x URA3t_BglII (bearing a BglII site). The PCR product was digested AscI/BglII and cloned into the AscI/BglII locus of pFA6a_GFP(S65T)_GEN3_7GA_ssr. PCR products amplified from the newly constructed module did not show ASR activity anymore. It was named pGUG (GFP-URA3T-GEN3; Figure 37e; a plasmid map is attached in "Appendix I"). The optimal PCR conditions determined were 2' initial denaturation at 94°C, 1' annealing at 60°C, 2'45" elongation at 72°C, 30 cycles, 7' final elongation at 72°C, Pwo polymerase (Roche) in the supplied reaction buffer adjusted to 4 mM MgSO₄.

C-Terminal GFP Fusion of Four Different Genes

The GFP module was developed for our studies described in "Chapter 1" and "Chapter 2". We were interested in the localisation pattern and the dynamics of AgSPA2 (see "Chapter 1"), AgBOI (see "Chapter 2"), AgCAP1 and AgCAP2. It was shown in yeast that C-terminal fusions to ScCAP1 and ScCAP2 were not fully functional (Yves Barral, personal communication). We therefore decided to integrate second copies of each of these genes that are C-terminally fused to GFP. For AgSPA2 and AgBOI the endogenous copy was directly fused to the GFP module. In all cases the approach via the yeast detour was followed, as we did not obtain transformants from direct transformations of *A.gossypii* with the PCR product.

pGUG was amplified with oligonucleotides for the selected ORFs: AgSPA2: AgSPA2_GFP5'fusion x AgSPA2_GFP3'fusion; AgBOI: 5'BOIGFPpGUG x 3'BOIGFPpGUG; AgCAP1: 5CAP1GFPpGUG x 3CAP1GFPpGUG; AgCAP2: 5CAP2GFPpGUG x 3CAP2GFPpGUG. The deletion set was 39 bp for AgSPA2, 25 bp for AgBOI and 50 bp for AgCAP1 and AgCAP2, respectively.

The PCR product for an AgSPA2-GFP fusion was transformed together with pAGSPA2 (see "Materials and Methods") into the yeast strain #259(pFS-28)-3. Transformants were verified for correct recombination of the PCR product with the plasmid; the 5'-linkage with the oligonucleotides AgSPA2GFPver x GFP2 and the 3'-linkage with AgSPA23'ver x G3 (Figure 38a&b). A 3180 bp Sall fragment from the constructed pAGSPA2-GFP plasmid (Figure 38c) was subcloned into

pUC19 (Yanisch-Perron et al., 1985) generating pTCAGSPA2-GFP. The fragment consists of the GUG module flanked by homologous regions to the AgSPA2 locus, 218 bp at its 5'-site and 224 bp at its 3'-site (Figure 38d). pTCAGSPA2-GFP was amplified in *E.coli*. 10 µg were digested with Sall and transformed into *Agleu2Δthr4Δ* (Figure 38d&e). Homokaryotic isolates were verified by PCR for correct integration of the module, the oligonucleotide pairs used were AgSPA2for1 x Green2 for the 5'-site and G3.2 x AgSPA2_rev1 for the 3'-site (Figure 38f). The transformants showed specific fluorescence and the fusion protein complemented the endogenous copy. The new strain was named AgSPA2-GFP (see

"Chapter 1).

For a C-terminal fusion to the AgBOI ORF the PCR product was co-transformed with pAGBOI into the yeast strain #259(pFS-28)-3 (see "Materials and Methods"). Verification of recombination on the generated plasmid pAGBOI-GFP was done with oligonucleotides pSM13_out3 x Green2 at the 5'-site and G3.2 x pSM_out-5th at the 3'-site (Figure 39a & b). A 3163 bp EcoRI/BamHI fragment from the constructed pAGBOI-GFP plasmid (Figure 39c) was subcloned into pUC19. The fragment carried the GUG module with homology to the AgBOI locus, 171 bp at the 5'-site and 254 bp at the 3'-site (Figure 39d). The generated plasmid, pTCAGBOI-GFP, was amplified in *E.coli* and

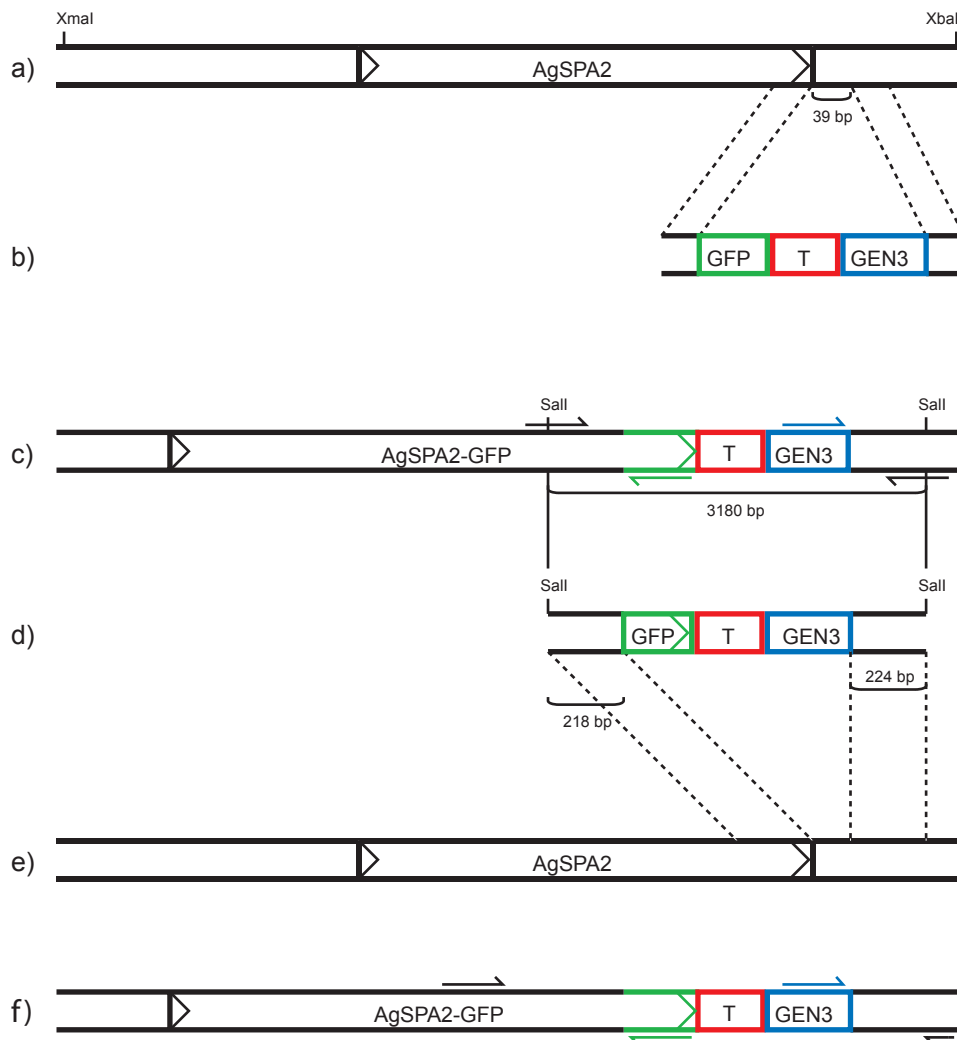


Figure 38

Construction of an AgSPA2-GFP strain

a) pAGSPA2, cloned XmaI/XbaI into pRS415. b) GUG amplified by PCR with oligonucleotides for C-terminal AgSPA2-GFP fusion. The deleted region in the AgSPA2 terminator is indicated. Regions of homology between the AgSPA2 locus on pAGSPA2 and the PCR cassette are indicated with dashed lines. c) pAGSPA2-GFP, oligonucleotides for verification are indicated by arrows. d) pTCAGSPA2-GFP with Sall sites used for subcloning. Lengths of homology flanks are shown. e) Chromosomal locus of AgSPA2 in the *Agleu2Δthr4Δ* strain. Regions of homology between the chromosomal AgSPA2 locus and pTCAGBOI-GFP are indicated with dashed lines. f) Chromosomal locus of AgSPA2 in the AgSPA2-GFP strain. Arrows indicate oligonucleotides for verification.

digested EcoRI/BamHI. 10µg were transformed into *Agleu2Δthr4Δ* (Figure 39e). Homokaryotic isolates were verified by PCR with the same oligonucleotide combination used for verification of the plasmid recombination (Figure 39f). The generated strain was named AgBOI-GFP. All strains showed specific fluorescence and the fusion protein complemented the endogenous copy (see "Chapter 2").

For a C-terminal GFP fusion of AgCap1p and AgCap2p the plasmids pAGCAP1 and pAGCAP2 were transformed with the respective PCR product. Verification for a correct recombination were done by PCR using oligonucleotides CAP1verfor x Green2 for the 5'-site and G3.2 x CAP1verrev

for the 3'-site in pAGCAP1-GFP; pAGCAP2-GFP was verified using CAP2verfor x Green2 for the 5'-site and G3.2 x CAP2verrev for the 3'-site (Figure 41a, b & c; Figure 42a, b & c).

AgCAP1-GFP and AgCAP2-GFP were integrated as second copies as described in "Chapter 4".

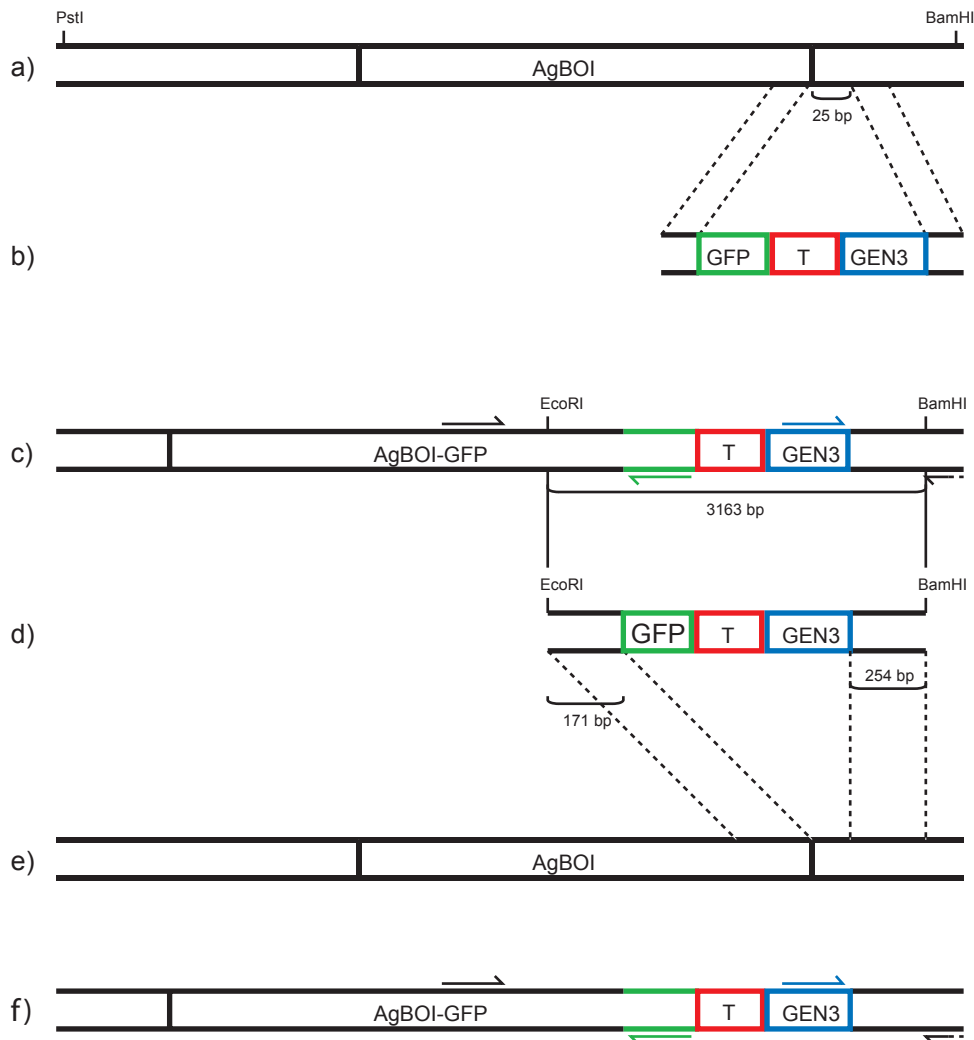


Figure 39

Construction of an AgBOI-GFP strain

a) pAGBOI, cloned PstI/BamHI into pRS415. b) GUG amplified by PCR with oligonucleotides for C-terminal AgBOI-GFP fusion. Regions of homology between the AgBOI locus on pAGBOI and the PCR cassette are indicated with dashed lines. The deleted region in the AgBOI terminator is indicated. c) pAGBOI-GFP, oligonucleotides for verification are indicated by arrows. d) pTCAGBOI-GFP with EcoRI/BamHI sites used for subcloning. Regions of homology between the chromosomal AgBOI locus and pTCAGBOI-GFP are indicated with dashed lines. e) Chromosomal locus of AgBOI in the *Agleu2Δthr4Δ* strain. Sites of recombination with pTCAGBOI-GFP are shown as dashed lines. f) Chromosomal locus of AgBOI in the *AgSPA2-GFP* strain. Arrows indicate oligonucleotides for verification.

Construction of an Integration Module Based on the AgADE2 Marker

Introduction

As we wanted to integrate second copies of AgCAP1-GFP and AgCAP2-GFP in *A.gossypii*, we decided to construct an integration module for *A.gossypii*. The strategy was to reconstitute a partially deleted AgADE2 locus to a functional locus with an integration cassette.

The *A.gossypii* strain used for integration should carry a partial deletion at the AgADE2 locus spanning the C-terminal coding region and the terminator region downstream of AgADE2. A module consisting of this deleted region flanked by sufficient homology regions to the chromosomal AgADE2 should be able to reconstitute the partially deleted locus by homologous recombination. The AgCAP1-GFP or AgCAP2-GFP fusions, respectively, cloned into the module downstream of the terminator but upstream of the 3'-flanking homology region could then be co-integrated at the AgADE2 locus.

A strain carrying AgCAP1-GFP or AgCAP2-GFP, respectively, at the AgADE2 locus would be G418s, clonNATs and leu-, so all three markers, GEN3, NAT1 and LEU2 were still available. This integration module could of course not only integrate GFP fusion constructs but any allele of interest.

Results and Discussion

Generation of an Integration Module with AgADE2 as New Selection System

In a first step we generated a partial deletion of the AgADE2 gene by PCR based gene targeting. GEN3 was amplified with oligonucleotides 5Agade2part x 3Agade2part and transformed into *Agleu2Δthr4Δ*. The homokaryotic transformants *Agade2Δ1* were verified by PCR with oligonucleotides Agade2verfor x GEN3_2.1 and Agade2verrev x GEN3_3.2. The total length of the deletion was 994 bp, 770 bp of the ORF encoding 310 aa - 566 aa and 224 bp downstream of the stop codon (Figure 40a & b). The inter ORF

region downstream of the AgADE2 ORF was 232 bp. We identified this following ORF as YAS 332, a gene that does not have an orthologue in *S.cerevisiae* and no significant homology to other proteins could be found. In the partial deletion introduced at the AgADE2 locus we also deleted the terminator region of YAS 332 to a remaining of 8 bp. The only phenotypic difference between the *Agade2Δ* and the *Agleu2Δthr4Δ* strain was a red colour accumulation in the *Agade2Δ1* mycelium. The integration module was constructed by subcloning the 1453 bp *HinDIII*/*EcoRI* fragment from bAG1773 into pBSIISK(+)^{ScaI} (pBSIISK(+)) (Short et al., 1988) with a point mutation in the *ScaI* site, introduced by site-directed mutagenesis

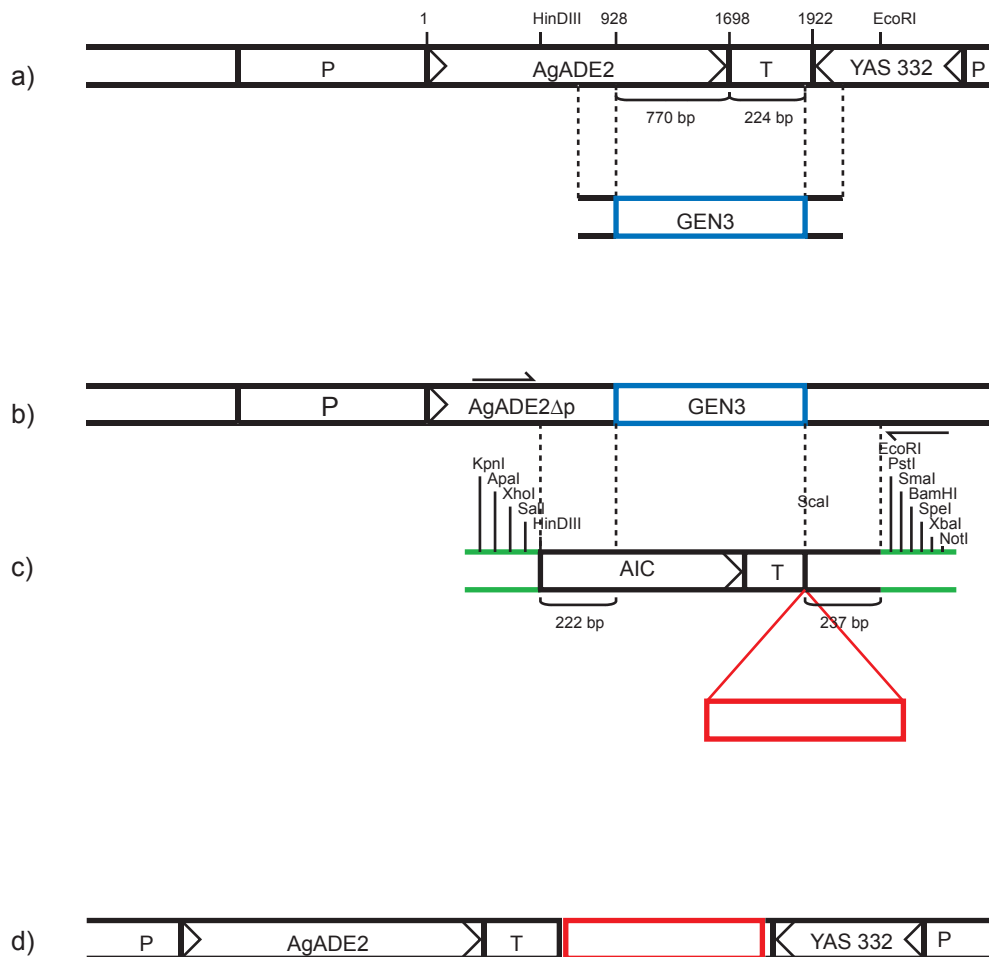


Figure 40

AgADE2 Integration Cassette (AIC): Construction and mode of action

a & b) Generation of an *Agade2Δ1* strain by PCR based gene targeting. Regions of homology between the AgADE2 locus and the PCR cassette are indicated with dashed lines. Numbering starts at the AgADE2 start codon. c) pAIC integration module. Sites used for subcloning from bAG1773 are *HinDIII* and *EcoRI* (also shown in a)). *ScaI* site for cloning the fragment of interest and restriction sites for excision of the module are indicated. Lengths of homology to the AgADE locus in *Agade2Δ1* are 222 and 237 bp, respectively. Regions of homology between the chromosomal AgADE locus and pAIC are indicated with dashed lines. d) Chromosomal AgADE locus after integration of pAIC carrying the fragment of interest. Standard oligonucleotides Redfor and Redrev used for verification are shown in b).

(Weiner et al., 1994) using the oligonucleotides killthescafor x killthescarev that bind in the β -lactamase coding region). The fragment beard 992 bp of the AgADE2 ORF encoding the C-terminal part and 461 bp downstream of the AgADE2 stop codon. At the 5'-site it shared 222 bp and at the 3'-site 237 bp homology to the truncated AgADE2 locus in AgADE2 Δ 1, respectively. A unique Scal

site was located at the beginning of the 237 bp downstream homology. The new plasmid was named pAIC (AgADE2 Integration cassette, Figure 40c; a plasmid map is attached in "Appendix II") Any fragment of interest can now be cloned into the Scal site of pAIC (Figure 40c). After amplification in *E.coli* the fragment can be recut with flanking homologies to the AgADE2 locus and transformed

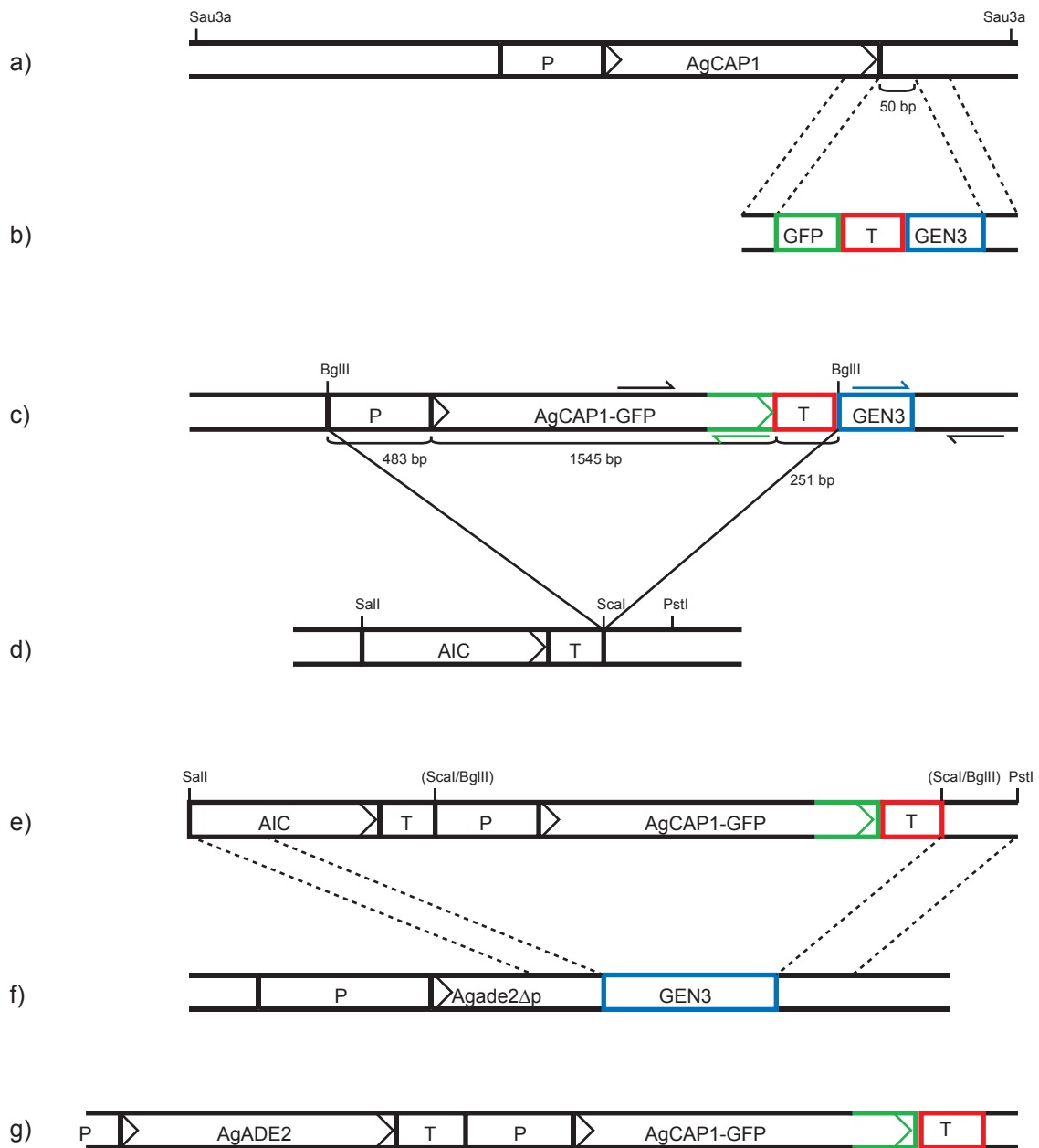


Figure 41

AgCAP1-GFP fusion and its integration at the AgADE2 locus

a) pAGCAP1 b) GUG amplified with oligonucleotides for C-terminal AgCAP1 GFP fusion. The deleted region in the AgCAP1 terminator is indicated. Dashed lines represent the homology between pAGCAP1 and the PCR cassette. c) pAGCAP1-GFP, oligonucleotides for verification are indicated by arrows. d) Cloning of a 2279 bp BglII fragment from pAGCAP1 into the Scal site of pAIC . Both restriction sites were destroyed. e) pAIC_AGCAP1-GFP; the cassette used for transformation into Agade2 Δ 1 was released by Sall/PstI digestion. f) Chromosomal locus of AgADE2 in the AgADE2 Δ 1 strain. Homology regions between pAIC_AGCAP1-GFP and the chromosomal AgADE2 locus in Agade2 Δ 1 is indicated with dashed lines. g) Chromosomal locus of AgADE2 in the AgCAP1-GFP strain after recombination. Oligonucleotides used for verification are shown in b).

into Agade2Δ1. The resulting strain will be ADE+, G418s (Figure 40d).

Integration of AgCAP1-GFP and AgCAP2-GFP Fusions Using the pAIC Module

The plasmid pAGCAP1-GFP (see "Chapter 3") was

digested with BglII. Blunt ends were generated in a "fill-in" reaction using a polymerase with a 5' - 3' exonuclease activity. The 2279 bp fragment was then subcloned into the *Scal* site of pAIC (Figure 41d & e). The new plasmid pAIC_AGCAP1-GFP carried the AgCAP1 ORF C-terminally fused to GFP without any remaining of the GEN3 module. The promoter region of AgCAP1 was 483 bp in

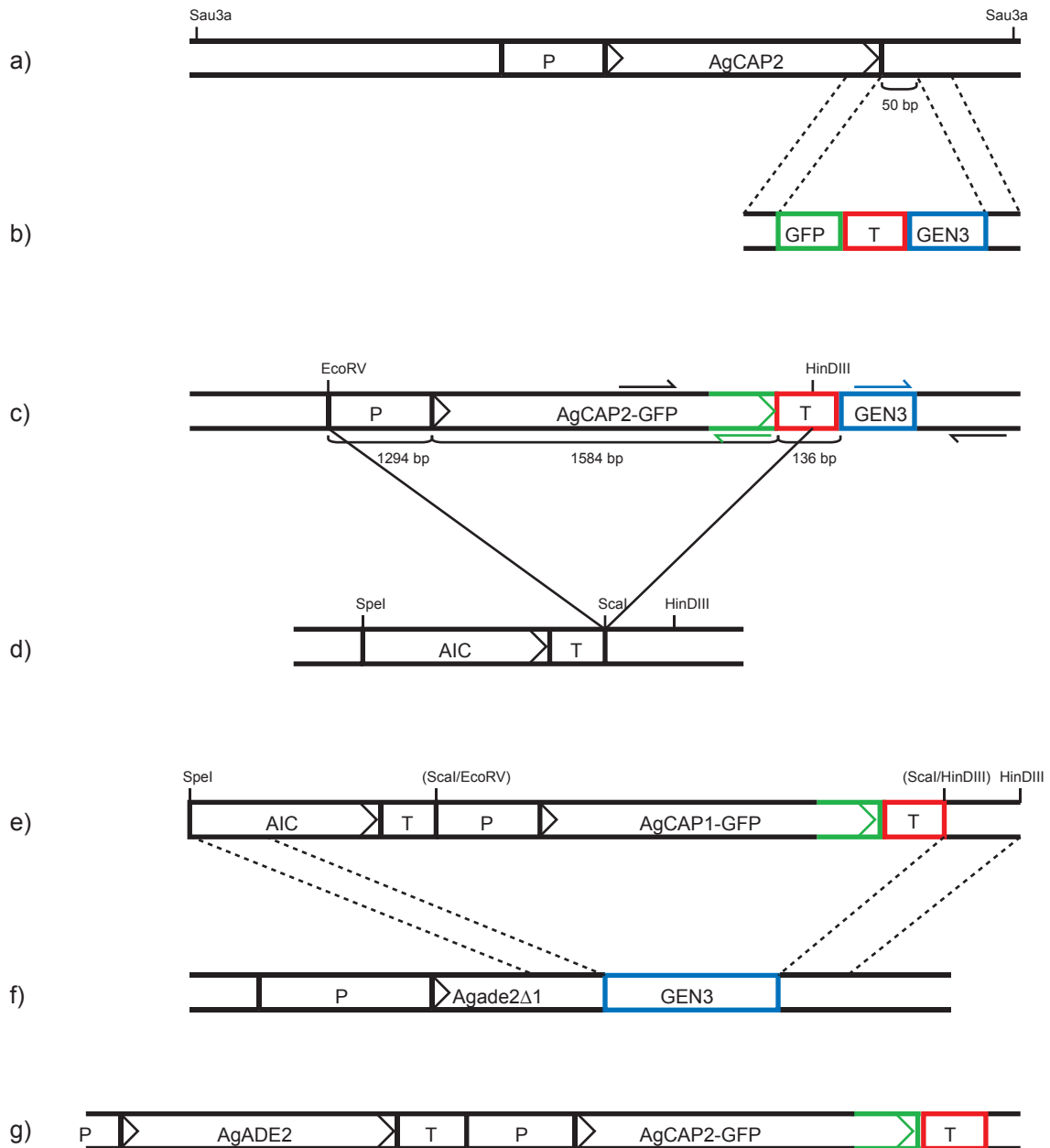


Figure 42

AgCAP2-GFP fusion and its integration at the AgADE2 locus

a) pAGCAP2 b) GUG amplified with oligonucleotides for C-terminal AgCAP2-GFP fusion. The deleted region in the AgCAP2 terminator is indicated. Dashed lines represent the homology between pAGCAP2 and the PCR cassette. c) pAGCAP2-GFP, oligonucleotides for verification are indicated by arrows. d) Cloning of a 3014 bp EcoRV/HinDIII fragment from pAGCAP2 into the *Scal* site of pAIC. All three restriction sites were destroyed. e) pAIC_AGCAP2-GFP; the cassette used for transformation into Agade2Δ1 was released by *SpeI*/*HinDIII* digestion. f) Chromosomal locus of AgADE2 in the Agade2Δ1 strain. Homology regions between pAIC_AGCAP2-GFP and the chromosomal AgADE2 locus in Agade2Δ1 is indicated with dashed lines. g) Chromosomal locus of AgADE2 in the AgCAP2-GFP strain after recombination. Oligonucleotides used for verification are shown in b).

length. pAIC_AGCAP1-GFP was amplified in *E.coli* and digested PstI/Sall to obtain the AgCAP1-GFP fusion gene with flanking homologies to the AgADE locus. 5 µg were transformed into the Agade2Δ1 strain. Homokaryotic transformants were obtained and named AgCAP1-GFP (Figure 41f & g). Verification was done by PCR using oligonucleotides Agade2verfor x Agade2verrev. The plasmid pAGCAP2-GFP was digested with EcoRV/HinDIII. Blunt ends were generated in a "fill-in" reaction using a polymerase with a 5' - 3' exonuclease activity. The 3014 bp fragment was then subcloned into the Scal site of pAIC (Figure 42d & e). The new plasmid pAIC_AGCAP2-GFP carried the AgCAP2 ORF C-terminally fused to GFP. The promoter region of AgCAP2 was 1294 bp in length, the ScURA3 terminator from the GUG module was shortened from 286 bp to 136 bp in length. pAIC_AGCAP2-GFP was amplified in *E.coli* and digested SpeI/HinDIII to obtain the AgCAP2-GFP fusion gene with flanking homologies to the AgADE locus. 5 µg were transformed into Agade2Δ1. Homokaryotic transformants were obtained and named AgCAP2-GFP (Figure 42f & g). Verification was done by PCR using oligonucleotides Agade2verfor x Agade2verrev.

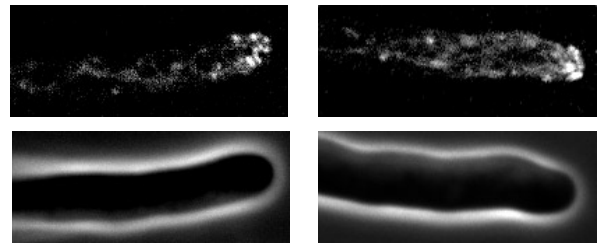


Figure 43
AgCAP1-GFP

Two examples of the localisation of AgCap1-GFP in hyphal tips of *A.gossypii*. Top represents the fluorescence picture, bottom the corresponding phase contrast picture. AgCap1p-GFP localised as polarised patches to the tip and as single patches at the hyphal cortex. The signal for AgCap2-GFP was even weaker.

The AgCAP1-GFP and AgCAP2-GFP strains showed specific fluorescence similar to what was observed for cortical actin patches in fixed Rhodamine-Phalloidine stainings (Figure 43 and 1A). However, the intensity of the GFP signal was weak in the AgCAP1-GFP strain and even weaker in the AgCAP2-GFP strain and thus did not serve well for analysis. We did not use these strains any further.

Materials and Methods

Molecular Cloning

General molecular cloning was done according to Sambrook et al., 2001. *E.coli* DH5((Hanahan, 1983) was used as a host strain for all plasmid work. Sequencing was performed on an ABI 377 automated sequencer using the BigDye Terminator Sequencing Kit. Enzymes for cloning were purchased at NEB, polymerases for PCR at NEB (Vent DNA polymerase), Pharmacia (Taq DNA polymerase) and Roche (Pwo DNA polymerase). Kits from Qiagen were used for plasmid DNA isolation and DNA extraction from agarose gels. P32-labeling of DNA for colony

hybridisation was done with a hexanucleotide random primer labelling kit (RPN 1600Z) from Amersham. Oligonucleotides used for sequencing and cloning are listed in Table 1.1, plasmids and BACs are listed in table 1.2.

Bioinformatic tools for alignment, database searching, protein analysis, primer selection and pattern recognition were used from the Wisconsin Package (Genetics Computer Group, Inc.). ProfileScans were performed at the ISREC ProfileScan Server <http://hits.isb-sib.ch/cgi-bin/PFSCAN>.

Table 1.1 Oligonucleotides for cloning, sequencing and verification PCR

Name	Sequence
G2	5'-GTTTAGTCTGACCATCTCATCTG-3'
G3	5'-TCGCAGACCGATACCAGGATC-3'
G2.1	5'-TGCCTCCAGCATAGTCGAAG-3'
G3.2	5'-CTCCAACCTCGGCACTATTTTAC-3'
V2*NAT1	5'-GTGTCGTCAAGAGTGGTACC-3'
V3*NAT1	5'-ACATGAGCATGCCCTGCCCC-3'
AgSPA25ver	5'-GTCAAAGAAACCCACACCC-3'
AgSPA3'verif	5'-GGCGGGCTAGTATAAATGTATC-3'
AgSPA2GFPver	5'-TGACCATTTTCGCTGACAAAC-3'
AG-OLIGO1865	5'-CATAAGTCATTTGCCAATAGC-3'
AG-OLIGO1237	5'-CAGGGCTCTTATGATGAACTTCC-3'
AG-OLIGO1710	5'-GCATTGATTACGCGCCGAG-3'
AG-OLIGO1927	5'-TCGAGTATTCCTACATGATGGC-3'
GEN3_BglII	5'-ATCAGATCTGGTGTATTTACC-3'
GEN3_PmeI	5'-AGCTTTGTTTAAACGATGAGGCCGTCTTTTGTTG-3'
7GAfor	5'-GGGGCCGGTGCAGGCGCTGGAGCTGGCGCCGGTGGTGGCGCA-3'
7GArev	5'-TGCGCCAGCACCGGCGCCAGCTCCAGCGCCTGCACCGGCCCC-3'
GFP_3_W	5'-CCGTGCCAGGTCCCTGGGGAGA-3'
GFP_3_C	5'-CTAGTCTCCCAGGGACCTGGCACGGAGCT-3'
URA3t_AscI	5'-GGCGCGCCATTATAAGTAAATGCATGTATAC-3'
URA3t_BglII	5'-GGAGATCTATGCGTCCATCTTTACAGTCC-3'
Agade2verfor	5'-TGCACCAGAACAACATATGCC-3'
Agade2verrev	5'-AAATGGACATTCAAATCCCCAG-3'
killthescafo	5'-TACTCACCAGTCACAGAAAAG-3'
killthescare	5'-TTCAACCAAGTCATTCTGAG-3'
GFP2	5'-TCCAATTTGTGTCCAAGAATG-3'
AgSPA2_for1	5'-CGCACTAAAAGAACACGGCAAC-3'
Green2	5'-ATCACCTTCACCCTCTCCAC-3'
AgSPA2_rev1	5'-ACGGAATGCCGCAGCAAAAAC-3'
pSM13_out3	5'-AACCAGGCCGATTCTGCGG-3'
pSM_out-5th	5'-AATTGACTCCTAACGAAGCTCC-3'
pAG1634rp_G1	5'-CACCAGCTTCTTACACTTCC-3'
pAG1634rp_G4	5'-AGACGACTGGCAGGTGTCTG-3'
AgADE2verfor	5'-TGCACCAGAACAACATATGCC-3'
AgADE2verrev	5'-AAATGGACATTCAAATCCCCAG-3'
CAP1verfor	5'-TGAAGACGGCAATGTGAAG-3'
CAP1verrev	5'-AACGACAGAAGGCTGGATGAG-3'
CAP2verfor	5'-TACCGCATTACCACAACCATC-3'
CAP2verrev	5'-CTTCAACATCTTCAACCACTACC-3'
1634-4th	5'-GAGGATTCTTGAAGGCACGG-3'
p13_out4	5'-AGATCAACCTTGTTCATGGC-3'

Table 1.2 Plasmids and BACs

Name	Reference
pGEN3	Wendland et al., 2000
pAG25	Goldstein and McCusker, 1999
opAG13790	Dietrich et al., 2001
pAGSPA2	(this study)

pAGSPA2ΔP	(this study)
pAGSPA2ΔP_TURA	(this study)
pFA6a_GFP(S65T)_kanMX	Wach et al., 1997
pFA6a_GFP(S65T)_GEN3	(this study)
pFA6a_GFP(S65T)_GEN3_7GA	(this study)
pFA6a_GFP(S65T)_GEN3_7GA_ssr	(this study)
pGUG	(this study)
bAG1773	Dietrich et al., 2001
pBSIISK(+)	Short et al., 1988
pBSIISK(+) ^{Sc}	(this study)
pAGSPA2-GFP	(this study)
pUC19	Yanisch-Perron et al., 1985
pTCAGSPA2-GFP	(this study)
pAGBOI	(this study)
pAGBOI-GFP	(this study)
pTCAGBOI-GFP	(this study)
pAGCAP1	Dietrich et al., 2001, originally opAG20010
pAGCAP2	Dietrich et al., 2001, originally opAG11951
pAGCAP1-GFP	(this study)
pAGCAP2-GFP	(this study)
pAIC	(this study)
pAIC_CAP1-GFP	(this study)
pAIC_CAP2-GFP	(this study)
pAG503	(this study)

Methods in *A.gossypii* Genetics

Sequence resources Any *A.gossypii* sequence information used in this work was taken from a whole genome sequencing approach (Dietrich et al., 2001).

Growth conditions *A.gossypii* was grown in liquid AFM (*Ashbya* Full Medium, 10 g/l yeast extract, 10 g/l Select Peptone 140 (Gibco BRL / LIFE TECHNOLOGIES), 20g/l glucose, 1 g/l myo-Inositol) using baffle shake flasks or on solid medium (AFM + 12 g/l agar granulated). For selection on the dominant drug resistance markers Geneticin (Calbiochem, 100% efficacy) or clonNat (WERNER Bio AGENTS, Jena, Germany) was added to the medium at concentrations of 200 µg/ml and 50 µg/ml, respectively. For auxotrophic selection using the LEU2 or ADE2 markers ASD drop out medium was prepared (*Ashbya* Synthetic Dextrose, 1.7 g/l YNB w/o amino acids and ammoniumsulfate (Difco), 0.78 g/l CSM-ADE / 0.69 g/l CSM-LEU (Bio101), 1 g/l Asn, 1 g/l myo-Inositol, 20 g/l Glucose, 12 g/l agar). Standard incubation temperature was at 30°C.

To isolate spores an AFM plate was inoculated with *A.gossypii* spores or mycelium in the centre. After growth for 7 d the mycelium was harvested with a sterile loop and resuspended in 1 ml of 2 mg/ml aqueous Zymolyase solution (Seikagaku, 20 U/µg) and incubated at 37°C for 1 h. The suspension was centrifuged at 2000 x g and the supernatant decanted. Three washing step with 0.03 % Triton X-100 were applied. Finally the spores were resuspended in 20 % glycerol and frozen at -70°C. The concentration was 1-2x10⁷ spores/ml.

Transformation *A.gossypii* was either

transformed replicative (Wright and Philippsen, 1991) or integrative (Steiner et al., 1995).

In replicative transformation pRS415 (Sikorski and Hieter, 1989) and pAG503 served as shuttle vectors. pRS415 carries a CEN/ARS element and the LEU2 gene from *S.cerevisiae* and complements *Agleu2Δ* strains (Mohr, 1997). pAG 503 is a pRS415 derivate in which the ScLEU2 gene was replaced with the GEN3 marker (see "Appendix III"). It can be used in G418^S strains and was tested in combination with wild-type, *Ag leu2Δ*, *thr4Δ* and *Ag leu2, Δthr4Δ, nat1^r* strains.

Integrative transformants were obtained by transformation of cloned and linearised DNA fragments or via PCR based gene targeting (Wendland et al., 2000, Baudin et al., 1993). GEN3 served as resistance marker against Geneticin. It encodes a phosphotransferase that is controlled by ScTEF2 promoter and terminator. Alternatively the NAT1 ORF alone amplified from pAG36 (Goldstein and McCusker, 1999) was used as resistance marker. A selected ORF was exchanged with the NAT1 ORF by PCR based gene targeting. The NAT1 ORF was then under the control of the endogenous promoter. NAT1 encodes a N-acetyltransferase that was used as a resistance marker against clonNat. Oligonucleotides used for PCR based gene targeting are listed in Table 1.3, strains are listed in Table 1.4.

For transformation of *A.gossypii* 100 ml of AFM were inoculated with spores to a concentration of ~7.5x10⁴ spores/ml. After 16-18 h the mycelium was harvested by filtration and washed with water once. It was incubated in 40 ml PD (50mM Phosphate-buffer pH 7.4, 25mM DTT) at 30°C with soft shaking for 30 min. The mycelium was filtrated again and washed with 40 ml of cold

STM (270mM Sucrose, 10 mM Tris pH 7.5, 1 mM MgCl₂). The competent mycelium was resuspended in 1-2 ml cold STM. 1-10 µg DNA resuspended in 50 µl of water was mixed with 150 µl of competent mycelium and transferred into a cold 4 mm electroporation cuvette (BioRad). The mycelium was electroporated (Gene Pulser, BioRad) at 100 Ω, 25 µF and 1.5 kV and resuspended in 1 ml AFM. Using the dominant drug resistance markers GEN3 or NAT1 the transformed mycelium was streaked on pre-dried AFM plates. After 5 h the plates were overlaid with 8 ml 0.5% agar containing 250 µg/ml Geneticin or 75 µg/ml clonNat, respectively. Primary transformants appeared after 2-3 days. Using auxotrophic markers the mycelium was allowed to recover for 5 h in 1 ml AFM. The mycelium was then washed twice with water and streaked onto the appropriate ASD drop out plates. Primary transformants appeared after 3-5 days. Primary heterokaryotic transformants were

transferred onto selective plates and allowed to sporulate. Spores were prepared and separated on selective plates using a micromanipulator (Singer Instruments) to obtain homokaryotic transformants.

Verification of the transformants was done by PCR (Wendland et al., 2000). The newly generated links at the transformed loci were amplified from genomic DNA and the size verified on agarose gels. Oligonucleotides used for verification are listed in Table 1.1. Standard oligonucleotides for verification of deletions generated with GEN3 are G3_2.1 and G3_3.2, for deletions generated with NAT1 are V2*NAT1 and V3*NAT1. They bind in the 5'-region and in the 3'-region of the respective marker.

A minimum of two independent homokaryotic transformants was claimed for each transformation. Experimental analysis was always done on at least two isolates demanding the same results.

Table 1.3 Oligonucleotides for PCR based gene targeting

Name	Sequence
SPA2-S1	5'-GTGACCGGCAACTCGCAGGACCGCTCGACATCCACTCGCGCACAGGCTAGGGATAACAGGGTAAT-3'
SPA2-S2	5'-CGCTTCACGTGGAAGTGGTCCTTCGGCAATAGATGGTCCGGCTGTAGGCATGCAAGCTTAGATCT-3'
AgSPA2_TURA3	5'-CTTAAGGAGGAAATAGAATACTTAAACTCCAAATTGGCGAAGTAGATTATAAGTAAATGCATGTATAC-3'
5Agade2part	5'-CGATTCTTGGGCTGCCGATGCCGCGGGGGTTCTCATCGATGGCTAGCTAGGGATAACAGGGTAAT-3'
3Agade2part	5'-CACAAAATTACTTGCCTCCTTGGAGCAGTTGTATAACTATTAGTAGGCATGCAAGCTTAGATCT-3'
AgSPA2_GFP	5'-AGCCTTAAGGAGGAAATAGAATACTTAAACTCCAAATTGGCGAAGGGTGCAGGCGCTGGAGCTG-3'
AgSPA2_GFP ^{5'fusion}	5'-CTCTCTGTGCTACGTGAAAAGAGCGAGCACTGTATTAGAGAAGTTAGGGACCTGGCACGGAGC-3'
AgSPA2_GFP ^{3'fusion}	5'-AACGAGTACTATGGCCTAGATCCGAAATATATGGGTGAGAAGATTGGTGCAGGCGCTGGAGCTG-3'
5'BOIGFPpGUG	5'-TTATTTATTAATCTGGCAGGACTGCTCTTTCGTGTTTATAATACAAGGGACCTGGCACGGAGC-3'
3'BOIGFPpGUG	5'-GCTATTAGCAACTATCGTCTAGGGAAAGATGCAGCGCAGGGGAAGGGTGCAGGCGCTGGAGCTG-3'
5CAP1GFPpGUG	5'-TAAGCTGTTTTAACTATCAGGCATTGTGAGCTAAGCTTTGAGTGGAGGGACCTGGCACGGAGC-3'
5CAP2GFPpGUG	5'-AACCGGGACAAGCACCAGGATTTAATCAAGGGCCTACAGGGCCTCGGTGCAGGCGCTGGAGCTG-3'
3CAP2GFPpGUG	5'-AACCAGGACAAGCACCAGGATTTAATCAAGGGCCTACAGGGCCTCGGTGCAGGCGCTGGAGCTG-3'
S1*BOI	5'-AGGATGAGTTTTTCGTTCAAGAAGGCGCTGAAGCTGACCGGGATGGCTAGGGATAACAGGGTAAT-3'
S2*BOI	5'-TCTTTCGTGTTTATAATACAGACTTTTCAATAGCACTTGAAATCAAGGCATGCAAGCTTAGATCT-3'
BOInat13'	5'-TCTTTCGTGTTTATAATACAGACTTTTCAATAGCACTTGAAATCAAGGGCAGGGCATGCTCATGTAG-3'
BOInat15'	5'-CCGCAAGACATCTCAAGAGCTGACTTACGGGTTGAGGACAGCAGGATGGGTACCCTCTTGACGAC-3'

Table 1.4 *Ashbya gossypii* strains

Name	Genotype	Reference
wild-type isolate		ATCC 10895
Ag ^{leu2Δ} thr4Δ*	leu2Δ, thr4Δ	Altmann-Johl and Philippsen, 1996, Mohr, 1997
Agspa2ΔC	Agspa2Δ::GEN3, leu2Δ, thr4Δ	
AgSPA2ΔP	SPA2Δ(978-3163)::GEN3, leu2Δ, thr4Δ	
AgSPA2-GFP	AgSPA2-GFP::GUG, leu2Δ, thr4Δ	
AgSPA2ΔP-GFP	SPA2Δ(978-3163)-GFP::GUG, leu2Δ, thr4Δ	
AgboiΔ	AgboiΔ::GEN3, leu2Δ, thr4Δ	
AgBOI-GFP	AgBOI-GFP::GUG, leu2Δ, thr4Δ	
AgboiΔSPA2-GFP	AgboiΔ::NAT1, AgSPA2-GFP::GUG, leu2Δ, thr4Δ	
Agade2Δ1	Agade2(310-566)Δ::GEN3, leu2Δ, thr4Δ	
AgCAP1-GFP	AgCAP1, AgCAP1-GFP, leu2Δ, thr4Δ, G418s	
AgCAP2-GFP	AgCAP2, AgCAP2-GFP, leu2Δ, thr4Δ, G418s	

*referred to as wild-type

Genomic DNA isolation The mycelium of a 50 ml o/n culture was harvested by filtration and washed once with water. 1 g of mycelium was incubated in 10 ml SPEZ (1 M Sorbitol, 10mM NaP pH 5.8, 10mM EDTA, 1 mg/ml Zymolyase) at 37°C for 1 h or until protoplastation. 1 ml 10 % SDS was added and the suspension was incubated at 37°C for 15 min. SDS was precipitated on ice for 30 min with 3.6 ml 3 M KAc. The suspension was centrifuged at 15000 x g for 15 min and the supernatant precipitated with 1 vol. of isopropanol. The solution was centrifuged at 15000 x g, the pellet washed with cold 70 % EtOH and dried. The pellet was resuspended in 1 ml TE containing 0.5 mg/ml RNase A (Roche) and incubated at 37°C for 1 h. The solution was phenol-chlorophorm extracted, precipitated, washed and resuspended in Tris pH 8.0 (Wright and Philippsen, 1991).

Cytoskeletal staining Visualization of the actin cytoskeleton was done using Phalloidin coupled fluorophores (acc. to Amberg, 1998, modified). *A.gossypii* was cultured in AFM to the desired stage. 1 ml of the culture was mixed with 100 µl 37 % formaldehyde (Fluka puriss. p.a.) and fixed for 10 min. Mycelia were centrifuged at 2000 x g, resuspended in PBS containing 4 % formaldehyde and incubated for 1 h. Mycelia were washed twice with PBST (PBS containing 0.03 % Triton X-100) and resuspended in 100 µl PBST. 10 µl Rhodamine-Phalloidin or Alexa488-Phalloidin (6.6 µM in MeOH, Molecular Probes Inc.) was added and the mycelia were incubated for 1 h in the dark. Mycelia were washed 5 times in PBST and resuspended in 50 µl mounting medium (50 mg p-phenylenediamine in 5 ml PBS, adjust pH to 8.0 with 0.5 M Na₂CO₃ pH 9.0, bring volume to 50 ml with glycerol). Alternatively, cells were fixed with paraformaldehyde (Fluka) if the fluorescence of GFP should be maintained. 1 ml of a cell culture was fixed for 30 min. with 1 ml of 4 % paraformaldehyde (Sambrook et al., 2001). Mycelia were washed twice with PBST and resuspended in mounting medium or stained for actin using Rhodamine-Phalloidin according to the protocol above.

Microscopy

Microscope set-up The microscopy unit used (as described in Hoepfner et al., 2000, modified) consisted of an Axioplan 2 imaging microscope (Carl Zeiss, Feldbach, Switzerland) with the objectives Plan Neofluar 100x Ph3 N.A.1.3, Plan Neofluar 63x Ph3 N.A.1.25, Plan Neofluar 40x Ph3 N.A.1.3 and Plan Aplanachromat 63x N.A.1.4. It was equipped with a 75 W XBO illumination source

controlled by a MAC2000 shutter and filter wheel system (Ludl Electronics, Hawthorne, NY). The camera was a TE/CCD-1000PB back illuminated cooled CCD camera (Princeton Instruments, Trenton, NJ). The following filter sets for different fluorophores were used: #10 for Alexa488 and #20 for Rhodamine (Zeiss), #41018 for GFP (Chroma Technology Corp., Brattleboro, VT, USA). GFP-Rhodamine double stainings were acquired with the mentioned filter sets except that the HQ500LP emission filter from filter set #41018 was replaced by a BP505-530 (Zeiss). The excitation intensity was controlled with different neutral density filters (Chroma). The setup including microscope, camera and Ludl controller was controlled by MetaMorph 4.1.7 software (Universal Imaging Corporation).

Image acquisition and processing The illumination time and light intensity for standard brightfield or fluorescence acquisitions was chosen to reach minimally 25 % of the maximal intensity that can be read by the camera. For multiple exposures of the same sample bleaching of the sample had to be taken into account. The z-distance in stack acquisitions was set to maximal 0.4 µm. Brightfield and single plane fluorescent images were scaled using the "scaling" drop-in in MetaMorph. Stacks were deblurred with MetaMorphy "remove shading" drop-in, flattened by "stack arithmetic" and scaled as mentioned above. For 3-D reconstructions stacks were first deblurred using AutoDeblur 7.0 (Universal Imaging Corporation) and reconstructed with MetaMorphy "3D reconstruction" drop-in. For time-lapse acquisition spores were cultured on a slide with a cavity (time-lapse slide, Merck) that was filled with medium (AFM, for fluorescent acquisitions 0.25 x AFM in respect to peptone, yeast extract and myo-Inositol, 1 x in respect to glucose). Spores were pre-incubated in a humid chamber without cover slip until they reached the required developmental stage. Then a cover slip was acquired. An acquisition set consisted of a brightfield image with optional three fluorescent images. The acquisition frequency varied from 0.5 min⁻¹ to 0.2 min⁻¹. The exposure time for the fluorescent images was reduced to 0.2-0.4 sec at 10-25% excitation intensity. Fluorescent pictures sets were processed as mentioned above and overlaid using MetaMorphy "overlay" drop-in. The time laps picture series was exported from MetaMorph as 8-bit TIFF files, converted to PICT files by Adobe Photoshop 6.0 (Adobe Systems Inc.) for Mac (Apple Computer Inc.) and converted to a QuickTime Movie (Apple Computer Inc.) by Adobe Premiere 4.2.1 for Mac. For time-lapse

acquisitions with a frequency of 0.5 h⁻¹ microscopy slides were covered with 1 ml molten AFM agar. Spores were spread on slides and allowed to germinate in a humid chamber to prevent drying of the agar. The slides were only removed from the humid chamber to acquire pictures.

Methods in Yeast Genetics

Culture conditions, transformation methods and DNA isolation were performed as described by Burke et al., 2000. Yeast strains used are listed in table 1.5.

ORF was kept in frame but shortened for 6558 bp. The GUG module (see "Chapter 3") was partly amplified by PCR with the oligonucleotide pair AgSPA2_TURA3 x AgSPA2_GFP3'fusion. The oligonucleotide AgSPA2_TURA3 has homology at its 3'-site to the ScURA3 terminator in GUG and carries 45 bp homology to the C-terminal coding region of the AgSPA2 ORF. AgSPA2_GFP3'fusion binds to the 3'-standard binding site in the GUG module. It carries 45 bp homology to the AgSPA2 ORF at its 3'-site. The gap between the two homology regions is 39 bp. The PCR product was

Table 1.5 Yeast strains

Name	Genotype	Reference
#259(pFS-28)3	lys2, his4, URA3, tef2Δ	Schirmaier and Philippsen, 1984

Cloning of pAGSPA2

The AgSPA2 ORF is 10179 bp in length and could be localized on an 11915 bp XmaI/XbaI fragment. Genomic Ashbya DNA was digested XmaI/XbaI. The digested DNA was separated by agarose gel electrophoresis. Fragments between 10.0 and 12.0 kbp were eluted and ligated with XmaI/XbaI digested pRS415 (Sikorski and Hieter, 1989). Positive pAGSPA2 clones were identified by a radioactive colony hybridisation. As a probe we used a 591 bp EcoRV fragment from opAG13790 covering a part in the N-terminal coding region of AgSPA2.

Generation of AgSPA2ΔP and Agspa2ΔC Strains

AgSPA2 was deleted by PCR based gene targeting using the resistance marker GEN3 (Wendland et al., 2000). The oligonucleotide pair used to amplify GEN3 was SPA2-S1 x SPA2-S2. The homology regions were selected to delete the whole ORF leaving the start and stop codon. The oligonucleotide pair used to verify the 5'-integration site is AgSPA25verif x G2.1, for the 3'-integration site AgSPA3'verif x G3.2. The deletion was made in the Agleu2Δthr4Δ strain.

To generate an AgSPA2ΔP strain a transformation cassette had to be generated first (in analogy to the C-terminal GFP fusion strategy described in "Chapter 1"). pAGSPA2 was digested using StuI/BtrI releasing 11 fragments from the AgSPA2 coding region. The linearised plasmid was religated to obtain pAGSPA2ΔP. The AgSPA2

then co-transformed with pAGSPA2ΔP into yeast strain #259(pFS-28)-3. Recombination on the plasmid was verified using oligonucleotide pair AgSPA2GFPverif x URA3t_BglII for amplification of the 5'-site and AgSPA23'verif x G3.2 for amplification of the 3'-site. The new plasmid pAGSPA2ΔP_TURA was digested EcoRV to release a 4444 bp fragment that was cloned into the EcoRV site of pBSISK(+) to generate pTCAGSPA2ΔP. This EcoRV fragment carries 1634 bp homology to the AgSPA2 ORF at the 5'-site of the StuI/BtrI deletion and remaining 686 bp between the StuI/BtrI deletion and the stop codon. At the 3'-site it carries 156 bp homology to the endogenous AgSPA2 terminator region. pTCAGSPA2ΔP was amplified in *E.coli*, digested with EcoRV and transformed into Agleu2Δthr4Δ. Verification was done on homokaryotic cells. The 5'-site was amplified with oligonucleotide pair AgOLIGO1865 x G3 and at the 3'-site using AgOLIGO1237 x URA3t_BglII. The deleted region in AgSPA2ΔP could not be amplified with the oligonucleotide pair AgOLIGO1927 x AgOLIGO1710 whereas this was possible in AgleuΔthr4Δ.

Generation of AgSPA2-GFP and AgSPA2ΔP-GFP Strains

The construction of an AgSPA2-GFP strain is described in "Chapter 1". To generate an AgSPA2ΔP-GFP strain, a transformation cassette had to be generated first (in analogy to the C-terminal GFP fusion strategy described in "Chapter

1"). pAGSPA2-GFP (see "Chapter 1") was digested Stul/BtrI to release a 6558 bp fragment generating pAGSPA2 Δ P-GFP. A 5214 bp EcoRV fragment from this plasmid was cloned into the EcoRV site of pBSISK(+) creating pTCAGSPA2 Δ P-GFP. The new plasmid harboured the GFP module fused to the partially deleted AgSPA2 ORF. The homology region prior to the Stul/BtrI deletion is 1634 bp in length, the region between the Stul/BtrI deletion and the GFP is 686 bp in length. At the 3'-site of the GUG module 156 bp of homology are located to the endogenous AgSPA2 terminator. pTCAGSPA2 Δ P-GFP was amplified in *E. coli* and digested with EcoRV. 10 μ g were transformed into Agleu2 Δ thr4 Δ to obtain AgSPA2 Δ P-GFP.

described in "Chapter 3".

Cloning of pAGBOI

The AgBOI ORF is 2955 bp in length. We could localise the complete ORF of AgBOI on a 4148 bp PstI/BamHI fragment. A library containing 8 - 12 kbp genomic *A. gossypii* inserts (obtained as a gift from K.-P. Stahmann, Forschungszentrum Jülich GmbH, D-52425 Jülich, Germany) was digested PstI/BamHI and separated on an agarose gel. Fragments between 3 - 5 kbp were eluted and ligated into PstI/BamHI digested pRS415. Positive pAGBOI clones were identified by a radioactive colony hybridisation. As a probe we used a 577 bp fragment that was amplified with the oligonucleotides AG1634rp_G1 x AG1634rp_G4 from genomic DNA.

Generation of Agboi Δ and Agboi Δ SPA2-GFP

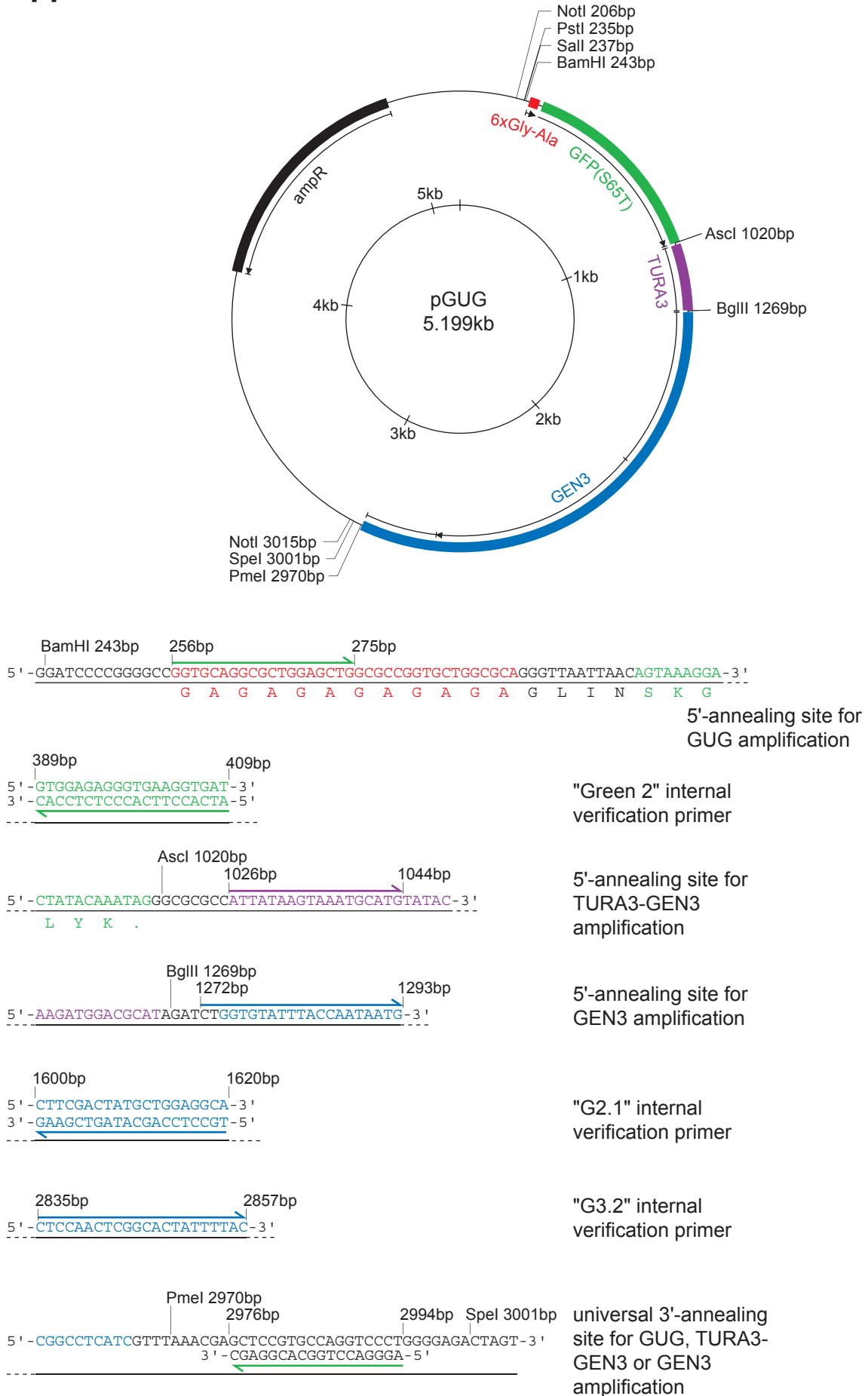
AgBOI was completely deleted by PCR based gene targeting using the GEN3 marker (Wendland et al., 2000). The oligonucleotide pair used to amplify GEN3 was S1*BOI x S2*BOI. The homology regions were selected to delete the whole ORF leaving the start and stop codon. The oligonucleotide pair used to verify the 5'-integration site was 1634-4th x G2.1, for the 3'-integration site G3.2 x p13_out-4. The deletion was made in the Agleu2 Δ thr4 Δ strain.

AgBOI was also deleted in the background strain AgSPA2-GFP with the resistance marker NAT1. The NAT1 ORF was amplified with oligonucleotides BOInat13' x BOInat15'. The homology regions were selected to replace the AgBOI ORF by the NAT1 ORF. The oligonucleotide pair used to verify the 5'-integration site was 1634-4th x V2NAT1*, for the 3'- integration site V3NAT1* x p13_out-4.

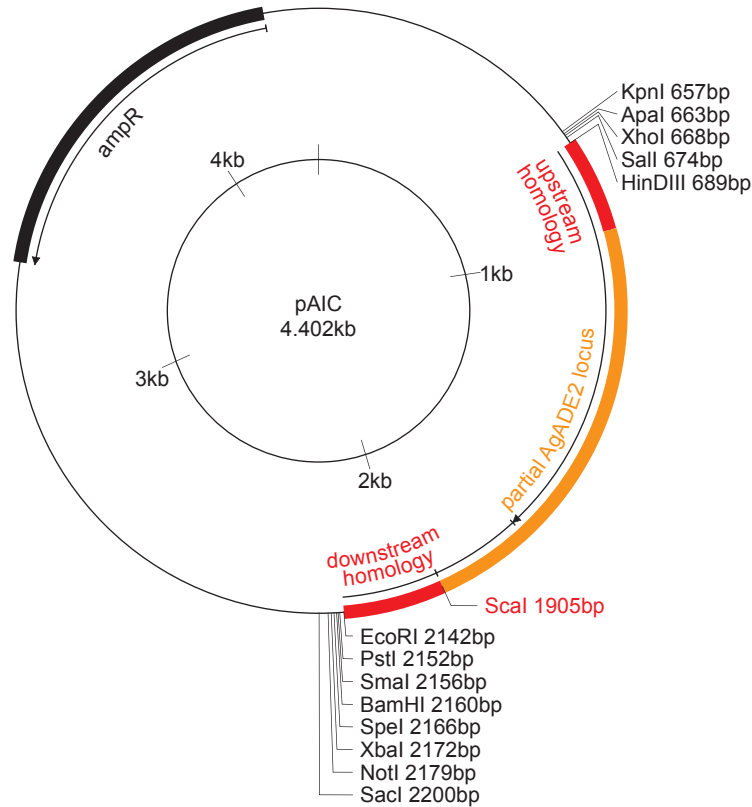
Generation of AgBOI-GFP

The construction of an AgBOI-GFP strain is

Appendix I



Appendix II



```

1824bp      1843bp
5' - CCATCAGCATAGGCACAACACTCCGCCGTAGTTGGTTTCAACAATTCGGCATATGCGACACGCGAAACCTGTTTTC
3' - GGTAGTCGTATCCGTGTTGAGGCGGCATCAACCAAGTGTAAAGGCGTATACGCTGTGCGCTTTGGACAAAG
    
```

"REDfor" internal
verification primer

```

Scal 1905bp      1947bp      1967bp
CGTTTCTAGTACTAATAGTTTATAACAACCTGCTCCAAGGAGCGCAAGTAATTTGTGAGGTTCCGACTTATGGC-3'
GCAAAGATCATGATTATCAATATGTTGACGAGGTTCCCTCGCGTTCATTAACAACACTCCAAGGCTGAATACCG-5'
    
```

"REDrev" internal
verification primer

```

-72bp      -51bp      HindIII 689bp
5' - TGCACCAGAAACAACATATGCCACCTATGCTACGCGCCAGCGCGGGTTGCTGACTCAATCCAGCTACGTGCCAAGCTT-3'
5' - ACGTGGTCTTGTTGTATACGGTGGATACGATGCGCGGTTCGCGCCAACGACTGAGTTAGGTCGATGCACGGTTCGAA-3'
    
```

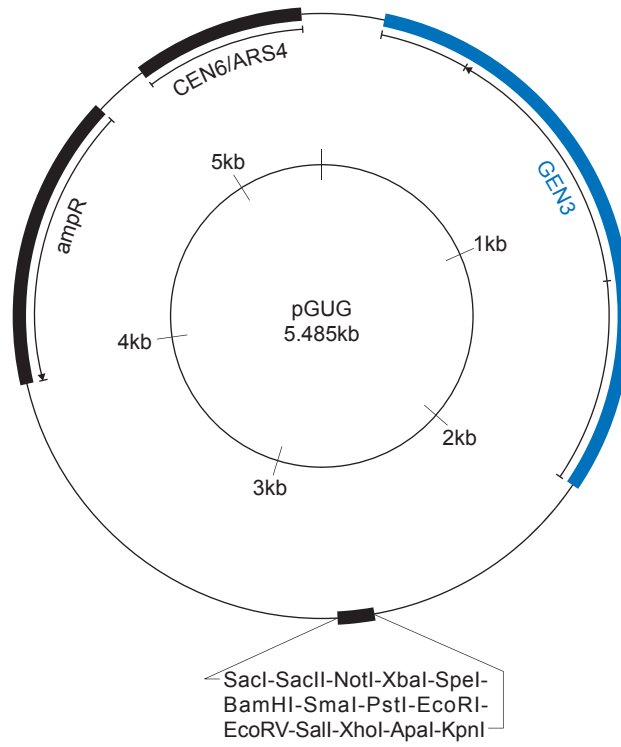
"Agade2verfor" external verification primer
binding 51bp upstream of the HindIII site in
the genomic AgADE2 locus

```

EcoRI 2142bp      +46bp      +68bp
5' - CTTTGAATTCACCGTTAAAAGTCAATATCTCCTATAGGGATTCTTCTTTTGTAGCTGGGGATTGAATGTCCATTT-3'
3' - GAAACTTAAAGTGCAATTTTCAGTATAGAGGATATCCCTAAGAAGAAAATCGACCCCTAAACTTACAGGTAAA-5'
    
```

"Agade2verrev" external verification primer
binding 46bp downstream of the EcoRI site in
the genomic AgADE2 locus

Appendix III



References

- Adamo, J.E., G. Rossi, and P. Brennwald. 1999. The Rho GTPase Rho3 has a direct role in exocytosis that is distinct from its role in actin polarity. *Mol Biol Cell*. 10:4121-33.
- Akada, R., J. Yamamoto, and I. Yamashita. 1997. Screening and identification of yeast sequences that cause growth inhibition when overexpressed. *Mol Gen Genet*. 254: 267-74.
- Altmann-Johl, R., and P. Philippsen. 1996. AgTHR4, a new selection marker for transformation of the filamentous fungus *Ashbya gossypii*, maps in a four-gene cluster that is conserved between *A. gossypii* and *Saccharomyces cerevisiae*. *Mol Gen Genet*. 250:69-80.
- Amberg, D.C. 1998. Three-dimensional imaging of the yeast actin cytoskeleton through the budding cell cycle. *Mol Biol Cell*. 9:3259-62.
- Amberg, D.C., J.E. Zahner, J.W. Mulholland, J.R. Pringle, and D. Botstein. 1997. Aip3p/Bud6p, a yeast actin-interacting protein that is involved in morphogenesis and the selection of bipolar budding sites. *Mol Biol Cell*. 8:729-53.
- Arkowitz, R.A., and N. Lowe. 1997. A small conserved domain in the yeast Spa2p is necessary and sufficient for its polarized localization. *J Cell Biol*. 138:17-36.
- Ashby, S.F., and W. Nowell. 1926. The fungi of stigmatomycosis. *Ann. Botany*. 40:69-84.
- Ayad-Durieux, Y., P. Knechtle, S. Goff, F. Dietrich, and P. Philippsen. 2000. A PAK-like protein kinase is required for maturation of young hyphae and septation in the filamentous ascomycete *Ashbya gossypii*. *J Cell Sci*. 113 Pt 24:4563-75.
- Baudin, A., O. Ozier-Kalogeropoulos, A. Denouel, F. Lacroute, and C. Cullin. 1993. A simple and efficient method for direct gene deletion in *Saccharomyces cerevisiae*. *Nucleic Acids Res*. 21:3329-30.
- Bauer, Y., and P. Philippsen. 2002. Publication in preparation.
- Bender, L., H.S. Lo, H. Lee, V. Kokojan, V. Peterson, and A. Bender. 1996. Associations among PH and SH3 domain-containing proteins and Rho-type GTPases in Yeast. *J Cell Biol*. 133:879-94.
- Brown, A., C. Gaillardin, J. Ernst, A. Dominguez, J. Pérez-Martin, F. Klis, R. Sentandreu, B. Hube, C. Kurischko, C. d'Enfert, and D. Maréchal. 2001. *Galar Fungail*, Novel Approaches for the Control of Fungal Disease.
- Burke, D., D. Dawson, and T. Stearns. 2000. *Methods in Yeast Genetics: A Cold Spring Harbor Laboratory Course Manual*. Cold Spring Harbour Press, New York. 205 pp.
- Casamayor, A., and M. Snyder. 2002. Bud-site selection and cell polarity in budding yeast. *Curr Opin Microbiol*. 5:179-86.
- Chant, J. 1999. Cell polarity in yeast. *Annu Rev Cell Dev Biol*. 15:365-91.
- Christiansen, T., A.B. Spohr, and J. Nielsen. 1999. On-line study of growth kinetics of single hyphae of *Aspergillus oryzae* in a flow-through cell. *Biotechnol Bioeng*. 63:147-53.
- Dietrich, F., S. Voegeli, A. Brachat, A. Lerch, K. Gates, P. Luedi, T. Gaffney, and P. Philippsen. 2001. Evolution of the *S.cerevisiae* genome: Lessons learned from the genome analysis of the fungus *Ashbya gossypii*. In XXth International Conference on Yeast Genetics and Molecular Biology, Prague, Czech Republic.
- Dietrich, F.S., J. Mulligan, K. Hennessy, M.A. Yelton, E. Allen, R. Araujo, E. Aviles, A. Berno, T. Brennan, J. Carpenter, E. Chen, J.M. Cherry, E. Chung, M. Duncan, E. Guzman, G. Hartzell, S. Hunicke-Smith, R.W. Hyman, A. Kayser, C. Komp, D. Lashkari, H. Lew, D. Lin, D. Mosedale, R.W. Davis, and et al. 1997. The nucleotide sequence of *Saccharomyces cerevisiae* chromosome V. *Nature*. 387:78-81.
- Drubin, D.G., and W.J. Nelson. 1996. Origins of cell polarity. *Cell*. 84:335-44.
- Errede, B., A. Gartner, Z. Zhou, K. Nasmyth, and G. Ammerer. 1993. MAP kinase-related FUS3 from *S. cerevisiae* is activated by STE7 in vitro. *Nature*. 362:261-4.

- Evangelista, M., K. Blundell, M.S. Longtine, C.J. Chow, N. Adames, J.R. Pringle, M. Peter, and C. Boone. 1997. Bni1p, a yeast formin linking cdc42p and the actin cytoskeleton during polarized morphogenesis. *Science*. 276:118-22.
- Evangelista, M., D. Pruyne, D.C. Amberg, C. Boone, and A. Bretscher. 2002. Formins direct Arp2/3-independent actin filament assembly to polarize cell growth in yeast. *Nat Cell Biol*. 4:32-41.
- Fujiwara, T., K. Tanaka, A. Mino, M. Kikyo, K. Takahashi, K. Shimizu, and Y. Takai. 1998. Rho1p-Bni1p-Spa2p interactions: implication in localization of Bni1p at the bud site and regulation of the actin cytoskeleton in *Saccharomyces cerevisiae*. *Mol Biol Cell*. 9:1221-33.
- Gehring, S., and M. Snyder. 1990. The SPA2 gene of *Saccharomyces cerevisiae* is important for pheromone-induced morphogenesis and efficient mating. *J Cell Biol*. 111:1451-64.
- Goldstein, A.L., and J.H. McCusker. 1999. Three new dominant drug resistance cassettes for gene disruption in *Saccharomyces cerevisiae*. *Yeast*. 15:1541-53.
- Gulli, M.P., and M. Peter. 2001. Temporal and spatial regulation of Rho-type guanine-nucleotide exchange factors: the yeast perspective. *Genes Dev*. 15:365-79.
- Hall, A. 1998. Rho GTPases and the actin cytoskeleton. *Science*. 279:509-14.
- Hanahan, D. 1983. Studies on transformation of *Escherichia coli* with plasmids. *J Mol Biol*. 166:557-80.
- Harris, S.D. 1997. The duplication cycle in *Aspergillus nidulans*. *Fungal Genet Biol*. 22:1-12.
- Heath, B.I. 1995. Integration and regulation of hyphal tip growth. *Can. J. Bot*. 73:131-139.
- Heim, R., and R.Y. Tsien. 1996. Engineering green fluorescent protein for improved brightness, longer wavelengths and fluorescence resonance energy transfer. *Curr Biol*. 6: 178-82.
- Hoepfner, D., A. Brachat, and P. Philippsen. 2000. Time-lapse video microscopy analysis reveals astral microtubule detachment in the yeast spindle pole mutant *cnm67*. *Mol Biol Cell*. 11:1197-211.
- Imamura, H., K. Tanaka, T. Hihara, M. Umikawa, T. Kamei, K. Takahashi, T. Sasaki, and Y. Takai. 1997. Bni1p and Bnr1p: downstream targets of the Rho family small G-proteins which interact with profilin and regulate actin cytoskeleton in *Saccharomyces cerevisiae*. *Embo J*. 16:2745-55.
- Johnson, D.I. 1999. Cdc42: An essential Rho-type GTPase controlling eukaryotic cell polarity. *Microbiol Mol Biol Rev*. 63:54-105.
- Kagami, M., A. Toh-e, and Y. Matsui. 1997. SRO9, a multicopy suppressor of the bud growth defect in the *Saccharomyces cerevisiae* rho3-deficient cells, shows strong genetic interactions with tropomyosin genes, suggesting its role in organization of the actin cytoskeleton. *Genetics*. 147:1003-16.
- Lengeler, K.B., R.C. Davidson, C. D'Souza, T. Harashima, W.C. Shen, P. Wang, X. Pan, M. Waugh, and J. Heitman. 2000. Signal transduction cascades regulating fungal development and virulence. *Microbiol Mol Biol Rev*. 64:746-85.
- Madden, K., and M. Snyder. 1998. Cell polarity and morphogenesis in budding yeast. *Annu Rev Microbiol*. 52:687-744.
- Maizel, J.V., Jr., and R.P. Lenk. 1981. Enhanced graphic matrix analysis of nucleic acid and protein sequences. *Proc Natl Acad Sci U S A*. 78:7665-9.
- Matsui, Y., R. Matsui, R. Akada, and A. Toh-e. 1996. Yeast src homology region 3 domain-binding proteins involved in bud formation. *J Cell Biol*. 133:865-78.
- Matsui, Y., and E.A. Toh. 1992. Yeast RHO3 and RHO4 ras superfamily genes are necessary for bud growth, and their defect is suppressed by a high dose of bud formation genes CDC42 and BEM1. *Mol Cell Biol*. 12:5690-9.
- Mayer, B.J. 2001. SH3 domains: complexity in moderation. *J Cell Sci*. 114:1253-63.

- Mohr, C. 1997. Genetic Engineering of the Filamentous Fungus *Ashbya gossypii*: Construction of a Genomic Library, Isolation of Genes for B-Isopropylmaltose dehydrogenase (LEU2) and a Protein Kinase (APK1) by Heterologous Complementation, and Characterization of Non-reverting mutants. PhD thesis, Biozentrum, University of Basel, Switzerland.
- Momany, M., and J.E. Hamer. 1997. Relationship of actin, microtubules, and crosswall synthesis during septation in *Aspergillus nidulans*. *Cell Motil Cytoskeleton*. 38:373-84.
- Momany, M., and I. Taylor. 2000. Landmarks in the early duplication cycles of *Aspergillus fumigatus* and *Aspergillus nidulans*: polarity, germ tube emergence and septation. *Microbiology*. 146 Pt 12:3279-84.
- Mosch, H.U., R.L. Roberts, and G.R. Fink. 1996. Ras2 signals via the Cdc42/Ste20/mitogen-activated protein kinase module to induce filamentous growth in *Saccharomyces cerevisiae*. *Proc Natl Acad Sci U S A*. 93: 5352-6.
- Ozaki-Kuroda, K., Y. Yamamoto, H. Nohara, M. Kinoshita, T. Fujiwara, K. Irie, and Y. Takai. 2001. Dynamic localization and function of Bni1p at the sites of directed growth in *Saccharomyces cerevisiae*. *Mol Cell Biol*. 21:827-39.
- Pagni, M., C. Iseli, T. Junier, L. Falquet, V. Jongeneel, and P. Bucher. 2001. trEST, trGEN and Hits: access to databases of predicted protein sequences. *Nucleic Acids Res*. 29:148-51.
- Pantaloni, D., and M.F. Carrier. 1993. How profilin promotes actin filament assembly in the presence of thymosin beta 4. *Cell*. 75: 1007-14.
- Pruyne, D., and A. Bretscher. 2000a. Polarization of cell growth in yeast. *J Cell Sci*. 113:365-75.
- Pruyne, D., and A. Bretscher. 2000b. Polarization of cell growth in yeast. *J Cell Sci*. 113:571-85.
- Rebecchi, M.J., and S. Scarlata. 1998. Pleckstrin homology domains: a common fold with diverse functions. *Annu Rev Biophys Biomol Struct*. 27:503-28.
- Robinson, N.G., L. Guo, J. Imai, E.A. Toh, Y. Matsui, and F. Tamanoi. 1999. Rho3 of *Saccharomyces cerevisiae*, which regulates the actin cytoskeleton and exocytosis, is a GTPase which interacts with Myo2 and Exo70. *Mol Cell Biol*. 19:3580-7.
- Roemer, T., L. Vallier, Y.J. Sheu, and M. Snyder. 1998. The Spa2-related protein, Sph1p, is important for polarized growth in yeast. *J Cell Sci*. 111:479-94.
- Sagot, I., S.K. Klee, and D. Pellman. 2002. Yeast formins regulate cell polarity by controlling the assembly of actin cables. *Nat Cell Biol*. 4:42-50.
- Sambrook, J., D.W. Russell, and J. Sambrook. 2001. *Molecular Cloning: A Laboratory Manual*. Cold Spring Harbor Laboratory. 999 pp.
- Schirmaier, F., and P. Philippsen. 1984. Identification of two genes coding for the translation elongation factor EF-1 alpha of *S. cerevisiae*. *Embo J*. 3:3311-5.
- Sheu, Y.J., Y. Barral, and M. Snyder. 2000. Polarized growth controls cell shape and bipolar bud site selection in *Saccharomyces cerevisiae*. *Mol Cell Biol*. 20:5235-47.
- Sheu, Y.J., B. Santos, N. Fortin, C. Costigan, and M. Snyder. 1998. Spa2p interacts with cell polarity proteins and signaling components involved in yeast cell morphogenesis. *Mol Cell Biol*. 18:4053-69.
- Short, J.M., J.M. Fernandez, J.A. Sorge, and W.D. Huse. 1988. Lambda ZAP: a bacteriophage lambda expression vector with in vivo excision properties. *Nucleic Acids Res*. 16: 7583-600.
- Sikorski, R.S., and P. Hieter. 1989. A system of shuttle vectors and yeast host strains designed for efficient manipulation of DNA in *Saccharomyces cerevisiae*. *Genetics*. 122:19-27.
- Snyder, M. 1989. The SPA2 protein of yeast localizes to sites of cell growth. *J Cell Biol*. 108:1419-29.
- Snyder, M., S. Gehrung, and B.D. Page. 1991. Studies concerning the temporal and genetic control of cell polarity in *Saccharomyces cerevisiae*. *J Cell Biol*. 114:515-32.

- Spohr, A., C. Dam-Mikkelsen, M. Carlsen, J. Nielsen, and J. Villadsen. 1998. On-line study of fungal morphology during submerged growth in a small flow-through cell. *Biotechnol Bioeng.* 58:541-53.
- Stapleton, D., I. Balan, T. Pawson, and F. Sicheri. 1999. The crystal structure of an Eph receptor SAM domain reveals a mechanism for modular dimerization. *Nat Struct Biol.* 6: 44-9.
- Steiner, S., J. Wendland, M.C. Wright, and P. Philippsen. 1995. Homologous recombination as the main mechanism for DNA integration and cause of rearrangements in the filamentous ascomycete *Ashbya gossypii*. *Genetics.* 140:973-87.
- Steinert, P.M., and D.R. Roop. 1988. Molecular and cellular biology of intermediate filaments. *Annu Rev Biochem.* 57:593-625.
- Thompson, J.D., D.G. Higgins, and T.J. Gibson. 1994. CLUSTAL W: improving the sensitivity of progressive multiple sequence alignment through sequence weighting, position-specific gap penalties and weight matrix choice. *Nucleic Acids Res.* 22:4673-80.
- Toya, M., Y. Iino, and M. Yamamoto. 1999. Fission yeast Pob1p, which is homologous to budding yeast Boi proteins and exhibits subcellular localization close to actin patches, is essential for cell elongation and separation. *Mol Biol Cell.* 10:2745-57.
- Trinci, A.P.J. 1970. Kinetics of apical and lateral branching in *Aspergillus nidulans* and *Geotrichum lactis*. *Trans. Br. Mycol. Soc.* 55:17-28.
- Valtz, N., and I. Herskowitz. 1996. Pea2 protein of yeast is localized to sites of polarized growth and is required for efficient mating and bipolar budding. *J Cell Biol.* 135:725-39.
- van Roessel, P., and A.H. Brand. 2002. Imaging into the future: visualizing gene expression and protein interactions with fluorescent proteins. *Nat Cell Biol.* 4:E15-20.
- Vasara, T., M. Saloheimo, S. Keranen, and M. Penttila. 2001a. *Trichoderma reesei* rho3 a homologue of yeast RH03 suppresses the growth defect of yeast sec15-1 mutation. *Curr Genet.* 40:119-27.
- Vasara, T., L. Salusjarvi, M. Raudaskoski, S. Keranen, M. Penttila, and M. Saloheimo. 2001b. Interactions of the *Trichoderma reesei* rho3 with the secretory pathway in yeast and *T. reesei*. *Mol Microbiol.* 42: 1349-61.
- Wach, A., A. Brachat, C. Alberti-Segui, C. Rebischung, and P. Philippsen. 1997. Heterologous HIS3 marker and GFP reporter modules for PCR-targeting in *Saccharomyces cerevisiae*. *Yeast.* 13: 1065-75.
- Wach, A., A. Brachat, R. Pohlmann, and P. Philippsen. 1994. New heterologous modules for classical or PCR-based gene disruptions in *Saccharomyces cerevisiae*. *Yeast.* 10:1793-808.
- Weiner, M.P., G.L. Costa, W. Schoettlin, J. Cline, E. Mathur, and J.C. Bauer. 1994. Site-directed mutagenesis of double-stranded DNA by the polymerase chain reaction. *Gene.* 151:119-23.
- Wendland, J. 2001. Comparison of morphogenetic networks of filamentous fungi and yeast. *Fungal Genet Biol.* 34:63-82.
- Wendland, J., Y. Ayad-Durieux, P. Knechtle, C. Rebischung, and P. Philippsen. 2000. PCR-based gene targeting in the filamentous fungus *Ashbya gossypii*. *Gene.* 242:381-91.
- Wendland, J., and P. Philippsen. 2000. Determination of cell polarity in germinated spores and hyphal tips of the filamentous ascomycete *Ashbya gossypii* requires a rhoGAP homolog. *J Cell Sci.* 113:1611-21.
- Wendland, J., and P. Philippsen. 2001. Cell polarity and hyphal morphogenesis are controlled by multiple rho- protein modules in the filamentous ascomycete *Ashbya gossypii*. *Genetics.* 157:601-10.
- Wright, M.C., and P. Philippsen. 1991. Replicative transformation of the filamentous fungus *Ashbya gossypii* with plasmids containing *Saccharomyces cerevisiae* ARS elements. *Gene.* 109:99-105.
- Yanisch-Perron, C., J. Vieira, and J. Messing. 1985. Improved M13 phage cloning vectors and host strains: nucleotide sequences of the M13mp18 and pUC19 vectors. *Gene.* 33:103-19.

Acknowledgements

I would first like to thank my thesis advisor Prof. Peter Philippsen for giving me the opportunity to do my thesis in his lab. Peter supported me in every way during my thesis and he had always an open ear for my concerns. We had a lot of intellectual exchange, especially on the developmental pattern of *Ashbya gossypii*. I enjoyed these discussions and I think that we achieved to uncover certain secrets of filamentous growth in *Ashbya gossypii* morphogenesis. Furthermore, I would also thank Peter for buying me all the microscopy gimmicks that I desired.

I am also very thankful Yasmina Bauer, Jürgen Wendland for giving me an introduction into *Ashbya gossypii* as a model organism and for very helpful discussions during the time of my thesis. I would also like Florian Schärer for introducing me into methods of molecular genetics.

Further I would like to thank the members of my thesis committee Marie-Pierre Gully and Yves Barral for suggestions on my project and fruitful discussions.

I would like to thank the members of the sequencing group, Fred Dietrich, Philippe Lüdi, Anita Lerch, Sophie Brachat and Sylvia Vögeli for providing me not only with excellent sequence information.

I additionally thank all present members of the lab, especially Amy Gladfelter for critically reading this manuscript, Dominic Höpfner for giving me an introduction into video-microscopy, Pesche Helfer, Katrin Hungerbühler, Andreas Kaufmann, Hans-Peter Schmitz, Philippe Laissue, Riccarda Rischatsch and Kamila Wojnowska, the former members

Christine Alberti-Segui, Michael Bloch, Nicole Liebundguth, Roger Schmidt and Olaf Sunnotel, a diploma student who was working on the establishment of the NAT1 marker and

Isabelle Barde and Isabelle Cognet, two summer students who were working on the CAP-GFP fusions and

Regula Niederhauser, Gisela Burkhalter, Silvie Germano and Doris Rossi.

Und am allermeisten danke ich meiner lieben Caroline.

Curriculum vitae

- Name Philipp Andreas Knechtle

- Date of birth 05.08.1972

- Place of birth Basel, Switzerland

- Nationality Swiss

- Education
 - Primary school 1979-1984
Oberwil, Basel, Switzerland
 - Secondary school 1984-1989
Oberwil, Basel, Switzerland
 - Grammar school 1989-1992
Oberwil, Basel, Switzerland
 - Basic studies in Biology 1993-1996
ETH, Zürich, Switzerland
 - Continued studies in Biology 1996-1997
Biozentrum, Basel, Switzerland
 - Diploma Thesis in Microbiology 1997-1998
with degree 5/6
in the lab of Prof. P. Philippson
Biozentrum, Basel, Switzerland
 - Ph.D. in Microbiology 1999-2002
with degree magna cum laude
(5.5/6) in the lab of
Prof. P. Philippson
Biozentrum, Basel, Switzerland

- Research experience
 - Postdoc at the Institut Pasteur 2002-
in the lab of Dr. Ch. d'Enfert working
on virulence factors in
Candida albicans

- Conferences
 - April 2000, 5th European Conference on Fungal Genetics (ECFG V),
Arcachon, France. Poster presentation "AgBOI, a gene involved
in maintenance of polargrowth of the filamentous fungus
Ashbya gossypii"
 - April 2001, 21st Fungal Genetics Conference, Asilomar, CA, USA.
Poster presentation "Control of polarity in the filamentous fungus
Ashbya gossypii"
 - April 2002, 6th European Conference on Fungal Genetics
(ECFG VI), Pisa, Italy.

-Publications

- Ayad-Durieux, Y., Knechtle, P., Goff, S., Dietrich, F. & Philippsen, P. A PAK- like protein kinase is required for maturation of young hyphae and septation in the filamentous ascomycete *Ashbya gossypii*. *J Cell Sci* 113 Pt 24, 4563-75. (2000).
- Wendland, J., Ayad-Durieux, Y., Knechtle, P., Rebischung, C. & Philippsen, P. PCR-based gene targeting in the filamentous fungus *Ashbya gossypii*. *Gene* 242, 381-91. (2000).
- Knechtle, P. Dietrich, F., Philippsen, P. Maximal Polar Growth Potential Depends on the Polarisome Component AgSpa2 in the Filamentous Fungus *Ashbya gossypii* (ready for submission)

Ich erkläre, dass ich die Dissertation

"AgSPA2 and AgBOI Control Landmarks of Filamentous Growth in the Filamentous
Ascomycete *Ashbya gossypii*"

nur mit der darin angegebenen Hilfe verfasst und bei keiner anderen Fakultät
eingereicht habe.

Basel, April 2002

Philipp Knechtle